THEORETICAL AND COMPUTATIONAL STUDIES OF LIQUID METALS AND LIQUID BINARY ALLOYS

Thesis submitted to Mizoram University
for the Degree of

Doctor of Philosophy

in

Chemistry

By

R. LALNEIHPUII

Regd. No. : MZU/PhD/473 of 15.05.2012

DEPARTMENT OF CHEMISTRY

SCHOOL OF PHYSICAL SCIENCES

MIZORAM UNIVERSITY,

TANHRIL, AIZAWL- 796004

May, 2017

MIZORAM UNIVERSITY

(A central University under the Act of Parliament)

Department of Chemistry

School of Physical Sciences

Dr. Raj Kumar Mishra
Assistant Professor

CERTIFICATE

This is to certify that the thesis entitled '*Theoretical and Computational Studies of Liquid Metals and Liquid Binary Alloys*' submitted by ***Miss. R. Lalneihpuii,*** for the degree of ***Doctor of Philosophy*** in the Mizoram University, Aizawl, Mizoram, embodies the record of original investigations carried out by her under my supervision. She has been duly registered and the thesis presented is worthy of being considered for the award of the Ph.D. degree. This work has not been submitted for any degree in any other university.

Dated: 11th May, 2017

(RAJ KUMAR MISHRA)

Supervisor

Tanhril Campus, Aizawl, Mizoram- 796004, India: Ph. 0389-2330832 (0): Cell: 09774379665
Email: rkmishramzu@yahoo.com

Declaration of the Candidate

Mizoram University

May, 2017

I, R. Lalneihpuii, hereby declare that the subject matter of this thesis is the record of work done by me, that the contents of this thesis did not form basis of the award of any previous degree to me or to the best of my knowledge to anybody else, and that the thesis has not been submitted by me for any research degree in any other University/Institute.

This is being submitted to the Mizoram University for the degree of Doctor of Philosophy in Chemistry.

(R. LALNEIHPUII)

Candidate

Regd. No. : MZU/PhD/473 of 15.05.2012

(Prof. DIWAKAR TIWARI)

Head

(Dr. Raj Kumar Mishra)

Supervisor

ACKNOWLEDGEMENTS

I express my sincere thanks to my research supervisor, *Dr. Raj Kumar Mishra*, Assistant Professor, Department of Chemistry, Mizoram University, for his untiring perseverance throughout my research work. His expert knowledge in theoretical and computational research and his valuable suggestions and guidance highly encourages me and improve my knowledge in theoretical Chemistry which make it possible to accomplish my research work.

I offer my sincere regards to the present and former Head, *Prof. Diwakar Tiwari* and *Dr. Muthukumaran, R.*, Department of Chemistry, School of Physical Sciences, MZU for their many help and guidance during my Ph. D research work.

I express my sense of gratitude to the present and former Deans, *Prof. R.C. Tiwari* and *Prof. R. K. Thapa*, School of Physical Sciences, MZU for their support and encouragements in accomplishing the research work.

I am also immensely thankful to all the faculty members of Department of Chemistry, MZU and all the non-teaching staff of the Departmentfor their valuable help and cooperation.

I am very happy to acknowledge the cooperation and help I received from my fellow research scholars, *Mr. Jay Prakash Rajan, Mr. C. Lalnuntluanga, Miss Lalrintluangi* and all the Research Scholars in the Department for their support and helping hand, which had been rendered while carrying out my research work.

I also acknowledge the UGC, New Delhi for their financial assistance through Rajiv Gandhi National Fellowship during the whole Ph. D research work.

Valuable support and encouragement that I had received from my Family during my research career is worth to be mentioned. My special thanks go to them for their endless love, constant support and prayers which make it possible to accomplish my research work.

Above all, I thank the Almighty God for his blessings, protection and guidance throughout this research works.

(R. LALNEIHPUII)

Regd. No. : MZU/PhD/473 of 15.05.2012

CONTENTS

CHAPTER-5

CHAPTER-6

CHAPTER-7

1. INTRODUCTION

1.1. BACKGROUND

Statistical mechanics is one of the fundamental branches of theoretical science. It concerns itself primarily with the prediction of the behavior of large numbers of atoms and molecules from the basic laws describing the interactions of small numbers of atoms or molecules. Within the broader field of theoretical chemistry and Physics, statistical mechanics occupies a central place between thermodynamics, which treats the behavior of bulk matter without reference to the possible validity of the atomic hypothesis, and quantum mechanics, which treats the electronic structure of single molecule but does not readily treat systems containing substantial numbers of unbounded atoms (Phillies, 2000).

Statistical mechanics requires a description of the motion of individual atoms and molecules. Such motion may be treated either with classical or quantum mechanics. In some cases (e.g., internal molecular motions or translational motions of light atoms (He, Ne) at low temperature) the use of quantum mechanics is mandatory. However, modern chemistry and modern statistical mechanics largely treat systems in which the quantum nature of matter is not readily apparent. To calculate the shape of molecules, the forces between them, or the stages of a chemical reaction, quantum mechanics is needed. To treat translational and rotational (but not internal vibration) of molecules in liquids classical mechanics is almost always good enough (Phillies, 2000).

The primary goal of statistical thermodynamics (also known as equilibrium statistical mechanics) is to derive the classical thermodynamics of materials in terms of the properties of their constituent particles and the interactions between them. Statistical Mechanics makes it possible to relate the macroscopic properties of a system to the

microscopic states and energy levels. The subject of statistical mechanics has been successfully applied in various fields including the prediction of the microscopic function, S(k) of liquid metals (Gosh et al., 2007; Taylor et al., 2001; Gopala Rao and Venkatesh, 1989). Statistical mechanics provides numerical relations between structures, dynamic and thermodynamic properties of liquid metals and alloys (Ma et al., 2013).

In a crystalline solids there is a perfect or regular arrangement of the atoms, molecules or ions with maximum attractive force, which is referred as lattice points in the three dimensional space. Such an arrangement is called space lattice and constituting particles can move from one lattice site to another with suitable amount of activation energy of diffusion.

Liquid state is the intermediate between solid state and gaseous state as regards to inter-particle forces, packing of particles, etc. In solids, there is close packing of molecules or atoms or ions. The definite and ordered arrangement of the constituents of solids extends over a large distance. This is termed as long range order. The liquid may be considered to have an ordered pattern over a short range instead of the entire mass i.e. short - range order while gases show no order at all.

Since molecules of liquids are not far apart from one another, the intermolecular forces are fairly strong. Characteristic properties of liquids arise from the nature and the magnitude of these intermolecular forces. Liquid structure is continuously changing because of the thermal motion of the particles. In solids as the temperature of the crystal is increased the frequencies with which the particles vibrate about their mean positions increased. The increase in thermal vibration of atom at elevated temperatures overcomes the potential energy which keeps the particles in their positions. As a result, some atoms which have kinetic energy greater than their potential energy jump out of

their positions of lowest energy and create vacancies, thus forming defects. The existence of vacancies also enables easy movements of atoms or ions in the crystal changing places with one another. This accounts for the phenomenon of diffusion in solids. If the number of such defects is increased by increasing the temperature, the network structure of crystal will collapse and becomes liquid.

The study on structural, dynamical and surface properties of liquid metals and alloys helps in various metallurgical processes and also help their study in solid state. The study of liquid state is considered to be very complicated due to irregular structure of liquids. Theoretical development on the structural and associated properties (dynamic, transport, surface, thermodynamics) of liquids become a big challenge in present time for complete understanding of liquid state. Metals have been extensively studied in the liquid phase by using classical and quantum statistical mechanics to understand their microscopic as well as macroscopic properties under equilibrium and non-equilibrium conditions. The structure of a liquid is investigated by means of X – rays scattering and Neutron diffraction techniques. X-ray diffraction has been found to be useful for the studies of liquids as liquids survived some features of lattice structure of solids. It was found that the wavelength of X-rays was of about the same order as the inter-atomic distances. If the crystal contains more than one kind of atoms, the atom containing greater number of electrons scatters the X-rays to a greater extend. The scattering factor, f of an atom is defined as

$$f = 4\pi \int_0^\infty \rho(r) \frac{\sin kr}{kr} r^2 dr \qquad (1.1)$$

Where $\rho(r)$ is the spherical symmetric electron density (number of electrons per unit volume) of the atom and $k = (4\pi/\lambda)\mathrm{Sin}\theta$, where λ is the wavelength of the X-rays and θ is the scattering angle.

It is difficult to differentiate a liquid and a solid on a microscopic level although their difference is very clear in everyday life. The static properties like Structure factor etc. cannot distinct between amorphous solids and liquids, and therefore the dynamical diffusion properties are also necessary to make the distinction (March and Alonso, 1998) between them. The atoms in liquid will diffuse away from their original position even at low temperature but the atoms in a solid will not self-diffuse in the absence of defect. Further, the diffusion phenomena and the temperature dependence in liquids both from microscopic and macroscopic points of view are one of the most difficult problems in condensed matter because temperature dependence of many body interactions should be taken into account. Hence the studies of atomic transport properties of liquid metals and liquid binary alloys are much more complicated than the study of structure alone (Wax et al., 2000). Many properties of the materials depend on the rate (at the given temperature) at which the atoms in liquids diffuse (Shimoji and Itami, 1986).

1.2. INTERMOECULAR FORCES IN LIQUIDS

In general liquids are characterized by their high density and finite compressibility. In order to discuss the interaction in liquids, it is necessary first to assume that the mutual interaction energy U of a liquid collection of N molecules is independent of intermolecular energy levels (Faber, 1972; Skhrishevsij, 1980).

It is assumed that the interactions between the neighboring molecules in liquids are not sufficiently strong to excite new vibrational or electronic levels or to influence the occupation of rotational levels (Faber, 1972; Skhrishevsij, 1980; Waseda, 1980). In terms of partition function, the internal degrees of freedom of the molecules can be

factored out, to leave the configurational or interaction part. Although it is the intermolecular forces of attraction and repulsion which lend the liquid and its properties (Glazov et al., 1969; Hafner and Kahl, 1984; Percus, 1962).

The square well (SW) potential has been successfully applied for studying of various liquids for long time (Gopala Rao and Murthy, 1974; Liu et al., 1998; Gopala Rao and Sathpathy, 1982; Venkatesh et al., 2003; Gopala Rao and Venkatesh, 1989; Venkatesh and Mishra, 2005; Dubinin et al., 2008; Dubinin et al., 2014; Yu et al., 2001). SW potential includes both repulsive and attractive parts and easy to solve numerically and hence it is most suitable for different theoretical techniques, such as integral equations or perturbation theories. The SW potential is an extension of hard sphere potential as it retains hard sphere repulsive properties but allows the particles to attract one another and this potential function is defined by

$$\begin{aligned} U^{SW}(r) &= \infty \quad \text{for } r < \sigma \\ U^{SW}(r) &= -\varepsilon \quad \text{for } \sigma \le r \le \lambda\sigma \\ &= 0 \quad \text{for } r > \lambda\sigma \end{aligned} \tag{1.2}$$

where λ and ε are the breadth and depth of the potential well, σ is the radius of the atom.

1.3. PERTURBATION THEORIES

Intermolecular forces generally separate into a harsh short-range repulsion and a long-range smoothly varying attraction. At high density the structure of the liquid is largely determined by geometric packing effects associated with the hard core of the potential. On the other hand, in a first approximation, the attractive forces give rise to a uniform background potential which provides the cohesive energy of the liquid and also affects their structures and associated properties. A further plausible approximation consists in modeling the harsh repulsion is due to the elastic interaction between hard

spheres. This amounts to a relating the properties of a given liquid to those of a hard-sphere "reference system" having equilibrium properties which are well known; the attractive forces can then be treated as a perturbation (Hansen and McDonald, 1976).

The general theory of perturbation treatment was first described by Zwanzig (Zwanzig, 1954) and the reference system is usually taken to be hard sphere system. We consider the positions of N atoms or molecules, as a sum of two terms namely the reference potential, $U_N^{(0)}$ and the perturbing potential, $U_N^{(1)}$. Thus we have

$$U_N = U_N^{(0)} + U_N^{(1)} \tag{1.3}$$

Examining various degrees of freedom, it is necessary to consider the energy contribution in calculating the canonical partition function. The partition function is more generally written in terms of Hamiltonian. The Hamiltonian operator is separated into two parts, one involving only the center of mass i.e. $\hat{H}_{cm}$ and the other involving the intra molecular degrees of freedom i.e $\hat{H}_{int}$, so that the total Hamiltonian $\hat{H}$ is written as

$$\hat{H} = \hat{H}_{cm} + \hat{H}_{int} \tag{1.4}$$

The canonical partition function (Q_T) according to the assumption can be separated and is given as

$$Q_T = \sum_{i,j} \exp\left[-\frac{E_i^{cm} + E_j^{int}}{k_B T}\right]$$

$$= \sum_i \exp\left[-\frac{E_i^{cm}}{k_B T}\right] \quad \sum_j \exp\left[-\frac{E_j^{int}}{k_B T}\right]$$

$$= Q_{cm}(N, V, T) \qquad Q_{int}(N, T) \tag{1.5}$$

Where k_B is the Boltzmann constant, T is the absolute temperature and other symbols have their usual meaning. It is to be noted that the internal degrees of freedom

depend only on the intra-molecular structure (hence effect of vibrational, rotational etc. are to be considered) and is independent of volume or density, whereas, translational degrees of freedom depend on center of mass (cm).

The translational Hamiltonian for the centre of mass $\hat{H}_{cm}$ for the system of 'N' particles in which the potential energy depends only on positions r_1, r_2,……,r_{3N} is given by

$$\hat{H}_{cm} = \sum_i \frac{P_{iX}^2 + P_{iY}^2 + P_{iZ}^2}{2m} + U_N\ (r_1, r_2, \ldots\ldots, r_{3N}) \tag{1.6}$$

P_{ix}, P_{iy}, P_{iz} are the three components of momentum vector P_i.

Assuming that the translational degrees of freedom are evaluated classically, Q_{cm} is given by

$$Q_{cm} = \frac{1}{N!\ h^{3N}} \int\ldots\int \exp\left[-\frac{H_{cm}}{k_B T}\right] dp^{3N}\ldots dr^{3N} \tag{1.7}$$

Substituting the value of H_{cm} from Eqn. (1.7) and integrating we get

$$Q_{cm} = \frac{Z_N}{N!\ \Lambda^{3N}} \tag{1.8}$$

Where

$$\Lambda = \left(\frac{h^2}{2\pi m k_B T}\right)^{1/2}$$

Λ is called thermal de Broglie wave length and

$$Z_N = \int\ldots\int \exp\left[-\frac{U_N}{k_B T}\right] d\bar{r}_1 \ldots d\bar{r}_N \tag{1.9}$$

Here U_N is the potential energy of interaction, which depends on the relative positions of N atoms or molecules. Z_N is called the configurational integral, which is involved in various distribution functions.

Substituting the value of U_N in Eqn. (1.9), the configurational integral, Z_N is obtained. The configurational integral of the hard spheres is given by $Z_N^{(0)}$, which is expressed as

$$Z_N^{(0)} = \int ... \int \exp\left[-\frac{U_N^{(0)}}{k_B T} \right] d\bar{r}_1 ... d\bar{r}_N \tag{1.10}$$

So, $Z_N = Z_N^{(0)} \frac{Z_N}{Z_N^{(0)}}$

$$= Z_N^{(0)} < \exp\left\{ -U_N^{(1)}/k_B T \right\} >_0 \tag{1.11}$$

$< \exp\left\{ -U_N^{(1)}/k_B T \right\} >_0$ indicates a canonical average in the unperturbed system.

1.4. INTEGRAL EQUATIONS AND CORRELATION FUNCTIONS

For simple liquids, which are characterized by spherically symmetric interaction, it is assumed that the force act through the centre of gravity and are pair decomposable i.e total 'N' body configurational energy can be represented as a sum of pair interaction and hence it can be written as

$$U_N(\bar{r}_1, \bar{r}_2 ..... \bar{r}_N) = \sum_{i<j}^{N} U(\bar{r}_{ij}) \tag{1.12}$$

The important four theories involving integral equations are Yvon - Born- Green equation (YBG) theory, the Hyper-netted chain (HNC) theory, the Percus – Yevick (PY) theory and the perturbation theory, which correlate the distribution function with potential function.

The YBG is the simplest of these and least accurate among the rest. The HNC and Percus – Yevick (PY) equations gives the idea of the direct correlation functions (DCF), C(r) which was first introduced by Ornstein and Zernike (OZ) in 1914 in their investigation of density fluctuations near the critical point. The linear response of a

system to a static external field is intimately related to structure factor. In establishing the link between these two we find that a second function appears in natural way; this is the DCF.

The PY (Percus and Yevick, 1957) and HNC (Baxter, 1967) approximation gives expression for C(r) in terms of g(r) and potential function U(r). These are given by

$$\text{PY}: \quad C(r) = g(r)\left[1 - \exp\left\{\frac{U(r)}{k_B T}\right\}\right] \tag{1.13}$$

$$\text{HNC}: \quad C(r) = g(r) - 1 - \ln g(r) - \frac{U(r)}{k_B T} \tag{1.14}$$

The well-known OZ equation involves direct correlation function between two particles which can be shown by following diagram (Hansen and McDonald, 1976)

C(1,2)={the sum of all distinct connected diagrams consisting of two white circles, labeled 1 and 2, black circles and f-bonds, and which are free of connecting circles}. (1.15)

C (1,2) = 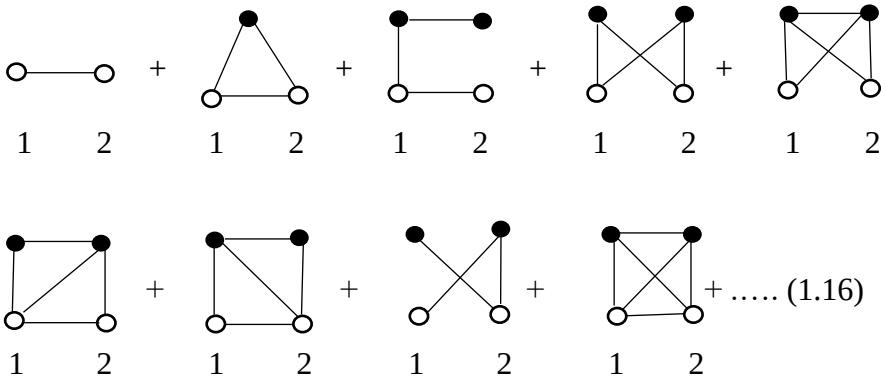

..... (1.16)

And thus OZ equation can be given as

$$h(1,2) = C(1,2) + \int \rho^{(1)}(3) C(1,3) C(3,2)\, d3 + \int\int \rho^{(1)}(3)\rho^{(1)} C(1,3)C(3,4)C(4,2) d3\, d4 + \ldots \tag{1.17}$$

Where h (1, 2) is the total correlation function between the two particles. First part of the right hand side represents the direct correlation between particle 1 and

particle 2, whereas the integral parts are due to various indirect correlations between particle 1 and 2 with many other particles present in the system. Above expression can be represented by the following diagram (Hansen and McDonald, 1976)

h(1,2)={ the sum of all distinct connected chain diagrams composed of black circles and c-bonds, terminated at each end by a white circle, labelled 1 and 2 respectively}. (1.18)

Specifically,

h(1,2) = 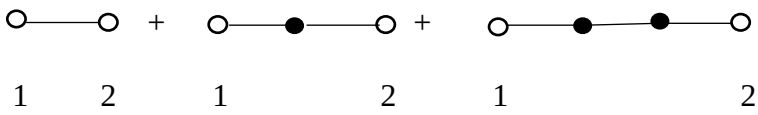 (1.19)

It describe the fact that the total correlation between particles 1 and 2 is due to, in part, the direct correlation function between 1 and 2, but also to the indirect correlation function via an increasing number of intermediate particles, corresponding to the integration variables 3, 4, etc. For a translational invariant and isotropic system the OZ relation becomes

$$h(r) = C(r) + \rho \int C(|r - r'|)\, h(r')\, dr' \tag{1.20}$$

1.5. STRUCTURAL CHARACTERISTICS IN LIQUIDS

The structural information about the liquid state can be obtained by X-ray diffraction technique. In liquid metals and alloys, the individual atoms work as scattering centers and the scattering results are presented as angle dependent scattering intensities, I(θ), where instead of the angle the variable k is used

$$k = \frac{4\pi}{\lambda} \mathrm{Sin}\,(\theta) \tag{1.21}$$

Here 2θ is the scattering angle and λ is the wavelength of the incident beam. The intensity in electron units scattered by a non-crystalline array of atoms at a scattering angle is given by 'Debye's equation'

$$I_{eu}^{coh}(k) = \sum_i \sum_j f_i f_j \frac{\sin kr_{ij}}{kr_{ij}} \tag{1.22}$$

Where f_i and f_j are the atomic scattering factors for the i^{th} and j^{th} atoms respectively, r_{ij} is the magnitude of the vector separating these two atoms. For monatomic liquids $f_i = f_j = f$. The summation in Debye's equation i.e. Eqn. (1.22) should performed at first for the atom at the origin and next extending to all atoms of the liquid specimen over all distances. Summation for the atom at the origin lead to unity, since in the limit as $r_{ij} \to 0$, $(\sin kr_{ij}/ kr_{ij}) \to 1$. If N is the total number of atoms,

$$I_{eu}^{coh}(k) = Nf^2 [1 + \sum_{i'} \frac{\sin kr_{ij}}{kr_{ij}}] \tag{1.23}$$

Where $\sum_{i'}$ excludes the atom at the origin. If it is assumed that there is continuous distribution of atoms, then above summation may be replaced by an integral. If ρ(r) is the density of atoms at distance r from the atom at the origin, then the number of atoms in the spherical shell of radius r and thickness dr is $4\pi r^2 \rho(r) dr$, then Eqn. (1.23) can be written as

$$I_{eu}^{coh}(k) = Nf^2 [1 + \int_0^\infty 4\pi r^2 \rho(r) \frac{\sin kr_{ij}}{kr_{ij}} dr] \tag{1.24}$$

If we take ρ as the constant average density of atoms, then Eqn. (1.24) can be written as

$$I_{eu}^{coh}(k) = Nf^2 [1 + \int_0^\infty 4\pi r^2 [\rho(r) - \rho] \frac{\sin kr_{ij}}{kr_{ij}} dr] + \int_0^\infty 4\pi r^2 \rho \frac{\sin kr_{ij}}{kr_{ij}} dr \tag{1.25}$$

The second integral is negligible since it corresponds to forward scattering (Clark, 1989). Hence Eqn. (1.25) can be written as

$$I_{eu}^{coh}(k) = Nf^{2}[1 + \int_{0}^{\infty} 4\pi r^{2}[\rho(r) - \rho]\frac{\sin kr_{ij}}{kr_{ij}} dr] \tag{1.26}$$

The structure factor of a liquid S(k), which is the autocorrelation function of the Fourier components of density of particles is defined as

$$S(k) = \frac{I_{eu}^{coh}(k)}{Nf^{2}} \tag{1.27}$$

So that,

$$\begin{aligned} S(k) &= 1 + \int_{0}^{\infty} 4\pi r^{2}[\rho(r) - \rho]\frac{\sin kr_{ij}}{kr_{ij}} dr \\ &= 1 + \int_{0}^{\infty} 4\pi r^{2}[g(r) - 1]\rho\frac{\sin kr_{ij}}{kr_{ij}} dr \end{aligned} \tag{1.28}$$

1.6. PAIR DISTRIBUTION FUNCTION (RADIAL DISTRIBUTION FUNCTION)

Radial distribution function is used to describe the probability of finding a particle (atom, molecule or ion) at a distance r if a particle is placed at the origin.

Equilibrium probability densities and distribution functions allow a complete but compact description of the microscopic structure of liquids and fluids, as well as providing a quantitative measure of the correlations between the positions of different particles. Further, more knowledge of the lowest order distribution function is generally sufficient to calculate most equilibrium properties of the system.

The normalized canonical probability density for a system of N identical particles can be taken as (Mc. Quarrie, 1976; Rice and Gray, 1963; Ross, 1956)

$$f_O^{(N)}(r^N, p^N) = \left(\frac{\Lambda}{h}\right)^{3N} \exp[-\beta K_N(p^N)] \frac{\exp[-\beta V_N(r^N)]}{Z_N(V,T)} \tag{1.29}$$

Where Λ is again the de Broglie wavelength and $K_N(P^N)$ is the kinetic energy term. The probability density factorizes into 3N independent Maxwellian distributions density for the components of the momenta of particles, and into a probability density for the coordinates which does not separate in general because of correlations between the positions of particles. We therefore define (Mc. Quarrie, 1976; Rice and Gray, 1963; Ross, 1956)

$$P_N^{(N)}(r_1,....,r_N)dr_1...dr_N = \frac{1}{Z_N} \exp[-\beta V_N(r_1,...,r_N)]\, dr_1....dr_N \tag{1.30}$$

as the probability of simultaneously finding particle 1 in a volume dr_1 around r_1, particle 2 in dr_2 around r_2, etc.

The n-body probability density $P_N^{(n)}$ is obtained from $P_N^{(N)}$ by integrating over the coordinates of the remaining N – n particles:

$$P_N^{(n)}(r_1,....,r_n) = \int ... \int P_N^{(N)}(r_1,....,r_N)\, dr_{n+1}....dr_N \tag{1.31}$$

As the mutual distances between the n particles increase, the correlations between their positions are expected to decrease. Consequently, in the limit $|r_i - r_j| \to \infty$ for all $1 \leq i, j \leq n$, the n-particle probability density will factorize into the product of n single-particle probability densities:

$$P_N^{(n)}(r_1,....,r_n) \simeq P_N^{(N)}(r_1).....P_N^{(1)}(r_n) \tag{1.32}$$

In this limit the position of each of the n particles is independent of the positions of the remaining n-1 particles. Advantage can be taken of the resulting factorization to define the n-particle distribution functions:

$$g_N^{(n)}(r_1,....,r_n) = \frac{P_N^{(N)}(r_1,...r_n)}{\prod_{i=1}^{n} P_N^{(1)}(r_i)} \tag{1.33}$$

We see that $g_N^{(n)}(r^n) \to 1$ for all n as the mutual distances between the n particles increase indefinitely. Strictly speaking the limit of infinite mutual distances makes sense only in the thermodynamic limit.

Here N is the total no's of particle in the system. n-particle correlation function can be given as

$$g^{(n)}(\bar{r}_1, \bar{r}_2.....\bar{r}_n) = \frac{1}{\rho^n} \rho^{(n)}(\bar{r}_1, \bar{r}_2.....\bar{r}_n) \tag{1.34}$$

Here ρ is the number density.

At this juncture, it is worth to mention that two particles correlation function $g^{(2)}(\bar{r}_1, \bar{r}_2)$ plays a very important role in understanding liquid state properties. Two particles correlation function is designated as pair distribution function g(r).

(1) There is zero probability of the two particles occupying the same space, hence g(r) at r = 0 is zero.

(2) At a distance r_0, which is the minimum of the potential energy curve between two particles, there is maximum probability of finding a particle and hence g(r) is expected to be maximum as a first approximation.

(3) As $r \to \infty$, there is no long – range order, and so $g(r) \to 1$.

(4) g(r) multiplies with number density gives local density ρ(r).

(5) The Fourier inverse of g(r) gives structure factor, S(k) in momentum space (k-space).

1.7. CORRELATION FUNCTIONS IN BINARY ALLOYS

In a binary alloy the scattering function depends upon, in general, three independent partial structure factors (PSFs), $S_{ij}(k)$ (Keating, 1963), which are Faber-Ziman (FZ) and Ashcroft-Langreth (AL) type partial structure factors (Mishra and Venkatesh, 2008). The pair correlation functions and potential parameters contribute mainly to describe the structure of alloys (Mishra and Venkatesh, 2008; Echendua et al., 2010; Gonz'alez and Gondz'alez, 2008). Thus, PSFs can be defined for a binary mixture as

$$S_{ij}(k) = \delta_{ij} + 4\pi\pi(_i\rho_j)^{1/2} \int_0^\infty \left[g_{ij}(r) - 1\right] r^2 j_0(r) dr \tag{1.35}$$

Here $j_0(r)$ is a spherical Bessel function of the zeroth order, δ_{ij} is the kronecker delta and it is defined as

$$\delta_{ij} = \begin{Bmatrix} 1 & \text{for} & i = j \\ 0 & \text{for} & i \neq j \end{Bmatrix} \tag{1.36}$$

Hence in a binary system in principle three partial structure factors are $S_{11}(k)$, $S_{22}(k)$ and $S_{12}(k)$. These $S_{ij}(k)$ are related to partial pair distribution function $g_{ij}(r)$ which give the probability that a particle of species i is at a distance r from one of the particle of a species j in a binary alloy.

$$g_{ij}(r) - 1 = \frac{1}{2\pi^2(\rho_i\rho_j)^{1/2}} \int_0^\infty \left[S_{ij}(k) - \delta_{ij}\right] k \sin(kr) dr \tag{1.37}$$

Keating (Keating, 1963) observed that by varying the scattering factor of two components, f_i and f_j, say by isotopic substitution, without altering the structure, it is possible to obtained three different curves for S(k), corresponding to three different values for the ratio f_1/f_2 and thus it is possible to evaluate $S_{11}(k)$, $S_{22}(k)$ and $S_{12}(k)$ by

solving three simultaneous equations for each value of k with assumption $S_{12}(k)= S_{21}(k)$.

The change in electrical resistivity on alloying is also available as an indicator of the variation of concentration, if the relation between concentration and resistivity is accurately known. Krishnan and Bhatia (Krishnan and Bhatia, 1944) pointed out that the temperature dependence of resistivity of an alloy is due to the corresponding temperature dependence of the concentration fluctuation in that alloy. Bhatia and Thornton (BT) (Bhatia and Thornton, 1970) generalized the above fluctuation approach and made it applicable at shorter wavelength and low temperatures also. Under the weak scattering approximation they defined three more correlation functions which are thermodynamically important and they are

(1) the particle density or number density or number-number correlation function, $S_{NN}(k)$

(2) the concentration-concentration correlation function (i.e. total concentration as in mole fraction), $S_{CC}(k)$

(3) the cross correlation between number and composition, the number-concentration correlation function, $S_{NC}(k)$

Further, to understand the mixing behavior of two elemental metals forming a binary alloy has always been a subject of considerable interest to physicist, chemist and metallurgist (Singh and Somer, 1997).

BT correlation functions have proved to be of great physical significance as they furnish important structural information about α', the chemical short-range order parameter (CSRO) in the system. Bhatia - Thornton fluctuations are linearly related to PSFs (AL or FZ) and can be presented as

$$\begin{bmatrix} S_{NN}(k) \\ S_{NC}(k) \\ S_{CC}(k) \end{bmatrix} = \begin{bmatrix} C_1 & C_2 & 2(C_1C_2)^{1/2} \\ C_1C_2 & -C_1C_2 & (C_2 - C_1)(C_1C_2)^{1/2} \\ C_1{C_2}^2 & {C_1}^2C_2 & -2(C_1C_2)^{1/2} \end{bmatrix} \begin{bmatrix} S_{i-i}(k) \\ S_{j-j}(k) \\ S_{i-j}(k) \end{bmatrix} \quad (1.38)$$

1.8. DIFFUSION, SURFACE AND SCALING PROPERTIES

Knowledge of diffusion in liquid state is very important for understanding the material processing and metallurgy. However, the experimental determination of the diffusivity in liquid state is difficult because it is not fully understood that how the diffusion coefficient depends on the structure and thermodynamics of the liquids as it can be understood in non-crystalline solids.

The diffusion coefficients of liquid metals have been evaluated from the well-known Einstein's formula of self-diffusion coefficient, $D\,(D = \frac{k_B T}{\xi})$ using the square well potential parameters. The friction coefficient, ξ is the sum of ξ_H, ξ_S and ξ_{SH}. Here ξ_H, ξ_S and ξ_{SH} are the friction coefficients due to hard part, soft part and soft-hard part respectively. These friction coefficients were computed on the basis of Helfand-Rice-Nachtrieb approach (Shimoji and Itami, 1986) using square well potential as soft part of the inter particle pair potential.

Friction coefficients were obtained by solving the following equations in repulsive and attractive regions of a square well potential (Venkatesh et al., 2003).

$$\xi = \frac{1}{3k_B T}\left[\int_0^t ds\langle F_H(t)F_H(t+s)\rangle + \left\{\int_0^t ds\langle F_S(t)F_S(t+s)\rangle + \int_0^t ds\langle F_S(t)F_H(t+s)\rangle\right\}\right] \quad (1.39)$$

Here F_H and F_S are the forces due to hard-core and soft-force.

Further, self-diffusion coefficients and mutual diffusion coefficients in binary liquids (Al-Cu and Ag-Cu) were computed by extending the Einstein's equation

$(D = \frac{k_B T}{\xi_i})$ for binary alloys. Here ξ_i is the friction coefficient due to i^{th} particle in a binary mixture.

The study of the relationship between structure and dynamics of metallic liquids is of major importance since their coupling governs different processes such as nucleation, crystal growth and glass transition (Pasturel and Jakse, 2015) and thus finding a correlation between them becomes a challenging task in condensed matter research. For this reason considerable attention has been paid on such problems by many workers. The relation between structure and dynamic properties using square well potential have been reported (Gopala Rao and Venkatesh, 1989; Venkatesh et al., 2003; Venkatesh and Mishra, 2005; Dubinin et al., 2009; Yu et al., 2001). The correlation between self-diffusion coefficients and their surface tension has also been studied by many authors with different approaches (Lu et al., 2005; Blairs, 2006). Lu et al. reported that the surface tension values are not well known experimentally even for many simple liquid metals (Lu et al., 2005).

A new correlation between surface tension and diffusion coefficient was established by incorporating modified Stokes - Einstein relation for square well potential with statistical mechanical expressions for surface tension and viscosity.

Surface entropy in considered liquids was also determined through temperature derivative of diffusion coefficients. Computed results were compared with available experimental data which gives us confidence in our square well calculations.

Dzugutov introduced a new universal scaling law relating the diffusion coefficients and the excess entropy of a liquid (Dzugutov, 1996). This information advances our knowledge of liquid transport properties. Recently many workers examined the scaling law proposed by Dzugutov (Dzugutov, 1996) for liquid metals

and binary liquid mixtures by *ab initio* molecular dynamic simulations (Jakse and Pasturel, 2015; Jakse and Pasturel, 2016; Hoyt et al., 2000; Samantha et al., 2004; Li et al., 2005) using embedded atom method (EAM). This study provides a relationship between the dynamic properties with microscopic static structural functions and with static thermodynamic quantity, S, entropy.

Thus one of the objectives of this thesis is to test the Dzugutov idea by computing the excess entropies for several liquids through a square well model of pair correlation functions and diffusion coefficients using atomistic scale computing.

1.9. SCOPE OF THE STUDY

When we know the properties of a material, we can know their applicability. So to evaluate various properties of the liquid metals and alloys we used SW model to compute the microscopic property structure factor and coordination number in liquid metals and liquid binary alloys. The computed structural functions were successfully employed in the same system for computing diffusion coefficients, surface tension, surface entropy, shear viscosity.

Recently developed universal scaling law, which correlates diffusion coefficient with excess entropy in real fluids, was tested for the considered systems. The scaling law study can predict correctly the diffusivity of pure fluids as well as binary fluid mixtures over a wide range of densities.

The study on structural, dynamical and surface properties of liquid metals and alloys helps in various metallurgical, industrial, material processing technologies and also help their study in solid state.

The structure of liquids is described by means of the correlation functions called the structure factor, which is shown to play an important role to obtain both equilibrium and non-equilibrium properties. Such liquid metals and alloys (Al-Cu and Ag-Cu) will be investigated through proposed model for which experimental results will be available, so that, we may compare theoretical calculations with experimental results.

At this juncture it is worth to mention that all structural and associated properties of binary alloys are to be evaluated using potential parameters of pure components.

2. STRUCTURE AND TRANSPORT PROPERTIES OF LIQUID METALS

2.1. INTRODUCTION

The auto correlation function, S(k) (where $k=(4\pi/\lambda)Sin\theta$) and its Fourier component g(r), pair correlation function (PCF) are most prominent quantities to characterize the structure of a liquid. Experimentally these quantities have been determined using neutron or X-rays scattering intensities. PCF is obtained by Fourier analysis of experimental S(k), which is a laborious and costly procedure. The analysis of results on structure and thermodynamic properties of liquid metals and alloys enable us to understand their structural ordering and complexities (Mishra and Venkatesh, 2008; Wax et al., 2000; Li et al., 2003; Lai et al., 1990). Hence, a detailed knowledge of the S(k) and g(r) is essential for a quantitative understanding of the structure of liquids and also sufficient to determine numerous other equilibrium and transport properties (Lai et al., 1990; Stadler et al., 1999; Balucani et al., 1993; Herrera et al., 1999).

The subject of statistical mechanics has been successfully applied in various fields including the prediction of the microscopic function, S(k) of liquid metals (Gopala Rao andVenkatesh, 1989; Gosh et al., 2007; Taylor et al., 2001). Wertheim (Wertheim, 1963) and Thiele (Thiele, 1963) (WT) solved Percus - Yevick's (PY) equation for hard sphere fluids to obtain the hard sphere direct correlation function $C_{hs}(r)$. Liquid metals static structure factors behave like hard sphere fluids and calculations for thermo-physical and thermodynamic properties with such reference system have been found to be reasonable in many cases (Zalid et al., 1999). However, we believe with other researchers that hard sphere reference system lacks realistic

properties because thermodynamics and the relation between thermodynamics with S(k)or g(r) are different for hard sphere and real fluids (Ravi et al., 2001; Venkatesh et al., 2005). Hence, it is important to include attraction between the particles in deriving structure factor of liquids. It must be mentioned that the hard sphere repulsive forces act up to a short – range and primarily determine the structure peak of a liquid and the relatively long - range uniform attractive part of the potential brings atoms in short – range order. Further, it is pointed out that the success of any theoretical model depends on its experimental confirmation (Prakash et al., 2004; Boulahbak et al., 1998). Thus in the present work the square-well (SW) attractive tail has been perturbed over Wertheim and Thiele (Wertheim, 1963; Thiele, 1963) solutions for hard sphere mixture to evaluate the direct correlation function C(k) in momentum space in order to compute S(k) of real liquids. The analytical solution of this model in the mean spherical model approximation (MSMA) was introduced by Rao and Murthy (Gopala Rao and Murthy, 1974; Gopala Rao and Murthy, 1975; Gopala Rao and Murthy, 1975). The model is applied to set of liquid metals to obtain microscopic structural characteristics with their application in the determination of various properties of the considered liquid metals.

The SW fluid is the simplest one possessing the basic characteristics of real fluids. It is an excellent model (Yu et al., 2001; Mishra and Venkatesh, 2008; Glazov and Aivazov, 1980; Li and Gong, 2004; Rah and Eu, 2002; Xin et al., 2001) for liquids in which internal degrees of freedom of individual particles are important. Here we considered that pair wise potential plays a significant role and multi-particle interactions do not play a major role.

The SW potential has been successfully applied for metallic liquids (Gopala Rao and Murthy, 1974; Gopala Rao and Murthy, 1975; Venkatesh and Mishra, 2005), colloidal particles (Asherie et al., 1996; Noro and Frenkel, 2000), hetro-chain molecules

(Zaccarelli, et al., 2001; Cui and Elliot, 2001) and complex systems (Zhou et al., 2002; Zhou et al., 1997).

Here we consider that the multi-particle interactions are due to the sum of pair wise interactions.

Transport coefficients such as diffusion and viscosity coefficients are important quantities not only for chemical engineer and chemist but also for life scientist, environmental administrators and workers in many other fields. Diffusion is involved in the efficiency of mass transfer equipment, the dispersion of pollutants, the dyeing of wool and the transport phenomena in living cells (Fei, W., Bart, H.J., 1998). Several authors have reported self-diffusion coefficients for real dense fluids interacting with hard sphere (HS) (Dymond, 1985; Speedy, 1987), Lennard - Jones (LJ) (Liu et al., 1998; Speedy et al., 1989; Yu and Gao, 1999) and Square-well (SW) (Liu et al., 1998; Yu et al., 2000; Venkatesh and Mishra, 2005). The viscosity parameter of liquids dictates their critical cooling rates for glass transition. On the other hand, it is not fully understand how they depend on structure and thermodynamic properties of liquid as well (Sonvane et al., 2012)

The study of coordination number, diffusion coefficient and viscosity of liquid metals is of fundamental importance and the better understanding of these properties is helpful in material processing technology. Coordination number of liquid metals is determined by integrating g(r) functions between first two minima. The shear viscosity, η_v is obtained by replacing the hydrodynamic radius in the Stokes - Einstein relation by the first peak position of g(r) and computed values of diffusion coefficients, D. To the best of our knowledge the limited work is available for η_v calculation of liquids metals and alloys. These are important dynamic properties which decide cooling rate of a liquid and these two governs the dynamics in fluids. While viscosity describes the

macroscopic transport of momentum by the collective motion of particles, atomic diffusion describes single-particle diffusive transport (Brilo et al., 2011).

2.2. THEORY

2.2.1. EVALUATION OF STATIC STRUCTURE FACTOR AND COORDINATION NUMBER

The SW is an extension of hard sphere potential as it retains hard sphere repulsive properties but allows the particles to attract one another and the interaction energy U(r) between two square well particles separated by a distance r is given by

$$\beta U(r) = \begin{cases} \infty & ; \quad r < \sigma \\ -\varepsilon & ; \quad \sigma < r < \lambda\sigma \\ 0 & ; \quad r > \lambda\sigma \end{cases} \tag{2.1}$$

where σ is the hard core diameter, σ (λ-1) and ε (<0) are the breadth and depth of the potential well, $\beta = 1/ k_B T$.

An important model system is the MSMA and was first proposed by Lebowitz and Percus (Lebowitz and Percus, 1966) which expressed g(r) and the direct correlation function C(r) as

$$\left.\begin{aligned} g(r) &= 0 && ; \quad r < \sigma \\ C(r) &= -U(r) / k_B T && ; \quad r > \sigma \end{aligned}\right\} \tag{2.2}$$

The Ornstein-Zernike direct correlation function (DCF) of one component liquid using the SW model in momentum space under MSMA can be written as

$$C(k) = C_{hs}(k) + C_{sw}(k). \tag{2.3}$$

with

$$\rho C_{hS}(k) = -[24\eta/(x)^6][\alpha(x)^3\{\sin(x\sigma x - x\cos(x)\} + \beta(x)^2 \{2x\sin(x) - (x^2-2)\cos x - 2\} + \gamma\{(4x^3 - 24x)\sin(x) - (x^4 - 12x^2 + 24)\cos x - 24\}]. \quad (2.4)$$

$$\rho C_{SW}(k) = [24\eta\varepsilon/k_B T]\ (x)^3\ [\sin(\lambda x) - \lambda x\cos(\lambda x) + x\cos(x) - \sin(x)]. \quad (2.5)$$

where x= kσ, ρ is the number density, ε and λ represent depth and breadth respectively, of the square well and the other terms that enter in Eqn. (2.4) are given by following expressions (Block et al., 1977).

$$\alpha = \frac{(1+2\eta)^2}{(1-\eta)^4} \quad (2.6)$$

$$\beta = -\frac{6\eta\,(1+\eta/2)^2}{(1-\eta)^4} \quad (2.7)$$

$$\gamma = \frac{\eta\alpha}{2} \quad (2.8)$$

where η is called packing fraction i.e. volume occupied by the atoms divided by total volume and is given by

$$\eta = \frac{\pi\rho\sigma^3}{6}. \quad (2.9)$$

The S(k) of one component liquid can be given in terms of C(k) as

$$S(k) = [1 - \rho C(k)]^{-1}. \quad (2.10)$$

The Fourier inversion of S(k) gives the radial distribution function, g(r).

$$g(r) = 1 + \frac{1}{2\pi^2\rho}\int_0^\infty k^2[S(k)-1]\frac{\sin(kr_{ij})}{kr_{ij}}dk. \quad (2.11)$$

Experimentally obtained g(r) provides limited information about the short range order of liquids but the nearest-neighbor coordination number,ψ, which can be obtained by integrating the g(r) function between the first two minimum i.e. the left edge of the first peak to the first minimum on the right hand side of the first peak, r_{min}. ψ

characterizes several types of short - range order present in the liquids. The microstructure of liquids can also be characterized by ψ.

$$\psi = 4\pi\rho \int_0^{r_{min}} g(r)\ r^2\ dr. \tag{2.12}$$

Here r_{min} is the first minimum of the radial distribution function.

2.2.2. EVALUATION OF DIFFUSION COEFFICIENTS AND VISCOSITY OF LIQUID METALS

The self-diffusion coefficients of all the concerned liquid metals is derived using well known Einstein's formula $D = \dfrac{k_B T}{\xi_H + \xi_S + \xi_{HS}}$. Here ξ_H, ξ_S and ξ_{HS} are the friction coefficients due to hard, soft and hard-soft part of the potential function respectively. In evaluating the ξ and in handling the soft potential contribution to kinetic equations we introduced the Helfand's Linear Trajectory Principle (Davis and Polyvos, 1966). This principle is used to calculate time integral of auto correlation function by replacing the actual trajectories of the interacting molecules with linear trajectories. Here particle is assumed to move along a linear trajectory without acceleration during the times affected by soft potentials of the remaining particles. Thus the inter-particle pair potential is separated into two parts i.e, $U(r) = U^H(r) + U^S(r)$ with

$$\begin{aligned} U^H(r) &= \infty, \quad r < \sigma \\ &= 0, \quad r > \sigma \end{aligned} \tag{2.13}$$

and

$$\begin{aligned} U^S(r) &= 0, \quad r < \sigma \\ &= U(r), \quad r > \sigma \end{aligned} \tag{2.14}$$

Accordingly the force may be divided into two terms, F_H a hard core contribution and F_S, a soft force, and one can write friction coefficient in the form as follows

$$\xi = \frac{1}{3k_B T}\left[\int_0^t ds\langle F_H(t)F_H(t+s)\rangle + \left\{\int_0^t ds\langle F_S(t)F_S(t+s)\rangle + \int_0^t ds\langle F_S(t)F_H(t+s)\rangle\right\}\right] \tag{2.15}$$

$$= \xi_H + \xi_S + \xi_{SH} \tag{2.16}$$

F(t) being the molecular force on a particle at time t and F(t+s) at time t+s.

$$\xi_H = \frac{8}{3}\rho\sigma^2(\pi m k_B T)^{1/2} g^{HS}(\sigma) \tag{2.17}$$

$$\xi_S = -\frac{1}{3}\frac{\rho}{4\pi^2}\left(\frac{\pi m}{k_B T}\right)^{1/2}\int_0^\infty \frac{1}{\rho} k^3 U^{SW}(k)[S(k)-1]dk. \tag{2.18}$$

$$\xi_{HS} = -\frac{1}{3}\rho g^{HS}(\sigma)\left(\frac{m}{\pi k_B T}\right)^{1/2} \times \int_0^\infty [k\sigma\cos(k\sigma) - \sin(k\sigma)]\, U^{SW}(k)dk. \tag{2.19}$$

Here $U^{SW}(k)$ is the Fourier transform of SW potential

$$U^{SW}(k) = \frac{4\pi\varepsilon}{k^3}[Ak\sigma\cos(Ak\sigma) - \sin(Ak\sigma) - k\sigma\cos(k\sigma) + \sin(k\sigma)] \tag{2.20}$$

The shear viscosity coefficient, η_v is obtained under the SW model with the Stokes - Einstein relation

$$\eta_v = \frac{k_B T}{2\pi r_{max} D} \tag{2.21}$$

Where k_B is the Boltzmann's constant, r_{max} is the first peak position of g(r) and D is the diffusion coefficient.

2.3. RESULTS AND DISCUSSION

The WT solution of PY hard sphere fluid within the MSMA with SW perturbation can be solved numerically with the input data: temperature, T, atomic density, ρ, and the SW parameters. The molar volumes of pure liquid metals given by Singh and Sommer (Singh and Somer, 1997) and hence the number density could be calculated. The input parameters of liquid metals were given by Rao and Murthy (Gopala Rao and Murthy, 1975) and were listed in Table 2.1.

TABLE 2.1. Input parameters of liquid metals with σ as the diameter, ε/k_B as the depth, λ as the breath of the square well potential and ρ as the number density.

Metals	Temperature (K)	σ (Å)	ε/k_B(K)	λ(Å)	ρ (10^{25} m^{-3})
Sodium	378	3.30	111.60	1.65	2430
Potassium	343	4.11	96.14	1.65	1276
Cesium	303	4.81	109.5	1.70	0813
Magnesium	953	2.75	127.82	1.43	3900
Aluminum	943	2.45	160.00	1.30	6459
Indium	433	2.83	173.76	1.70	3686
Lead	613	2.97	70.00	1.4	3099
Silver	1273	2.60	500.00	1.75	5159
Copper	1423	2.25	300.00	1.68	7408
Gold	1373	2.60	600.00	1.73	5271

The first peak position of g(r) and S(k) are of considerable interest (Kalidoss and Ravi, 2002). The first peak positions and peak heights of the computed S(k) and g(r)for

all the considered liquid metals were presented in Table 2.2 with their experimental data (Waseda, 1980), which give the detailed information regarding the principal peak and structural characteristics of the metals. It can be seen from Table 2.2 that the agreement between our computed S(k) and the experimental results (Waseda, 1980) around the first peak appears to be very good. But in the case of Cs, Ag and Cu the peak heights from the calculation were slightly lower than that from the experiment but the peak positions were same. It is pointed out that the principal peak dominates in evaluating transport properties of real liquids. Similar trend was observed by Rao and Murthy (Gopala Rao and Murthy, 1974; Gopala Rao and Murthy, 1975; Gopala Rao and Murthy, 1975) while calculating S(k) for four liquid metals using the SW model under the random phase approximation. The difference in peak heights for these three metals may be due to existence of some small atomic cluster in these liquids which is not signifying by this model. However, other properties obtained with the same parameter were in fair agreement with the experimental values.

TABLE 2.2. Theoretical and experimental values of first positions (k) and peak heights S(k); first peak positions (r) and peak heights g(r) of liquid metals.

Metals	First Peak of S(k)				First Peak position g(r)			
	Theoretical		Experimental		Theoretical		Experimental	
	k ($Å^{-1}$)	S(k)	k ($Å^{-1}$)	S(k)	r (Å)	g(r)	r (Å)	g(r)
Na	2.0	2.7	2.0	2.7	3.6	3.24	3.7	2.42
K	1.6	2.6	1.6	2.6	4.5	2.80	4.6	2.35
Cs	1.4	2.5	1.4	2.7	5.0	3.61	5.1	2.58
Mg	2.5	2.5	2.4	2.5	2.9	2.84	3.1	2.46
Al	2.7	2.4	2.7	2.4	2.7	2.47	2.8	2.83
In	2.3	2.4	2.3	2.5	3.0	2.64	3.1	2.66
Pb	2.3	2.5	2.3	2.5	3.2	2.37	3.2	2.98
Ag	2.6	2.3	2.6	2.5	2.8	2.98	2.8	2.58
Cu	3.0	2.4	3.0	2.7	2.5	2.35	2.5	2.75
Au	2.6	2.4	2.6	2.5	2.8	2.68	2.8	2.77

The calculated results for S(k) of these metals at their respective temperatures along with their experimental results in the entire momentum space were depicted in Fig. 2.1. The agreement between the computed results and the experimental results (Waseda, 1980) is good throughout the k regions. It can be seen from Fig. 2.1 that structure factors of all the considered metals become constant around one in high k region. It shows the presence of short range order in liquid materials. Further, it may be noted that the simulation result with different approaches (Waxet al., 2000; Herrera et al., 1999; Boulahbak et al., 1998) for the peak height and position of S(k) of number of

liquid metals did not agree well with experiment. However, *ab initio* molecular dynamic simulation for the study of the structure and dynamic properties of liquids has been widely considered by research community (Dahlborg et al., 2013).

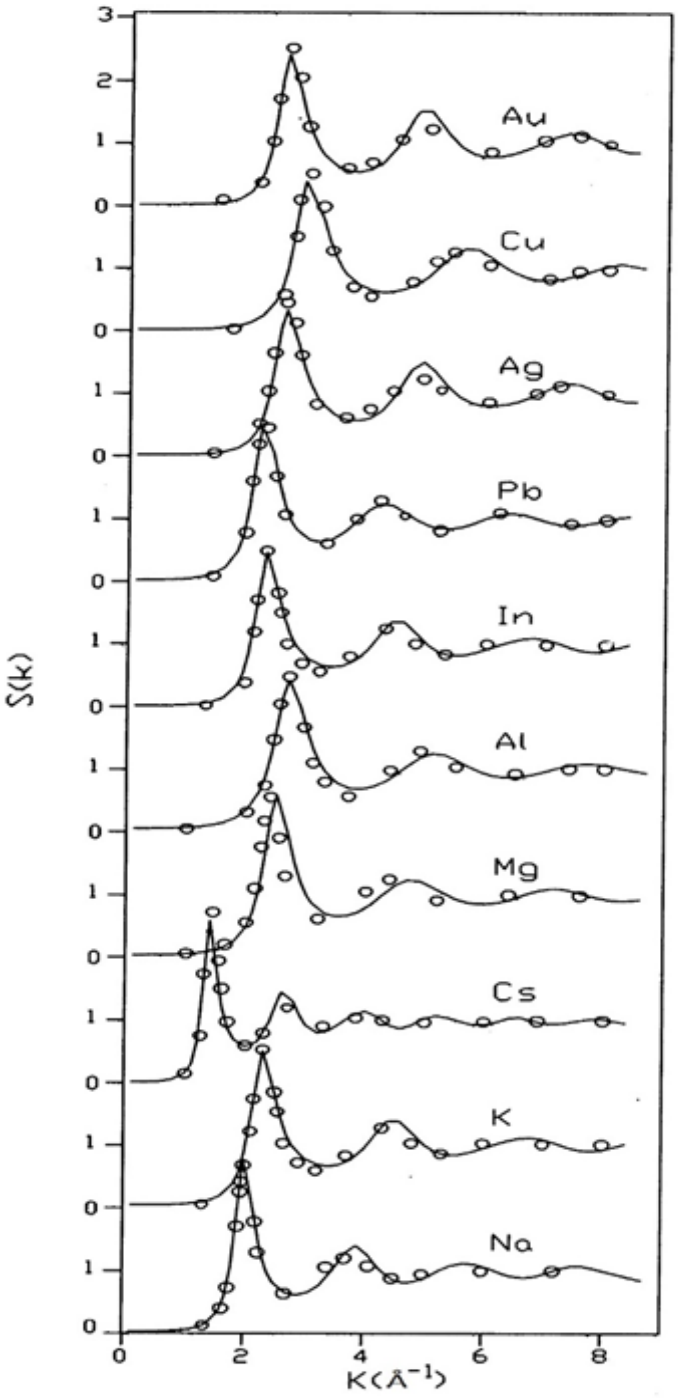

Fig. 2.1. S(k) against k for liquid metals; (——) present calculated results, (o o o) experimental results.

The peak positions and peak heights of the g(r), computed from Eqn. (2.11), for all the considered metals along with their experimental values (Waseda, 1980) were listed in Table 2.2 and also presented in Fig. 2.2(a) and Fig. 2.2(b). The ratio of the positions of the first and second peaks of the calculated and the experimental g(r) for all the liquids taken under investigation is about 0.51 and 0.53 respectively. This suggests that the model calculation of g(r) gives the structural properties of real liquids fairly well.

Computed results for g(r) were compared with the available experimental results and presented in Figs. 2.2(a) and 2.2(b). There is a good agreement between theoretical values and experimental values (Waseda, 1980).

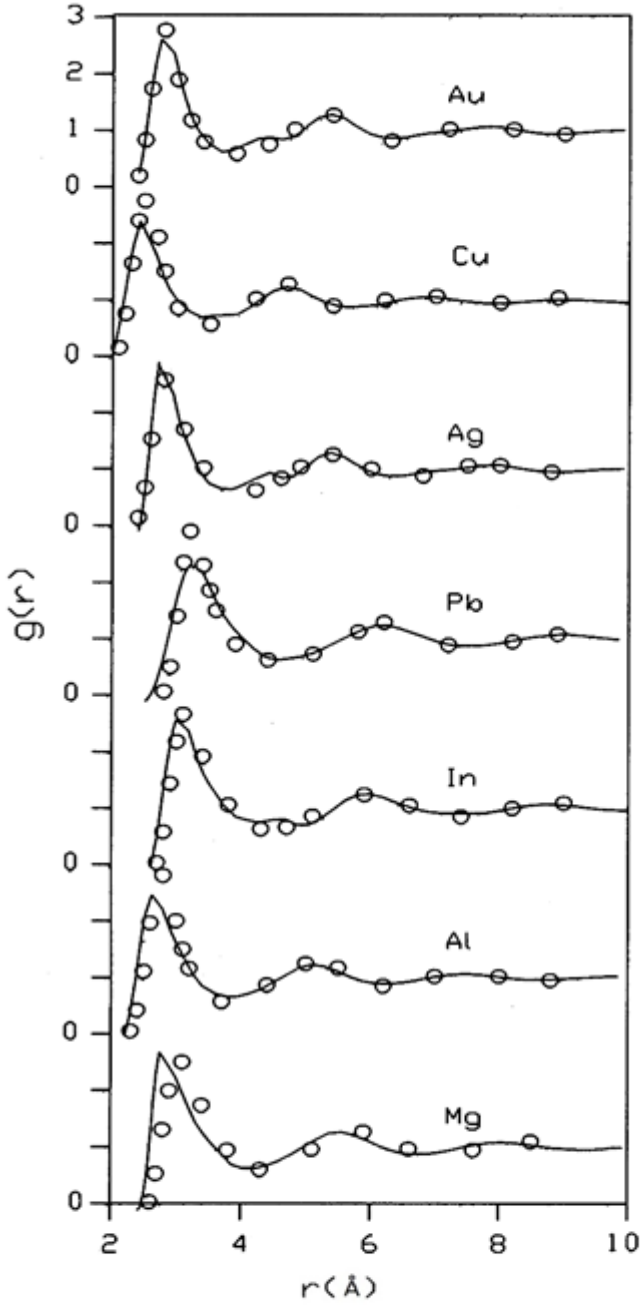

Fig. 2.2(a). g(r) against r for liquid metals; (——) presents calculated results. (o o o)experimental results.

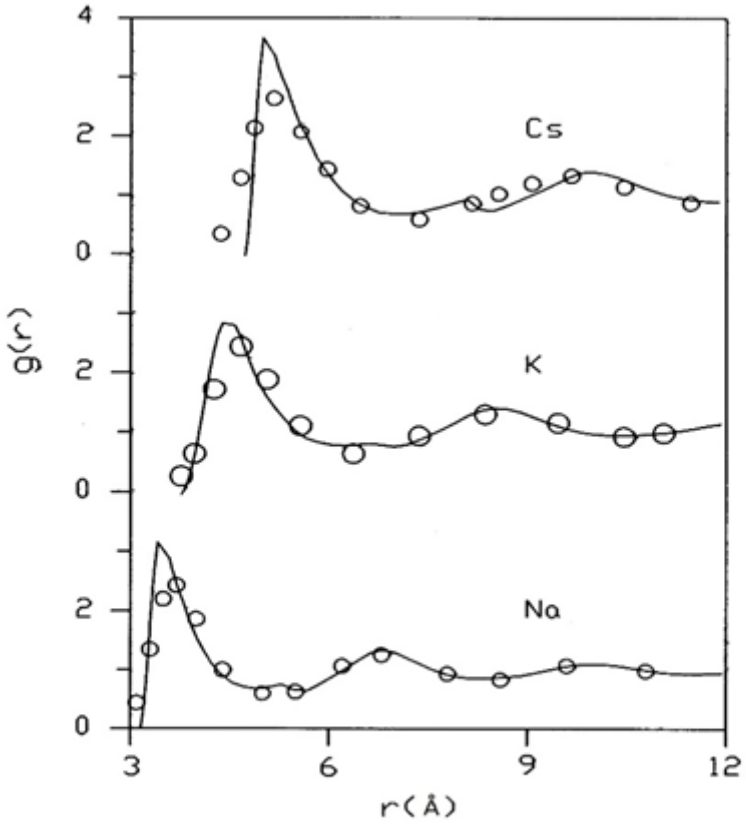

Fig. 2.2(b). g(r) against r for liquid metals; (——) presents calculated results, (o o o) experimental results.

The computed g(r) were used for determination of short range order parameters such as the shortest atomic distance, first peak position in g(r) and the first coordination cell. The knowledge of the distance between the nearest neighbor atoms in crystalline and liquid phases of a metal helps in understanding the mechanism of crystal lattice destruction during the melting (Zhakova and Afanayeva, 2008). Further it is pointed out that the first maximum cannot give the detailed representation of the inside structure of the first atomic coordination shell.

The deviation of g(r) from unity is a measure of the local order around the reference atoms. There are few maxima and minima in the g(r) which rapidly damped

around unity, where the first maximum corresponds to the position of the nearest neighbors around an origin atom.

The nearest-neighbor distance, a, and the first coordination numbers (ψ) were obtained by using Eqn. (2.12), for liquid metals and the computed values are presented with their corresponding experimental results (Tao, 2005) in Table 2.3. In all cases the first peak and first minimum lie between σ to $\lambda\sigma$. The computed values of ψ for the considered metals lie between 10.3 and 11.4 and that of the experimental values lie between 10.4 and 11.6. It is worth to mention here that the variation in values of ψ even for simple liquids depends on the theoretical approach of the computation (Tao, 2005). Detailed study of the first cell coordination number in liquid and crystalline form of the metals helps to understand the local structure in two phases (Li et al., 2003). ψ of liquid metals is also an important parameter that influences many of the properties of liquid metals such as density, viscosity and diffusivity (Cahoon, 2004).

TABLE 2.3. First minimum position of computed g(r); theoretical and experimental values of first coordination number (ψ) of liquid metals.

Metals	First minimum position of g(r)	$\psi_{Computed}$	$\psi_{Experimental}$
Na	4.9	10.5	10.4
K	6.2	10.8	10.5
Cs	7.0	11.4	-
Mg	4.2	10.2	10.9
Al	3.9	11.2	11.5
In	4.3	11.4	11.6
Pb	4.5	10.5	10.9
Ag	3.8	10.6	11.3
Cu	3.4	10.7	11.3
Au	3.7	10.3	10.9
		Average =10.7	11.03

$$\text{Average percentage deviation} = \frac{(\psi\text{average})\text{computed} - (\psi\text{average})\text{experimental}}{(\psi\text{average})\text{computed}} \times 100$$

Table 2.3 illustrates that the computed values of ψ are in good agreement with the experimental data. The computed average ψ of the ten liquid metals is 10.76 which is closed to the experimental average ψ of the considered metals which is 11.03 and the average deviation is of around ±2.51 pct. This shows that the theoretical and computational method presented in this work is suitable for the determination of coordination number of liquid metals. Computed values of friction coefficients ξ_H, ξ_S

and ξ_{HS} are presented in Table 2.4. ξ_H is dominating in all cases however ξ_S and ξ_{HS} also contribute significantly in case of all the liquid metals.

TABLE 2.4. Friction coefficients of liquid metals due to hard sphere ξ_H, square well ξ_S and hard sphere- square well interaction ξ_{HS}.

Metals	$\xi_H \times 10^{-13}$(Kg/s)	$\xi_S \times 10^{-13}$(Kg/s)	$\xi_{HS} \times 10^{-13}$(Kg/s)
Na	7.41	1.56	1.94
K	7.55	1.12	1.58
Cs	7.56	1.50	1.89
Mg	11.78	1.36	1.19
Al	11.98	1.76	1.07
In	18.14	4.39	5.38
Pb	25.59	2.04	1.75
Ag	42.28	8.25	12.56
Cu	31.96	2.78	4.53
Au	62.19	11.05	18.65

The diffusivity in liquid metals has been evaluated under LT principle (Venkatesh and Mishra, 2005) using well known Einstein equation for coefficient of diffusion (Berne and Pecora, 2000). Computed results are compared with available experimental results (Shimoji and Itami, 1986) and presented in Table 2.5. The shear viscosity coefficient, η_v is obtained under the SW model with the Stokes - Einstein relation. Computed results are compared with the available experimental data (Shimoji and Itami, 1986) in Fig. 2.5.

TABLE 2.5. Theoretical and experimental values of Diffusion coefficient, D (10^{-9} m^2/sec) and Shear viscosity (η_v) of liquid metals.

Metals	D(10^{-9} m^2/sec)		η_V(mPas)	
	theort.	expt.	theort.	expt.
Na	4.70	4.23	0.49	0.70
K	4.28	3.76	0.39	0.54
Cs	2.18	2.31	0.61	0.68
Mg	5.23	5.63	1.38	1.25
Al	4.93	4.87	1.56	1.46
In	2.10	2.60	1.51	-
Pb	2.87	2.19	1.47	2.61
Ag	2.61	2.55	3.8	3.70
Cu	4.85	3.97	2.6	3.50
Au	2.10	-	5.3	4.30

The SW potential is analytically solved and successfully applied for computing static structure factor, coordination number and thermodynamic properties of the considered liquids which are important information for metallurgical industry. Our results indicate that the SW model leads to a good agreement between computed and experimental results of structure factors and derived associated properties and hence such kind of theoretical works increase our confidence in present model. This model calculation provides an option to use the SW potential in the framework of the MSMA to derive the various thermo-physical and thermodynamic properties of liquid metals without using any adjustable parameter.

Coordination number calculations with number density and square well parameters are important findings to understand phase change at microscopic level. Thus the results of this chapter prove the usefulness of square well model in predicting various properties of liquid metals. Perturbation theory with hard sphere reference system is a good first approximation for the study of static and dynamic properties of liquid metals.

3. THERMO-PHYSICAL, THERMODYNAMIC, SURFACE AND SCALING PROPERTIES IN LIQUID METALS

3.1. INTRODUCTION

Statistical mechanics provides numerical relations between structures, dynamic and thermodynamic properties of liquid metals and alloys (Ma et al., 2013). In the last fifty years, studies on static and dynamical properties of liquid metals and alloys have been reported by different theoretical models and computer simulation techniques. However, all these model calculations and simulations provide a better understanding about microscopic structural characteristic and thermodynamics of liquid metals and alloys. Understanding a relationship between the transfer coefficients, thermodynamic properties, surface properties, thermo-physical properties and structural properties remains one of the most challenging task in the condense matter (Li et al., 2005; Li et al., 2004; Korkmaz and Korkmaz, 2009; Korkmaz, et al., 2006; Korkmaz and Kormaz, 2007; Yokoyama, 2000).

Inter-atomic forces are the key factor in molecular dynamic simulations also. The effective *ab initio* method to attain a high level of accuracy using embedded atom method (EAM) or the glue model is still expensive and are not easy to implement (Adebayo et al., 2005). It is rather difficult to determine some properties of a material by systematic theoretical calculations with many body potential functions. The Lennard-Jones potential was extensively tested for various liquid state theories in various computational experiments or within different theoretical approaches such as integral equations or

perturbation theories (Lang et al., 1999). Adebayo et al. investigated the temperature dependent structure and associated properties of liquid Al and Mg using Lennard-Jones potential (Adebayo et al., 2005). They observed a discrepancy in the first peak position and peak height at higher temperature (1063K and 1153K). They also reported that the Lennard-Jones model predict the Stokes – Einstein equation very poorly. Further, it may be noted that molecular dynamic simulation results of first peak of S(k) of liquid Al did not agree well with experiment especially at the principal peak position (Ji and Gong, 2004). It is worth to mention here that first peak of structural functions dictate various properties of materials. But in this square well model calculation on liquid Al, an excellent agreement was found between theory and experiment (Mishra and Venkatesh, 2008). Alfe and Gillan in their work with *ab initio* calculations on first-Principles Calculation of Transport Coefficients observed that model calculation predict value of viscosity based on the Stokes - Einstein equation with 40% accuracy (Alfe and Gillan, 1998).

Several authors have reported that the surface properties of liquids are very much depending on their bulk micro structural characteristics and their transport properties (Lu and Jiang, 2005; Blairs, 2006; Lu and Jiang, 2005; Gosh et al., 2007; Yokoyamoa and Tsuchiya, 2002). The surface tension and temperature coefficient of the surface tension, S_v ($S_v = -\frac{d\gamma}{dT}$) have been reported for most of the metallic melts (Nogi et al., 1985; Gosh et al., 2007; Yokoyamoa and Tsuchiya, 2002; Lu and Jiang, 2005). Several theories have been reported in last fifty years (Chacon et al., 1984; Yokoyamoa and Tsuchiya, 2002; Lu and Jiang, 2005) which provides a microscopic description of liquid metal surfaces. However, there is still uncertainty regarding

absolute values of γ_{ST} and particularly its temperature derivative which is called surface entropy due to the effect of impurities (Lu and Jiang, 2005).

In this thesis, self-diffusion coefficient, D, of liquids were determined using microscopic structure S(k), g(r) and pair wise interaction SW. Obtained D of considered liquids were employed in the determination of surface tension, γ_{ST}, recently published by many authors with different approaches (Lu and Jiang, 2005; Blairs, 2006). It is reported that the γ_{ST} is not well known experimentally even for many simple metals (Lu and Jiang, 2005).

In recent years different scaling laws relating the equilibrium thermodynamic properties, excess entropy with dimensionless transport coefficients have been reported by many authors (Li et al., 2005; Dzugutov, 1996; Rosenfeld, 1999; Samanta et al., 2004; Yokoyama, 1998). The Dzugutov universal scaling law (Yokoyama, 1998) is very important function among many scaling laws, which links the dynamic behavior of a liquid particle with pair correlation function, g(r), microscopic reducing parameter Γ and excess entropy. Dzugutov in his original work approximated the excess entropy per particle by two body approximations, which is denoted as S_2 and defined by

$$S_2 = -2\pi\rho \int_0^\infty \{g(r)\ln[g(r)] - [g(r) - 1]\}\, r^2 dr \qquad (3.1)$$

Here ρ is the number density. Yokoyama has modified Dzugutov's two body approximation by the term S_E (Yokoyama and Tsuchiya, 2002). The S_E per atom in liquid metals is the difference between the total thermodynamic entropy and that of the equivalent ideal gas.

In last two decades a considerable efforts have been made using molecular dynamics simulation to verify the Dzugutov's universal scaling law by other researchers

with embedded atom method (EAM) or Stillinger-Weber scheme or Tersoff potential or glue potential or second-moment approximation of tight-binding scheme for several liquid metals and alloys (Hoyt et al., 2000; Li et al., 2005; Rosenfeld, 1999; Samanta et al., 2004; Yokoyama, 1998; Yokoyama and Tsuchiya, 2002; Kreckelberg et al., 2009), by Dzugutov himself with Lennard-Jones and hard sphere potential functions. Recently, Ma et al. tested the scaling law in colloidal monolayers using optical microscopy and particle tracking techniques (Blairs, 2006).

The SW fluid is basic one possessing all characteristics of real liquid and the SW potential has been successfully applied for studying of various liquids for long time (Gopala Rao and Venkatesh, 1989; Venkatesh and Mishra, 2005; Venkatesh et al., 2003; Gopala Rao and Murthy, 1974; Liu et al., 1998; Gopala Rao and Sathpathy, 1982; Dubinin et al., 2009; Dubinin et al., 2014; Yu et al., 2001). Study of thermophysical and thermodynamic properties of liquids and their relation with microscopic structure functions are of long interest (Gosh et al., 2007; Qian et al., 1990; Ivanov and Berezutski, 1996; Nath and Joarder, 2005; Shih and Stroud, 1985).

We agree with other workers that the Dzugutov's hypothesis for dimensionless quantities must be tested with different form of inter atomic interactions (Hoyt et al., 2000). Thus the universal scaling law was tested by estimating the excess entropy of liquid metals as function of reduced diffusion. Technologically important surface properties like γ and its temperature derivative i.e. surface entropy, S_v ($S_v = -\frac{d\gamma}{dT}$) were studied through D and its temperature derivatives. Computed g(r) was employed to obtain Γ.

Further, new equations have been derived through equation of state of the SW potential (Gopala Rao and Joarder, 1976) and employed them to compute long wavelength limit of S(k) i.e. S(0) in liquid metals. S(0) can be related with various thermo-physical and thermodynamic properties of liquids (Blairs, 2007).

3.2. THEORY

The statistical mechanical approach is also useful to predict the relationship between various thermo physical and thermodynamic properties (March, 1999).

3.2.1. EVALUATION OF DEBYE TEMPERATURE

Another important quantity that is calculated is the Debye temperature θ_D. The Debye temperature plays the same role in the theory of lattice vibrations as the Fermi temperature plays in the theory of electrons in metal. Both are a measure of the temperature, separating the low temperature region where quantum statistics must be used from the high temperature region where classical statistical mechanics is valid.

The structure of many liquid metals in the vicinity of their melting temperature shows a similar characteristic as their structure in solid phase (Glazov and Aivazov, 1980; Tatarinova, 1988*).* During the melting of metals, partial breaking of bonds occur; as temperature increases a change in the melt structure can be observed which leads to post melting effects – an anomaly of structure sensitive properties (Diffusion, sound velocity, viscosity, etc.). The change in this structure with temperature can be predicted by a quantity called scaled flux (Panfilovich and Sagadeev, 2000) which is proportional to Debye temperature.

Recently Singh and Ali (Singh and Ali, 2013) computed the Debye temperature, θ_D of a number of liquid metals and presented a comparison between Debye temperature of crystalline, amorphous and liquid phases of metals. They found that the θ_D of several metals for amorphous state are lowered on average by 40% from the corresponding crystalline phase and are lowered by 6% to the corresponding values of liquid phase. This is well-known fact that metallic glasses shows some features of liquid metals (Li et al., 2003; Mishra et al., 2002) and hence computed diffusion coefficients were verified by calculating θ_D, using the equation obtained by Lal and Singh (Lal and Singh, 1993).

$$\theta_D = \frac{96\, D\, h}{k_B r_{max}^{\,2}}. \tag{3.2}$$

Here h is Planck's constant, k_B is Boltzmann's constant, r_{max} is the nearest-neighbor distance in g(r) and D is the self-diffusion coefficient of liquid metals.

3.2.2. EVALUATION OF SURFACE TENSION AND SURFACE ENTROPY OF LIQUID METALS

The detail studies of surface properties of condensed matter help in understanding their metallurgical processing.

The surface tension of elemental liquids can be given by statistical mechanical approach under zeroth order approximation as (Fowler, 1937)

$$\gamma_{ST} = \frac{\pi\rho^2}{8}\int_0^{\infty}\frac{d\,U(r)}{dr}\,g(r)r^4 dr. \tag{3.3}$$

Born and Green (Born and Green, 1949) derived the coefficient of viscosity of liquid metals using statistical mechanical approach as

$$\eta_V = \frac{2\pi\rho^2}{15}\left(\frac{m}{K_B T}\right)^{1/2}\int_0^{\infty}\frac{dU(r)}{dr}g(r)\,r^4 dr. \quad (3.4)$$

Here m is the atomic mass of the liquid metals. Eqns. (3.3) and (3.4) were derived on a strong scientific basis for hard sphere model but it is not easy to get the numerical solution of the integral equations. As we know that the statistical mechanics also provides various useful relationships between structure and thermodynamic properties of liquids.

A striking result can be obtained using Eqns. (3.3) and (3.4) with the well-known Stokes-Einstein relation, $\eta_V = k_B T/(2\pi r_{max} D)$, here r_{max}, the nearest neighbor distance, can be taken as first peak position of g(r) for real liquids as (Shimoji and Itami, 1986)

$$\gamma_{ST} = \frac{(k_B T)^{3/2}}{m^{1/2}}\,\frac{15}{32\pi\, r_{max}\, D}. \quad (3.5)$$

Since, D can be evaluated from well-known Einstein's relation using the SW long range interaction and hence the surface tension of liquid metals is obtained through Eqn. (3.5).

A study on temperature dependent structural and dynamic properties of materials enhances our knowledge and understanding about their surface and bulk properties. The temperature derivative of surface tension i.e., surface entropy of pure liquid at constant volume is defined as (Gosh et al., 2007)

$$S_V = -\frac{d\gamma}{dT} \quad (3.6)$$

$$\frac{d\gamma}{dT} = \gamma\left[\frac{1}{T} - \frac{1}{\sigma}\frac{d\sigma}{dT} + \frac{1}{\xi}\frac{d\xi}{dT}\right]. \quad (3.7)$$

$$\frac{d\xi}{dT} = \frac{d\xi^{H}}{dT} + \frac{d\xi^{S}}{dT} + \frac{d\xi^{SH}}{dT}. \tag{3.8}$$

The temperature derivative of friction coefficients for liquid metals is taken from (Venkatesh and Mishra, 2005).

3.2.3 SCALING LAW FOR SQUARE WELL LIQUID METALS

In order to test the Dzugutov scaling law for diffusion for liquid metals, we compute the collision frequency and excess entropy with SW model under RPA. Rosenfeld (Rosenfeld, 1999) defines the reduced transport coefficients in terms of reducing by macroscopic parameters, density and temperature, however, microscopic reducing parameters like hard sphere collision frequency, Γ and inter atomic distance σ (hard sphere diameter) according to Enskog theory (Chapman and Cowling, 1970) were chosen for deriving normalized diffusion. This concept was also extended by Li et al. for defining the reduced (Li et al., 2005) transport coefficients. Further, reduced transport coefficients were scaled by exponential of excess entropy with different values of pre-exponential factors (Hoyt et al., 2000; Blairs, 2006; Born and Green, 1949; Li et al., 2005; Dzugutov, 1996; Rosenfeld, 1999; Samanta et al., 2004; Yokoyama, 1998: Yokoyama et al., 2002).

As we have already mentioned that SW liquids possess all characteristics of real liquids. Thus we define the Γ for SW liquids in terms of g(r) from Eqn. (2.11) as

$$\Gamma = 4r_{max}^{2} g(r_{max}) \rho \left(\frac{\pi k_B T}{m}\right)^{1/2} \tag{3.9}$$

Here, r_{max} and $g(r_{max})$ are first peak position and value of pair correlation function respectively, m is the mass of diffusing species in atomic unit and other symbols have

their usual meanings. Dzugutov (Dzugutov, 1996) defined the reduced diffusion coefficient, and we modified for SW liquids

$$D^* = \frac{D}{\Gamma\, r_{max}^2} \tag{3.10}$$

There are various universal relations for different dimensionless physical parameters proposed for simple metals on the basis of corresponding state theory using characteristics parameters of different ionic potentials (Prakash et al., 2004).

The Dzugutov scaling law (Dzugutov, 1996) modified by Yokoyama (Yokoyama, 1998: Yokoyama et al., 2002) can be given as

$$D^* = a\, e^{k_B/S_E} \tag{3.11}$$

Where 'a' is a constant (a = 0.049), S_E is the excess entropy per atom expressed in units of k_B. Results of S_E for liquid metals can be represented in the form following equation:

$$S_E = \log \frac{D}{0.049\, \Gamma\, r_{max}^2} \tag{3.12}$$

3.2.4. EQUATION OF STATE FOR SQUARE WELL LIQUIDS

The structure factor in long wavelength limit, S(0), which is an important parameter to evaluate various properties of liquid state (Iwamatsu, 1990) was derived through equation of state in random phase approximation for SW fluids (Gopala Rao and Joarder, 1976)

$$\frac{PV}{RT} = \frac{1+\eta+\eta^2}{(1-\eta)^3} - \frac{4\varepsilon\,\lambda\,(\lambda^3-1)}{k_B T} \tag{3.13}$$

$$\left[\frac{V}{RT} + \frac{P}{RT}\frac{dV}{dP}\right]_T = \frac{d}{dP}(1+\eta+\eta^2)\times\frac{1}{(1-\eta)^3} - (1+\eta+\eta^2)\times\frac{(-3)}{(1-\eta)^4}(-1)\frac{d\eta}{dP} - \frac{4\varepsilon\,\lambda\,(\lambda^3-1)}{k_B T}\frac{d\eta}{dP}$$

(3.14)

$$\text{here, } \frac{d\eta}{dP} = \frac{\pi\sigma^3}{6}\frac{d\rho}{dP} = \frac{\pi\sigma^3}{6}\rho\beta_1 = \eta\beta_1 \qquad \beta_T = -\frac{1}{V}\frac{dV}{dP} \tag{3.15}$$

$$\left[\frac{V}{RT} + \frac{P}{RT}(-\beta_T)\right] = \frac{(\eta\beta_T + 2\,\eta.\eta\beta_T)}{(1-\eta)^3} + \frac{3(\eta^2+\eta+1)\,\eta\beta_T}{(1-\eta)^4} - \frac{4\varepsilon\,(\lambda^3-1)}{k_B T}\times\eta\beta_T$$

(3.16)

$$= \frac{\eta\beta_T\,[(1-\eta)\;(2\eta+1)+(3\eta^2+3\eta+3)]}{(1-\eta)^4} - \frac{4\varepsilon\,(\lambda^3-1)}{k_B T}\times\eta\beta_T$$

$$= \frac{\eta\beta_T\;(2\eta+1-2\eta-\eta+3\eta^2+3\eta+3)}{(1-\eta)^4} - \frac{4\varepsilon\,(\lambda^3-1)\,\eta\beta_T}{k_B T}$$

$$\frac{V}{RT} - \beta_T\frac{PV}{RT} = \frac{\eta\beta_T\;(\eta^2+4\eta+4)}{(1-\eta)^4} - \frac{4\varepsilon\,(\lambda^3-1)\,\eta\beta_T}{k_B T}$$

$$\frac{V}{RT} = \beta_T\frac{PV}{RT} + \frac{\eta\beta_T\;(\eta^2+4\eta+4)}{(1-\eta)^4} - \frac{4\varepsilon\,(\lambda^3-1)\,\eta\beta_T}{k_B T}$$

$$= \eta\beta_T\left[\frac{1}{\eta}\frac{PV}{RT} + \frac{\eta^2+4\eta+4}{(1-\eta)^4} - \frac{4\varepsilon\,(\lambda^3-1)\,\eta\beta_T}{k_B T}\right]$$

$$= \eta\beta_T\left\{\frac{1}{\eta}\left[\frac{1+\eta+\eta^2}{(1-\eta)^3} - \frac{4\varepsilon\,(\lambda^3-1)}{k_B T} + \frac{\eta^2+4\eta+4}{(1-\eta)^4} - \frac{4\varepsilon\,(\lambda^3-1)}{k_B T}\right]\right\}$$

$$= \eta\beta_T\left\{\frac{1+\eta+\eta^2}{\eta(1-\eta)^3} - \frac{4\varepsilon\,(\lambda^3-1)}{k_B T} + \frac{\eta^2+4\eta+4}{(1-\eta)^4} - \frac{4\varepsilon\,(\lambda^3-1)}{k_B T}\right\}$$

$$= \eta\beta_T\left\{\frac{(1-\eta)1+\eta+\eta^2+\eta(\eta^2+4\eta+4)}{\eta(1-\eta)^4}-\frac{8\varepsilon(\lambda^3-1)}{k_BT}\right\}$$

$$= \eta\beta_T\left\{\frac{1+\eta+\eta^2-\eta-\eta^2-\eta^3+\eta^3+4\eta^2+4\eta}{\eta(1-\eta)^4}-\frac{8\varepsilon(\lambda^3-1)}{k_BT}\right\}$$

$$= \eta\beta_T\left\{\frac{4\eta^2-4\eta+1}{\eta(1-\eta)^4}-\frac{8\varepsilon}{k_BT}(\lambda^3-1)\right\} \quad (3.17)$$

$$\frac{V}{RT} = \beta_T\left\{\frac{4\eta^2+4\eta+1}{\eta(1-\eta)^4}-\frac{8\varepsilon}{k_BT}(\lambda^3-1)\right\} \quad (3.18)$$

S(0) is related to isothermal compressibility, β_T as (Kalidoss and Ravi, 2002)

$$S(0) = \rho k_B T \beta_T \quad (3.19)$$

$$S(0) = \frac{1}{\left[\frac{(2\eta+1)^2}{(1-\eta)^4}-\frac{8\varepsilon\eta}{k_BT}(\lambda^3-1)\right]} \quad (3.20)$$

where η is called packing fraction i.e. volume occupied by the atoms divided by total volume and is given by $\eta = \frac{\pi\rho\sigma^3}{6}$. k_B is the Boltzman constant, T is the working temperature, ε is the SW depth and λ is the SW breadth.

3.3. RESULTS AND DISCUSSION

The surface, thermo-physical and thermodynamic properties of all the considered liquid metals were given in this Chapter. The Wertheim's (Wertheim, 1963) solutions of PY hard sphere fluid were perturbed with SW potential and solved numerically for liquid metals (Gopala Rao and Murthy, 1975) using temperature, T, ρ, and three parameters of SW potential.

TABLE 3.1. Theoretical and experimental values of Debye temperature, θ_D and Surface tension γ_{ST} of liquid metals

Metals	Temp (K)	$\theta_{DComputed}$ (K)	$\theta_{DLiterature}$ (K)	$\gamma_{STComputed}$ (Nm^{-1})	$\gamma_{STExperimental}$ (Nm^{-1})
Na	378	167.34	97.20	0.176	0.200, 0.197
K	343	97.37	59.20	0.096	0.110, 0.112
Cs	303	40.17	-	0.082	0.069, 0.070
Mg	953	286.51	-	0.418	0.557, 0.583
Al	943	311.53	294.00	0.801	0.867, 1.070
In	433	107.48	-	0.380	0.561
Pb	613	129.12	81.00	0.211	0.457, 0.462
Ag	1273	152.77	164.10	1.026	0.925, 0.910
Cu	1423	357.51	244.40	1.030	1.310, 1.320
Au	1423	123.38	121.60	1.200	1.145, 1.138

Lal and Singh (Lal and Singh, 1993) proposed a relationship between Debye temperatures, θ_D with self-diffusion coefficient for metallic glasses. Since it has been established that metallic glasses may be considered as super cooled liquids (Li et al., 2003; Mishra et al., 2002) hence this relationship was tested for all the considered liquid metals using square well model of diffusion. θ_D is an important parameter to inform the bonding and structural deformation of metals. Computed values for θ_D are summarized in Table 3.1 and compared with recently calculated and published values by Singh and

Ali (Singh and Ali, 2013). The agreement can be considered satisfactory, for the reasons mentioned already.

The surface tension is related with self-diffusion coefficients of liquids. Since self-diffusion coefficients of liquids were determined using microscopic structural functions along with SW potential and hence computed γ_{ST} is also related microscopic structure of liquids.

Computed values of γ_{ST} with their experimental values (Lu and Jiang, 2005) were also presented in Table 3.1 and satisfactory agreement was found between them.

The surface entropy of liquid metals through analytical expression for the temperature derivative of the SW model of D under linear trajectory principle was given. The temperature coefficient of the surface tension for pure liquid metals were derived by other workers (Iada and Guttrie, 1993) which depends on critical temperature and the temperature coefficient of density of liquid metals. It is mentioned that the critical temperature for many liquid metals is still unknown (Iada and Guttrie, 1993). Present model calculation also involves temperature coefficient of atomic density of liquid metals but there is no use of any critical temperature in our model calculation.

Since, temperature coefficient of density of liquid metals should have negative value hence a negative surface entropy were observed for all liquid metals. In some of binary liquid alloys, positive temperature coefficient of surface tension was reported this is due to having very positive excess free energy (Joud et al., 1973).

The computed results on the temperature coefficient of surface tension along with their experimental results (Lee et al., 2004) are presented in Table 3.2.

Table 3.2. Theoretical and experimental values of Surface tension (γ), Surface entropy, ($S_V = -d\gamma/dT$) isothermal compressibility, $\beta_T(10^{-11}\ m^2\ N^{-1})$ of liquid metals.

Metals	Temp	$S_V = -d\gamma/dT\ (mNm^{-1}K^{-1})$		$\beta_T(10^{-11}\ m^2\ N^{-1})$	
	(K)	theort.	expt.	theort.	expt.
Sodium	378	0.083	0.10	19.99	19.0
Potassium	343	0.057	0.08	40.47	38.2
Caesium	303	0.044	0.06	67.15	68.8
Magnesium	953	0.096	0.15	6.14	4.0
Aluminium	943	0.119	0.15	5.91	2.42
Indium	433	0.075	-	15.34	-
Lead	613	0.275	0.28	12.44	-
Silver	1273	0.230	0.17	2.54	2.2
Copper	1423	0.250	0.28	2.00	1.5
Gold	1423	0.270	-	1.99	1.3

From Table 3.2, one can be observed that there is a good agreement between theoretical and experimental results (Yokoyama and Tsuchiya, 2002), which shows the one more applicability of the analytical derivation of temperature derivative of D. The agreement between present computations with experimental results of η_v, for liquid metals (Yokoyama and Tsuchiya, 2002; Brandes, 1983) was found to be satisfactory.

The resulting correlation between D and γ_{ST} finds successful application for the estimation of γ_{ST}. Debye temperatures of liquid metals were calculated using diffusion data obtained through square well model.

The structure factor in long wavelength limit, S(0), is related to isothermal compressibility of liquid metals. Table 3.2 shows the computed results for β_T using equation of state of SW potential. There is a fair agreement between the computed value and the experimental values (Blairs, 2007; Singh et al., 2007; Ganesh and Wisdom, 2006) these shows the success of the SW perturbation theory.

S_E for liquid metals was calculated by employing the SW model of diffusion in Dzugutov scaling law. The computed values are in accordance with (Hoyt et al., 2000) which is shown in Fig. 3.1.

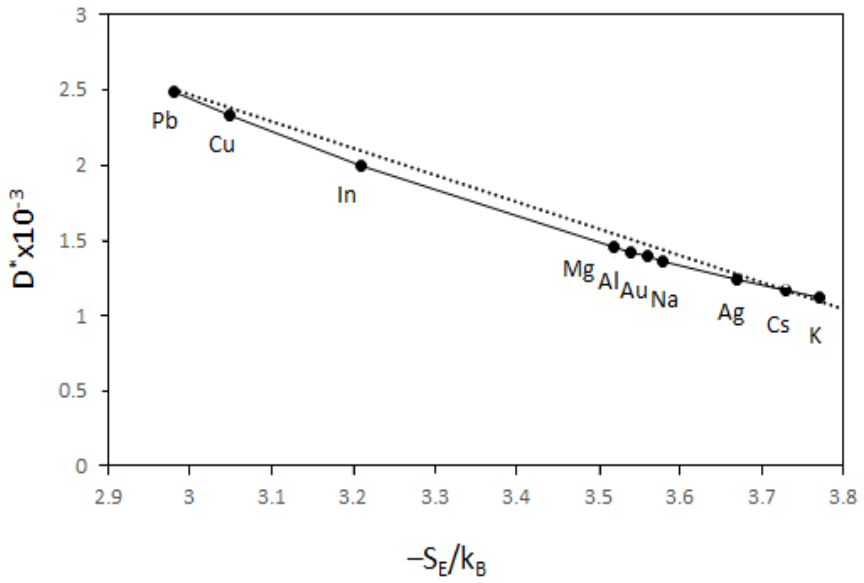

Fig. 3. 1. The scaled diffusion coefficient, D^* vs the excess entropy, S_E of liquid metals. The dashed line is the relationship found in original work of Dzugutov.

The computed values of S_E for all liquids are in order of three, a similar trend was observed by other researchers for nine liquids (Glazov and Aivazov, 1980). The excess entropy measurements of most of the liquid metals are yet to be determined experimentally, and therefore, the computed results of S_E for liquid In, Au and Ag could not be compared with experimental values.

Table 3.3. The Collision frequency (Γ), the Scaled diffusion (D^*) and Excess entropy ($-S_E/k_B$) of liquid metals.

Metals	Temp (K)	$\Gamma(10^{12}\ s^{-1})$	D^*x10^{-3}	$-S_E/k_B$	
				theort.	expt.
Sodium	378	26.74	1.36	3.58	3.46
Potassium	343	18.06	1.14	3.77	3.47
Caesium	303	7.16	1.17	3.73	3.57
Magnesium	953	37.69	1.45	3.52	3.38
Aluminium	943	44.43	1.42	3.54	3.55
Indium	433	10.99	1.98	3.21	-
Lead	613	9.66	2.48	2.98	3.94
Silver	1273	16.083	1.24	3.67	-
Copper	1423	21.931	2.33	3.05	3.44
Gold	1423	12.979	1.39	3.56	-

From Table 3.3, it can be seen that the difference between theoretical and experimental values for entropy lies in the range 0.01 to 0.96. But the overall agreement is quite good except in case of Pb. Such discrepancy was also observed by Yokoyama.

4. PARTIAL AND TOTAL STRUCTURAL CHARACTERISTICS OF LIQUID BINARY ALLOYS

4.1. INTRODUCTION

Alloys are industrial or commercial materials, which are grown from molten state. Liquid alloys have short-range order and their properties are much more difficult to understand than those of crystalline phases. The mixing behavior and dynamics in binary liquids are still not well understood. These complexities can be explained theoretically through correlation functions in disordered systems. Therefore, the studies of the properties of binary liquid alloys demands extensive theoretical investigations (Koirala et al., 2014).

It has been proved (Zernike and Prins, 1927) in one dimensional model that certain distances receive special weight in the formation of interface and this was carried on to three dimensional cases as in liquids. The impossibility of interpenetration of atoms and the existence of inter-atomic binding imply that certain arrangements of any given atom with respect to its neighbors are more probable than others. These investing introduced the idea of distribution function, which if known would facilitate the prediction X-ray pattern to be expressed for the any given substance.

X-ray diffraction measurements have been made on a large number of liquids including solutions and liquid metals. The results for liquid metals and alloys are summarized in reviews by Dubinin (Dubinin et al., 2014), Shimoji and Itami (Shimoji and Itami, 1986), Singh and Somer (Singh and Somer, 1997) and Wang et al. (Wang et al., 2009).

The structural, thermodynamic, transport and surface properties of binary liquid alloys have been extensively studied by various workers and is of long interest and many theoreticians have long been attempting to understand the properties of liquid alloys on the basis of the interactions between atoms or molecules (Flory, 1942; Harrision, 1966; Lebowitz, 1964; Faber, 1972; Shimoji, 1977; Bhatia et al., 1973; Alonso and March, 1982; Singh et al., 1990; Singh and Somer, 1992; Novakovic, 2010; Gopala Rao and Venakatesh, 1989; Dahlborg et al., 2013; Jakse and Pasturel, 2015; Jakse and Pasturel, 2016). The thermodynamic excess functions, static structure factors are well known experimentally, however, theoretical interpretation and evaluation need improvement (Echendua et al., 2010).

Studies of X – ray and neutron scattering from liquid metals and alloys give information about the atomic distribution, which is obtained by Fourier analysis of the experimentally observed scattering intensity. The pioneering work on X – ray diffraction was carried out by Gingrich (Gingrich, 1952), Gingrich et. al. (Gingrich and Henderson, 1952) and others (Orton et al., 1960; Enderby and North, 1968).

In a binary alloy the scattering function depends upon, in general, three independent partial structure factors and two scattering functions. Keating (Keating, 1963) suggested that in principle three partial structure factors (PSFs) $S_{11}(k)$, $S_{22}(k)$ and $S_{12}(k)$ are required to specify the structure of liquid binary alloys. It is difficult to obtain these partial structure factors experimentally. Of course isotope enrichment offers a method of obtaining another set of experimental data but complete enrichment is rather difficult.

In present work, the Ashcroft and Langreth (AL) type partial structure factors (Ashcroft and Langreth, 1967) are calculated through a perturbation model using square

well attractive tail as a perturbation over Lebowitz solution (Lebowitz, 1964) of statistical mechanical model of Percus-Yevick equation (Percus and Yevick, 1957) for hard sphere mixtures. The PSFs can be used in the evaluation of the total structure factor (TSF), number of nearest neighbors, thermodynamic properties, electrical resistivity, diffusion coefficients and many other properties. The hard sphere reference system with square well attractive part is the simplest one, possessing the basic characteristics of a real fluids. The success of square well model in the calculation of concentration dependent various properties of liquid Al-Cu and Ag-Cu binary alloys because they are size effect alloys in which the pair wise potential plays a significant role and multi-particle interactions do not play a vital role.

In this chapter a detailed discussion of the structural properties of Al-Cu and Ag-Cu alloys is presented. Many authors have been reported concentration and temperature dependent structural, transport and thermodynamic properties of liquid Al-Cu and Ag-Cu alloys using different theoretical techniques, computational simulations and experimental methods with specific instrumentation arrangement: for liquid Al-Cu alloys (Wang et al., 2009; Zhang et al., 2010; Brillo et al., 2008; Cheng et al., 2009: Brillo et al., 2006; Dahlborg et al., 2013; Dahlborg et al., 2007; Xiong et al., 2015; Zhang et al., 2009; Murdy et al., 2008; Eskin et al.,2005; Schmitz et al., 2014); for liquid Ag-Cu alloys (Lukens and Wagner, 1975; Novakovic et al., 2005; Brillo et al., 2004; Itami et al., 2000; Jha et al., 2014; Siwiec et al., 2013). Despite of a lot of experimental and theoretical effort devoted to the study of liquid alloys, the microscopic structural functions and their relation with thermo-physical and thermodynamic properties of the liquids are still not well understood. Interest to liquid metals and liquid alloys is motivated by their many

physical-chemical properties (Gopala Rao and Venkatesh, 1989; Murdy et al., 2008; Schmitz et al., 2014; Huang et al., 2011; Canales et al., 1998).

Copper has been the most common alloying element almost since the beginning of the aluminum industry and copper is added as the major alloying component in many of the alloys developed. Liquid Al-Cu alloys are studied extensively as it plays an important role in lightweight casting, in lead-free soldering (Schmitz et al., 2014) due to the presence of low temperature eutectic compositions. They have low melting point and are chemically inert substrates hence easy-to-handle experimentally. The Ag-Cu system is also interesting for a number of technical and industrial applications in joining processes. Such applications are brazing, soldering and welding. Moreover Ag-Cu alloys are also used in high temperature bonding applications. Pure silver is soft and ductile at room temperature. However, it can be hardened by alloying it with other element. Copper is the favorite hardener and is normally employed in the production of sterling silver (Jha et al., 2014).

The structural description at the atomic scale of liquid metals and alloys usually employs the radial distribution function (RDF) which is obtained through Fourier transform of structure factors (SFs) in binary alloys. Thus we present three PSFs in both the alloys; TSFs were obtained through these three PSFs and two scattering factors.

4.2. THEORY

For a systems containing more than one kind of atoms, the intensity of the X-ray scattering can be written as

$$\frac{I_{coh}}{N} = \langle f^2 \rangle + \langle f \rangle^2 \int_0^\infty 4\pi r^2 [\rho(r) - \rho] j_O(kr)\, dr \qquad (4.1)$$

Where $j_O(r)$ is the Bessel function of the zeroth order. Further

$$< f > = \sum_{i=1}^{n} C_i f_i \tag{4.2}$$

$$< f^2 > = \sum_{i=1}^{n} C_i f_i^2 \tag{4.3}$$

and

$$\rho(r) = \frac{\sum_{i=1}^{n}\sum_{j=1}^{n} C_i f_i f_j \rho_{ij}(r)}{[\sum_{i=1}^{n} C_i f_i]^2} \tag{4.4}$$

where C_i is the atomic percent of i^{th} atom in the alloy, f_i and f_j are the scattering factors of i^{th} and j^{th}-type atoms respectively, $\rho_{ij}(r)$ is the number of j-type atoms per unit volume at the distance r from an i-type atom and n is the number of atoms.

$$\rho(r) = [C_1 f_1^2 \rho_{11}(r) + C_2 f_2^2 \rho_{22}(r) + 2C_1 C_2 f_1 f_2 \rho_{12}(r)]\ [C_1 f_1 + C_2 f_2]^{-2} \tag{4.5}$$

Considering $C_1\rho_{12}(r) = C_2\rho_{21}(r)$, the total structure factor for binary system can be written as

$$S(k) = \frac{C_1^2 f_1^2}{< f >^2} I_{11}(k) + \frac{C_2^2 f_2^2}{< f >^2} I_{22}(k) + \frac{2C_1 C_2 f_1 f_2}{< f >^2} I_{12}(k) \tag{4.6}$$

where

$$I_{11}(k) = 1 + \int_0^{\infty} 4\pi r^2 [\frac{\rho_{11}(r)}{C_1} - \rho]\, j_0(kr)\, dr \tag{4.7}$$

$$I_{22}(k) = 1 + \int_0^{\infty} 4\pi r^2 [\frac{\rho_{22}(r)}{C_2} - \rho]\, j_0(kr)\, dr \tag{4.8}$$

$$I_{12}(k) = 1 + \int_0^{\infty} 4\pi r^2 [\frac{\rho_{12}(r)}{C_2} - \rho]\, j_0(kr)\, dr \tag{4.9}$$

As mentioned earlier we use hard sphere reference system as it dominates in deciding the structural aspects of liquids but we note that this reference system lacks realistic properties and hence the hard sphere solution of PercusYevick's equation obtained by Lebowitz is perturbed with square well attractive tail under Mean Spherical Model Approximation (MSMA) to obtain the direct correlation function (DCF) as

$$C_{ij}(r) = \begin{cases} C_{ij}^{0}(r) & ; \quad 0 < r < \sigma_{ij} \\ -\varepsilon_{ij}/k_B T & ; \quad \sigma_{ij} < r < \lambda_{ij}\sigma_{ij} \\ 0 & ; \quad r > \lambda_{ij}\sigma_{ij} \end{cases} \tag{4.10}$$

where $C_{ij}^{0}(r)$ stands for the Hard Sphere solution of Percus - Yevick's equation, σ_{ij}, λ_{ij} and ε_{ij} are the hard sphere diameter, Potential energy breadth and depth respectively of the Square well potential of i^{th}species. The mixed parameters are determined through the use of Lorentz-Berthelot rules (Gopala Rao and Das, 1987). Thus, the mixed parameters are given by

$$\left.\begin{aligned} \sigma_{12} &= (\sigma_1 + \sigma_2)/2 \\ \varepsilon_{12} &= (\varepsilon_{11}\ \varepsilon_{22})^{1/2} \\ \lambda_{12} &= \frac{\lambda_{11}\sigma_1 + \lambda_{22}\sigma_2}{2\sigma_{12}} \end{aligned}\right\} \tag{4.11}$$

The radial distribution function, $g_{ij}(r)$ is related to the correlation function, $h_{ij}(r)$ as given equation

$$h_{ij}(r) = g_{ij}(r) - 1 \tag{4.12}$$

Further, $h_{ij}(r)$ is related to the DCF through the generalized OZ equation for a system containing more than one species can be written as

$$h_{ij}(r) = C_{ij}(r) + \sum_{1=1,2} \rho_1 \int C_{i1}(\bar{r} - \bar{r}')\ h_{j1}(\bar{r}')\ d\bar{r} \tag{4.13}$$

where ρ_1 is the bulk density of 1^{th} species. Fourier transforming the OZ equation and using convolution theorem $h_{ij}(k)$ can be obtained as

$$h_{ij}(k) = C_{ij}(k) + \sum_{1=1,2} \rho_1 C_{i1}(k) \; h_{j1}(k) \tag{4.14}$$

For a binary system with

i = 1, j = 1

$$h_{11}(k) = C_{11}(k) + \rho_1 C_{11}(k) h_{11}(k) + \rho_2 C_{12}(k) h_{12}(k) \tag{4.15}$$

i =1, j = 2

$$h_{12}(k) = C_{12}(k) + \rho_1 C_{11}(k) h_{21}(k) + \rho_2 C_{12}(k) h_{22}(k) \tag{4.16}$$

i = 2, j = 1

$$h_{21}(k) = C_{21}(k) + \rho_1 C_{21}(k) h_{11}(k) + \rho_2 C_{22}(k) h_{12}(k) \tag{4.17}$$

i = 2, j = 2

$$h_{22}(k) = C_{22}(k) + \rho_1 C_{21}(k) h_{21}(k) + \rho_2 C_{22}(k) h_{22}(k) \tag{4.18}$$

These equations on solving for $h_{ij}(k)$ give rise to

$$h_{11}(k) = [\, C_{11}(k) \; \{1 - \rho_2 C_{22}(k)\} + \rho_2 C_{12}^2(k) \,][B(k)]^{-1} \tag{4.19}$$

$$h_{22}(k) = [\, C_{22}(k) \; \{1 - \rho_1 C_{11}(k)\} + \rho_1 C_{12}^2(k) \,] [B(k)]^{-1} \tag{4.20}$$

$$h_{12}(k) = h_{21}(k) = C_{12}(k) \; [B(k)]^{-1} \tag{4.21}$$

where B(k) is given by

$$B(k) = [1 - \rho_1 C_{11}(k) - \rho_2 C_{22}(k) + \rho_1 \rho_2 C_{11}(k) C_{22}(k) - \rho_1 \rho_2 C_{12}^2(k)] \tag{4.22}$$

Further, we have the result connecting the partial structure factor $S_{ij}(k)$ and $h_{ij}(k)$ as

$$S_{ij}(k) = \delta_{ij}(k) + (\rho_i \rho_j)^{1/2}[h_{ij}(k)] \quad (4.23)$$

where δ_{ij} is the kronecker delta and is defined as

$$\delta_{ij} = \begin{cases} 1 & \text{for} \quad i = j \\ 0 & \text{for} \quad i \neq j \end{cases} \quad (4.24)$$

The partial structure factors $S_{11}(k)$, $S_{22}(k)$ and $S_{12}(k)$ were solved by taking the Fourier transformation of $h_{ij}(k)$ given by (Gopala Rao and Satpathy, 1990)

$$S_{11}(k) = \{1 - \rho_1 C_{11}(k) - \rho_1 \rho_2 C_{12}^2(k)/[1 - \rho_2 C_{22}(k)]\}^{-1} \quad (4.25)$$

$$S_{22}(k) = [1 - \rho_1 C_{11}(k)]\ S_{11}(k)\ /\ [1 - \rho_2 C_{22}(k)] \quad (4.26)$$

$$S_{12}(k) = (\rho_1 \rho_2)^{1/2}\ C_{12}(k)\, S_{11}(k)\ /\ [1 - \rho_2 C_{22}(k)] \quad (4.27)$$

Thus the evaluation of partial structure factors depend on the computation of $C_{ij}(k)$ the direct correlation function as obtained by them can be written as

$$C_{ij}(r) = -[a_i + b_i r + d\ r^3] \quad ; \quad r < \sigma_i \quad (4.28)$$

$$C_{12}(r) = -\ a_1 \quad ; \quad r < \lambda \quad (4.29)$$

$$= -[a_1 + \{b(r-\lambda)^2 + 4\lambda d(r-\lambda)^3 + d(r-\lambda)^4\}/r] \ ; \ \lambda < r < \sigma_{12} \quad (4.30)$$

$$= 0 \quad ; \quad r > \sigma_{12} \quad (4.31)$$

Here

$$\lambda = (\sigma_2 - \sigma_1)/2 \quad (4.32)$$

$$\eta_i = \pi \rho_i \sigma_i^3 / 6 \quad (4.33)$$

$$\eta = \eta_1 + \eta_2 \quad (4.34)$$

$$\alpha = \sigma_1 / \sigma_2 \quad (4.35)$$

$$a_1 = \{(\eta_1 + \alpha^3 \eta_2)(4 + 4\eta + \eta^2) - 3\eta_2 (1-\alpha)^2 [1 + \eta_1 + \alpha(1 + \eta_2)] \\ (1 + 2\eta_1 - \eta_2) + (1 - \eta^3) - 3\eta_1 \eta_2 (1-\eta)(1-\alpha)^2\}\ (1-\eta)^{-4} \quad (4.36)$$

$$\alpha^3 a_2 = \{(\eta_1 + \alpha^3\eta_2)(4 + 4\eta + \eta^2) - 3\eta_1 (1-\alpha)^2 [1 + \eta_1 + \alpha(1+\eta_2)] \\ (1 - \eta_1 + 2\eta_2) + (1-\eta^3)\alpha^3 - 3\eta_1\eta_2 (1-\eta)(1-\alpha)^2 \alpha\}(1-\eta)^{-4} \quad (4.37)$$

$$\beta_1 = b_1\sigma_1 = -6[\eta_1 g_{11}^2 + \eta_2 (1+\alpha)^2 \alpha g_{12}^2 / 4] \quad (4.38)$$

$$\beta_2 = b_2\sigma_2 = -6[\eta_2 g_{22}^2 + \eta_1 (1+\alpha)^2 g_{12}^2 / 4\alpha^3] \quad (4.39)$$

$$\gamma_1 = d\sigma_1^3 = [\eta_1 a_1 + \alpha^3 \eta_2 a_2]/2 = \alpha^3\gamma_2 \quad (4.40)$$

$$b\sigma_2 = -3(1+\alpha)[\eta_1 g_{11}/\alpha^2 + \eta_2 g_{22}] g_{12} \quad (4.41)$$

$$g_{11} = [(1+\eta/2) + 3\eta_2 (\alpha-1)/2](1-\eta)^{-2} \quad (4.42)$$

$$g_{22} = [(1+\eta/2) - 3\eta_1 (\alpha-1)/2\alpha](1-\eta)^{-2} \quad (4.43)$$

$$g_{12} = [(1+\eta/2) + 3(1-\alpha)(\eta_1 - \eta_2)/2(1+\alpha)](1-\eta)^{-2} \quad (4.44)$$

and finally obtaining the total structure factor

$$S(k) = \sum_{i=1}^{2}\sum_{j=1}^{2} (C_i C_j)^{1/2} \frac{f_i(k) f_j(k)}{C_1 f_1^2(k) + C_2 f_2^2(k)} S_{ij}(k) \quad (4.45)$$

Where $f_j(k)$ and $f_j(k)$ are the atomic scattering factors taken from literature (Venkatesh et al., 2003) and C_i and C_j are the atomic fractions of the i^{th} and j^{th} species respectively.

Thus for the binary alloy, the total structure factor can be written as

$$S(k) = [C_1 f_1^2 S_{11}(k) - 2(C_1 C_2)^{1/2} f_1 f_2 S_{12}(k) + C_2 f_2^2 S_{22}(k)] \times [C_1 f_1^2 + C_2 f_2^2]^{-1} \quad (4.46)$$

The partial structure factors are then Fourier transform to get the partial radial distribution functions, $g_{ij}(r)$ as

$$g_{ij}(r) - 1 = \frac{1}{2\pi^2(\rho_i\rho_j)^{1/2}} \int_0^{\infty} [S_{ij}(k) - \delta_{ij}] k \sin(kr)\, dr \qquad (4.47)$$

Here δ_{ij} is the kronecker delta and is given in Eqn. (4.24).

The partial radial distribution functions are used to calculate the coordination number as

$$Z_{ij} = 4\pi\rho_{ij} \int_0^{r_{min}} g_{ij}(r)\, r^2\, dr. \qquad (4.48)$$

4.3. RESULTS AND DISCUSSION

The TSFs characterizes the structure of binary alloys were evaluated at five different concentrations of Cu in Al-Cu alloys and at six different concentrations of Cu in Ag-Cu alloys. Those concentrations were chosen in both these alloys because the experimental results were available. A necessary condition in the application of Lebowitz solution is $\sigma_{22}>\sigma_{11}$. Here σ_{11} corresponds to the diameter of Cu and σ_{22}correspond to the diameter of Al in Al-Cu melts

4.3.1. Concentration dependent Structural characteristics in Al-Cu Alloys

4.3.1.1. *Partial and Total Structure factors in Al-Cu alloys:*

The hybrid potential parameters $\sigma_{ij,}$ ε_{ij} and λ_{ij} were obtained by Lorentz-Berthelot rule using SW parameters of pure components (Venkatesh and Mishra, 2005; Mishra and Venkatesh, 2008). The input parameters used in the present calculations are listed in Table 4.1.

Table 4.1. Input parameters of liquid Al-Cu alloys with σ_{ii} as the diameter, ε_{ii}/k_B as the depth, λ_{ii} as the breath of the square well potential and ρ_n as the number density

	σ_{ii} (Å)	ε_{ii}/k_B	λ_{ii}	ρ_n
Cu	2.35	300	1.68	0.07408
Al	2.43	160	1.30	0.05235

In the present calculations the concentrations are expressed in terms of atomic fraction of Cu i.e., C_1. The peak positions and peak heights of the concentration dependent PSFs and TSFs, S(k) of the liquid Al-Cu alloys are presented in Table 4.2, which give the detailed information regarding the principal peak and structural characteristics of the binary melts at different compositions. The first peak positions of S(k) are shifted from 2.7$Å^{-1}$ to 2.8$Å^{-1}$ with increasing atomic percent of Cu from 10% to 40%. Roa and Bandyopadhayay also observed in their work on Mg-Zn melt that the maximum shift towards the larger k value with increase in the concentration of Zn in the melt. The amplitude of the first peak increases with increase in the atomic percent of Cu except in 17% Cu in Al-Cu alloys which is the eutectic composition of that alloy. The increase in the height of the peaks with increase in Cu concentration suggests that formation of bonds happen in the melt and that Cu atoms forms Cu-Cu cluster in the Al bulk melts. Similar trend were observed for Ag-Sn (Gopala Rao and Satpathy, 1990), Cu-Bi (Gopala Rao and Satpathy, 1990) and in case of Ag-In (Venkatesh et al., 2003). At the same time some of the original Cu-Cu bonds are destroyed and some new Al-Cu bonds have been formed. The increase in heights of the peaks with increase in atomic percent of Cu from 10% to 40% suggests the amount of forming bonds increases. Similar trend was observed for the

same alloy at 17% and 33% Cu (Brillo et al., 2006) and in Fe-Al alloy (Roik et al., 2014). But at the eutectic composition of the melt i.e, 17% Cu there is no increase in peak heights which suggests that the amount of destroyed bonds also increases in the melt.

Table 4.2. Theoretical and experimental values of first peak positions, k and peak heights S(k) of Al-Cu alloys at different compositions of Cu.

% Cu in Al-Cu	Temp K	k_{11}(Å^{-1})	S_{11}(k)	k_{22}(Å^{-1})	S_{22}(k)	k_{12}(Å^{-1})	S_{12}(k)	k(Å^{-1})	S(k)
10	973	2.7	1.11	2.7	2.18	2.7	0.36	2.7	2.12
17	1023	2.8	1.20	2.8	2.11	2.8	0.46	2.8	2.09
25	973	2.8	1.36	2.8	2.21	2.8	0.66	2.8	2.29
33	1023	2.8	1.51	2.8	2.17	2.8	0.78	2.8	2.38
40	1023	2.8	1.69	2.8	2.16	2.8	0.91	2.8	2.53

The partial Cu-Cu atomic distribution i.e, S_{11}(k) in Table 4.2 differs significantly from the structure factor of liquid Cu (Taylor et al., 2001), indicating the disappearance of Cu-like structure upon alloying. However the partial structure factor related to the Al-Al distribution i.e, S_{22}(k) in Table 4.2 resembles the structure of pure Aluminium (the first peak positions and peak heights of pure Al do not differ much) (Wertheim, 1963).

Further TSFs along with their experimental data illustrated in Fig. 4.1 throughout the k-space. TSFs become constant around one in high k region.

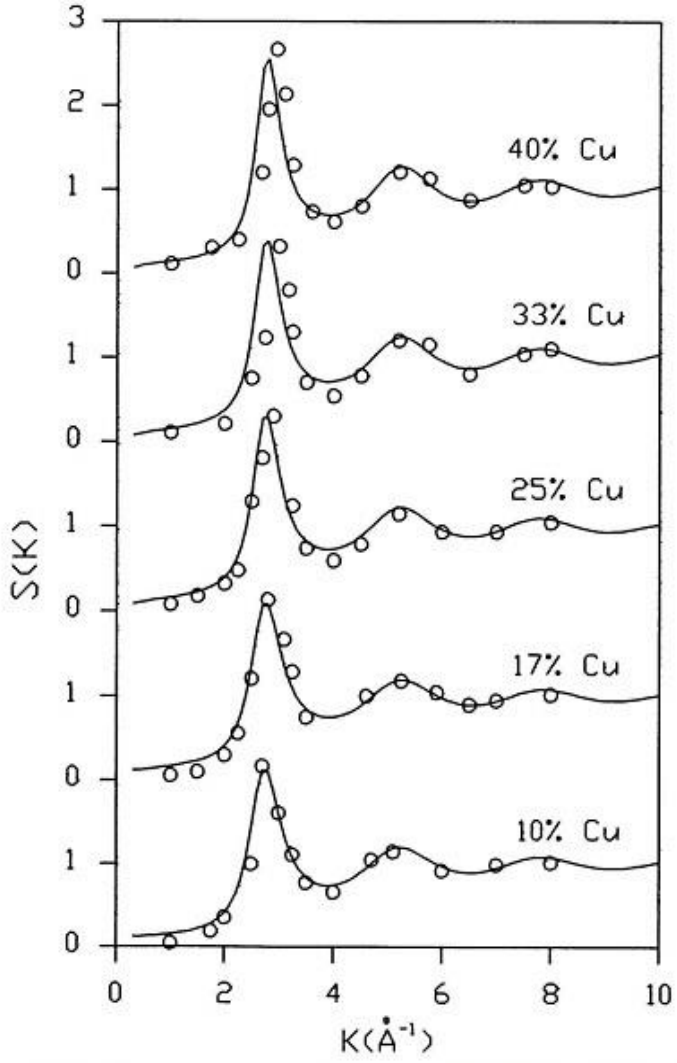

Fig. 4.1. Total structure factor S(k) versus k at different atomic percent of Cu in Al-Cu alloys. (——) theoretical values, (o o o) experimental values.

A discrepancy in peak height was observed with increase in atomic percent of Cu. This may be due to the fact that the melting point of Cu is 1353K while the working temperatures are 973K and 1023K. Hence one can presumed that the noble metal Cu may exist in the alloy as an amorphous material at the working temperatures which are much lower than Cu melting point. PSFs are also presented in Figs. 4.2 to 4.4 in entire momentum space.

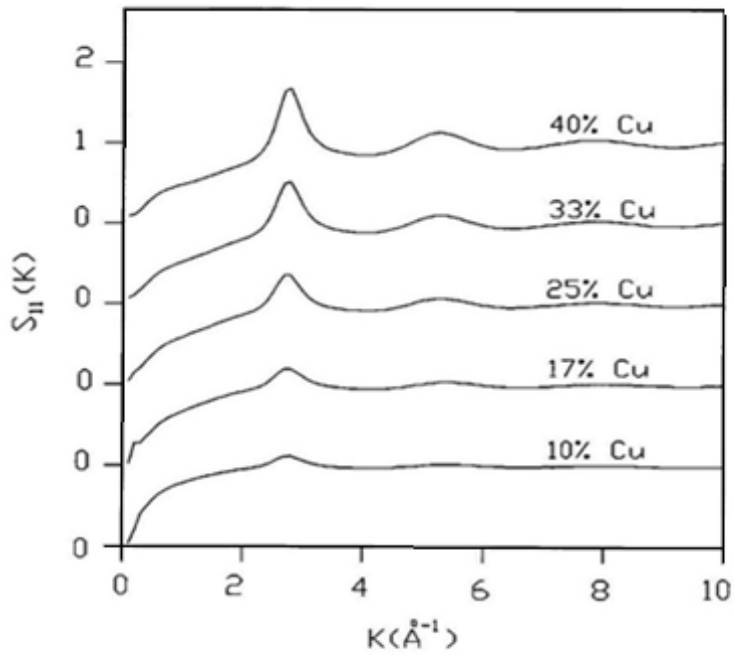

Fig. 4.2. $S_{11}(k)$ versus k at different atomic percent of Cu in Al-Cu alloys.

As seen from Figs. 4.2 and 4.3, the peak heights of $S_{11}(k)$ and $S_{22}(k)$ increases with increasing atomic percent of Cu and Al respectively. This tendency was also exhibited in Ag-Sn alloy (Rao and Satpathy, 1990), and in Ag-In alloys (Venkatesh et al., 2003).

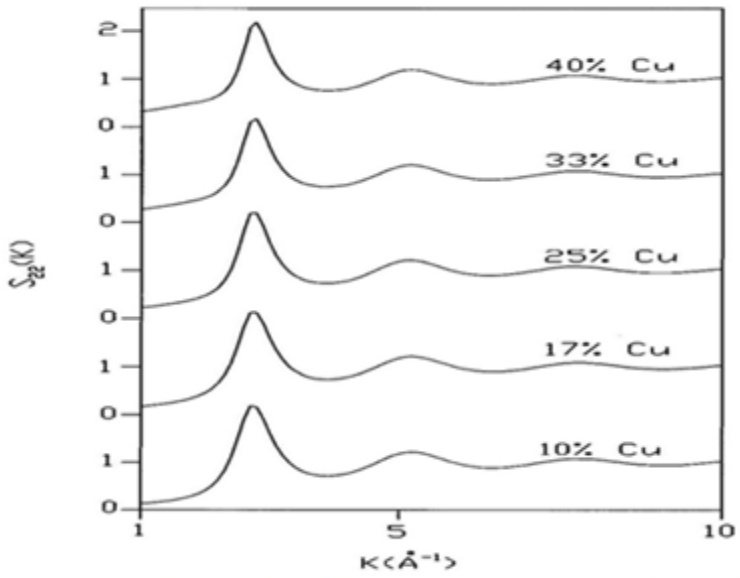

Fig. 4.3. $S_{22}(k)$ versus k at different atomic percent of Cu in Al-Cu alloys.

The peak height of $S_{12}(k)$ increases from 0.36 to 0.91 as the atomic percent of Cu increases from 10 to 40. As seen from Table 4.2, the peak height of $S_{12}(k)$ is lower than other partial structure factors ($S_{11}(k)$ and $S_{22}(k)$) at all compositions which may be due to the segregation of Cu in Al-Cu alloys.

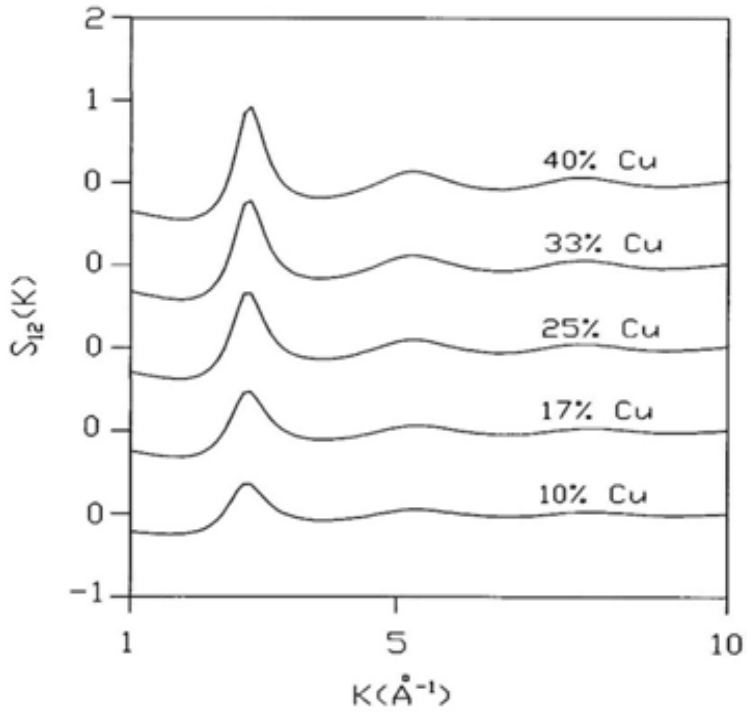

Fig. 4.4. $S_{12}(k)$ versus k at different atomic percent of Cu in Al-Cu alloys.

Dahlborg et al., observed a bump (pre peak) centered at k=1.5 $Å^{-1}$ in their elastic neutron scattering experiment at 10%, 17.1% and 25% Cu for Al-Cu melts (Dahlborg et al., 2013) however, with quasi elastic intensity measurement performed by (Dahlborg et al., 2007) at all composition of Al-Cu melts at 973K and1173 K a bump can be seen only for the 25% Cu. The present model does not show such pre-peaks or almost negligible prepeaks.

4.3.1.2. *Partial and Total radial distribution functions in Al-Cu alloys:*

Partial and total pair correlation functions were obtained by the Fourier transform of partial and total structure factors. The computed values of radial distribution function g(r), of liquid Al-Cu alloys at different atomic percent of Cu were presented in Fig. 4.5 along with the available experimental values. The agreement between experiments (Wang et al., 2009; Brillo et al., 2008) and the theory at all concentrations are good especially in light of peculiar nature of Al-Cu alloy. There is a discrepancy in peak height between theory and experiment at 40% of Cu which may be due to the existence of some Cu cluster at the working temperature 1023K as it has been mentioned that the melting temperature of Cu is 1353K. However, the peak position at this concentration does not change. The first peak of g(r) for all compositions is located around 2.6Å and height decreases with increasing the atomic percent of Cu in Al-Cu alloys. The computed results of the radial distribution functions agree well with the experiments (Wang et al., 2009; Brillo et al., 2008) for all compositions, especially both the locations and amplitudes of their peaks, providing strong support for accuracy liquid structures using SW model.

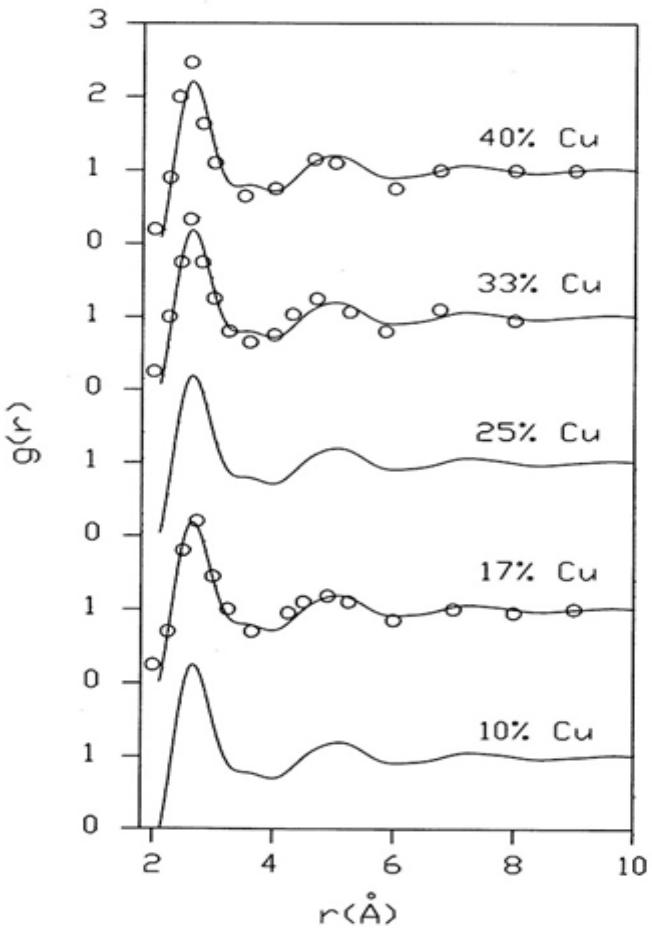

Fig. 4.5. Radial distribution function g(r) versus r at different atomic percent of Cu in Al-Cu alloys; (——) theoretical values, (o o o) experimental.

The partial radial distribution functions (PRDFs) are shown in Table 4.3. As seen from Table 4.3 as the atomic percent of Cu in Al-Cu alloys increases the amplitude of the first peak of the PRDFs increases and the peak positions are almost invariant with compositions. The peak positions are located at around 2.6 Å. From the PRDFs we obtained the nearest neighbor distances between Cu-Cu, Al-Al and Al-Cu which are given in Table 4.3. It can be seen from Table 4.3 that the separation between Al-Al atomic pairs are the longest, so it is assumed that the higher proportion of Al atoms in a cluster the larger that cluster must be. This condition favors compound forming behavior between Al and Cu as in case of experimental work on Al-Cu alloy (Brillo et al., 2006).

Table 4.3. Theoretical and experimental values of first peak positions, r and peak heights g(r) of Al-Cu alloys at different compositions of Cu.

% Cu in Al-Cu	Temp K	r_{11}(Å)	g_{11}(r)	r_{22}(Å)	g_{22} (r)	r_{12}(Å)	g_{12}(r)	r_{max}(Å)	g(r)
10	973	2.64	1.99	2.69	2.46	2.63	2.36	2.67	2.24
17	1023	2.63	2.11	2.69	2.48	2.63	2.39	2.66	2.19
25	973	2.63	2.33	2.69	2.53	2.63	2.45	2.65	2.18
33	1023	2.62	2.31	2.69	2.53	2.62	2.48	2.64	2.18
40	1023	2.61	2.38	2.68	2.55	2.61	2.51	2.62	2.21

4.3.1.3. *Partial and Total Coordination number in Al-Cu alloys:*

The partial and total coordination numbers of the Al-Cu alloy at different atomic percent of Cu were calculated at 1373 K because experimental results were only available at this temperature. The computed values were shown in Table 4.4. As seen from Table 4.4, the total coordination number increases from 11.16 to 13.32 with increasing composition of Cu. The coordination number of pure liquid Al is 11.5 (Kita et al., 1994) and we find a total coordination number at 90% Al is 11.16, which favors our model calculation for this microscopic parameter as with increasing Al% binary mixture shifting towards one component system. In fact the distance between Al-Al atoms is around 2.69Å while that between Cu-Cu is 2.63Å which is nearly corresponds to diameter of Al and Cu respectively. The existence of constant inter-atomic separation may be due to segregation within atomic dimensions i.e., clusters may exist (Gopala Rao and Satpathy., 1990; Gopala Rao and Sathpathy, 1982). Xiong et al. (Xiong et al., 2015) found in their work

on liquid $Al_{75}Cu_{25}$ using X-ray diffraction and electrostatic levitation measurements together with the *ab initio* molecular dynamic simulation in the temperature range from 800 to 1600 K that a linear increase in total coordination number with increasing concentration of Cu. The same trend is also observed in present calculations. Cu coordination number, Z_{11} increases from 0.87 to 3.72. This increase in coordination number may be due to the existence of Cu in amorphous form in the alloy as mention above at present working temperatures or Cu-clustering may increase with increasing Cu composition. However, the coordination number 6 is common in copper in crystalline state but in the present computations the partial coordination numbers as a function of composition shows that there is a good miscibility of Cu in Al-Cu alloy at lower atomic percent of Cu at 1373K.

Table 4.4. Partial and total coordination number of Al-Cu alloys at different compositions of Cu at 1373K.

% Cu in Al-Cu	Z_{11}	Z_{22}	Z_{12}	Total coordination number, Z
10	0.87	8.04	2.25	11.16
17	1.58	7.57	2.84	11.99
25	2.50	6.87	3.41	12.78
33	3.06	6.30	3.80	13.06
40	3.72	5.62	3.98	13.32

With increase in composition of Cu, coordination number of Al, Z_{22}, decreases from 8.04 to 5.62 as shown in Table 4.5. It means that binary mixture shifting towards

Cu at lower compositions of Al. Pure Al has face centred cubic (fcc) structure with coordination number 12 in the solid state. The total coordination number, Z of Al-Cu alloy at 10 atomic percent of Cu is 11.16 and it increases with increase in composition of Cu. The computed values of coordination numbers compared with the available experimental values are also shown in Fig. 4.6.

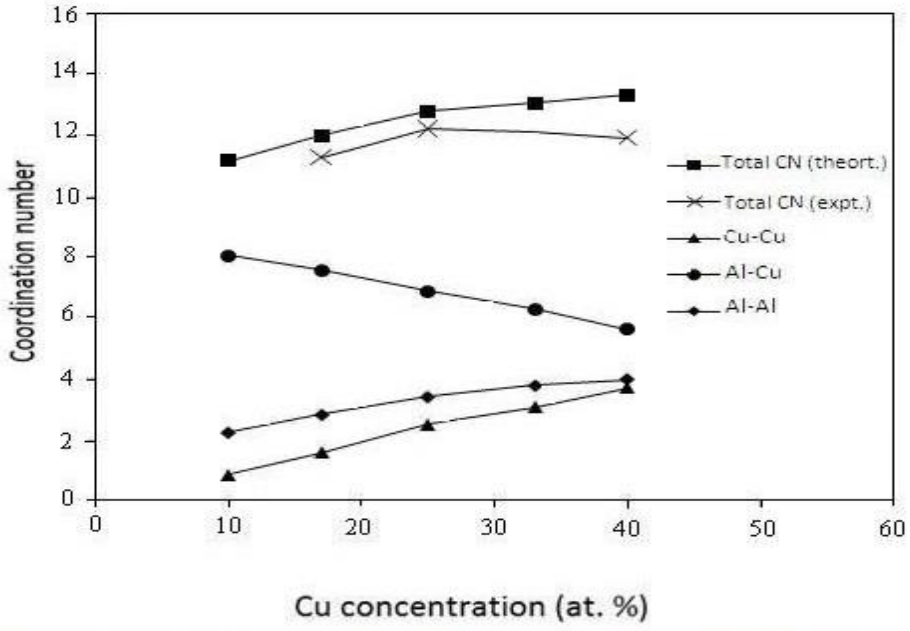

Fig. 4.6. Partial and Total coordination number of liquid Al-Cu alloys at different atomic percent of Cu.

4.3.2. Concentration dependent structural Characteristics in Ag-Cu alloy

4.3.2.1. *Partial and Total Structure factor in Ag-Cu alloys:*

The Ag-Cu alloy is also of great theoretical interest because it resembles a model glass forming with Lennard-Jones potential function (Vardeman and Gezelter, 2001). The SW input parameters σ_{ij}, ε_{ij} and λ_{ij} for Ag-Cu alloys are listed in Table 4.5. Here 1 stands for Cu and 2 for Ag and so σ_{11} corresponds to the diameter of Cu and σ_{22} correspond to the diameter of Ag.

Table 4.5. Input parameters of liquid Ag-Cu alloys with σ as the diameter, ε/k_B as the depth and λ as the breath of the square well potential

% Cu in Ag-Cu	Temp (K)	σ_{ii} (Å)	σ_{jj} (Å)	ε_{ii}/k_B	ε_{jj}/k_B	λ_{ii}	λ_{jj}
16.5	1173	2.39	2.63	300	500	1.68	1.75
28	1138	2.39	2.63	300	500	1.68	1.75
37	1078	2.39	2.63	300	500	1.68	1.75
50	1123	2.38	2.62	300	500	1.68	1.75
71	1193	2.36	2.61	300	500	1.68	1.75
85	1273	2.35	2.60	300	500	1.68	1.75

In the present calculations the concentrations are expressed in terms of atomic fraction of Cu i.e., C_1. The concentration dependent principal peak positions and intensity of PSFs and TSFs are presented in Table 4.6. As seen from Table 4.6, the peak heights and positions of the TSFs is almost constant i.e., this alloy does not show any unusual features with composition and temperature. Lukens and Wagner also observed similar trend in their work on liquid Ag-Cu alloys using X-ray diffraction (Lukens and Wagner, 1975). In Ag-Cu alloys, position of first peak of S(k) is shifting from 2.7 $Å^{-1}$ to 2.9 $Å^{-1}$ as the concentration of Cu increases from 16.5% to 85% and the amplitude of the first peak decreases from 16.5% Cu to 37% Cu after that increases up to 85% Cu. Thus, the positions of the first maxima of TSFs lie between the principal peak positions of liquid Ag and Cu which are 2.6 $Å^{-1}$ and 3.0 $Å^{-1}$ respectively as mentioned in Chapter 2.

Table 4.6. Partial and total structure factors with first peak positions, k and peak heights S(k) of Ag-Cu alloys at different compositions of Cu.

% Cu in Ag-Cu	Temp (K)	k(Å^{-1})	S_{11}(k)	k(Å^{-1})	S_{22} (k)	k(Å^{-1})	S_{12}(k)	k(Å^{-1})	S(k)
16.5	1173	2.8	1.25	2.7	2.53	2.7	0.64	2.7	2.76
28	1138	2.8	1.45	2.7	2.33	2.7	0.75	2.7	2.70
37	1078	2.8	1.60	2.7	2.15	2.8	0.84	2.7	2.60
50	1123	2.8	1.83	2.8	1.92	2.8	0.93	2.8	2.70
71	1193	2.9	2.22	2.8	1.56	2.8	0.82	2.8	2.60
85	1273	2.9	2.53	2.8	1.29	2.9	0.69	2.9	2.75

The increase in the height of the peaks with increase in atomic percent of Cu from 37% to 85% suggests the amount of forming bonds increases and those Cu atoms forms Cu-Cu cluster in the Ag-Cu melts. Similar trend was observed for the same alloy at different composition of Cu (Lukens and Wagner, 1974). The increase in heights of the peaks with increase in atomic percent of Cu from 37% to 85% and the shifting of the peak position from 2.7 to 2.9 Å suggests that the TSFs is shifting towards liquid Cu structure factor.

TSFs in entire momentum space along with their experimental values (Lukens and Wagner, 1975) were illustrated in Fig. 4.7.

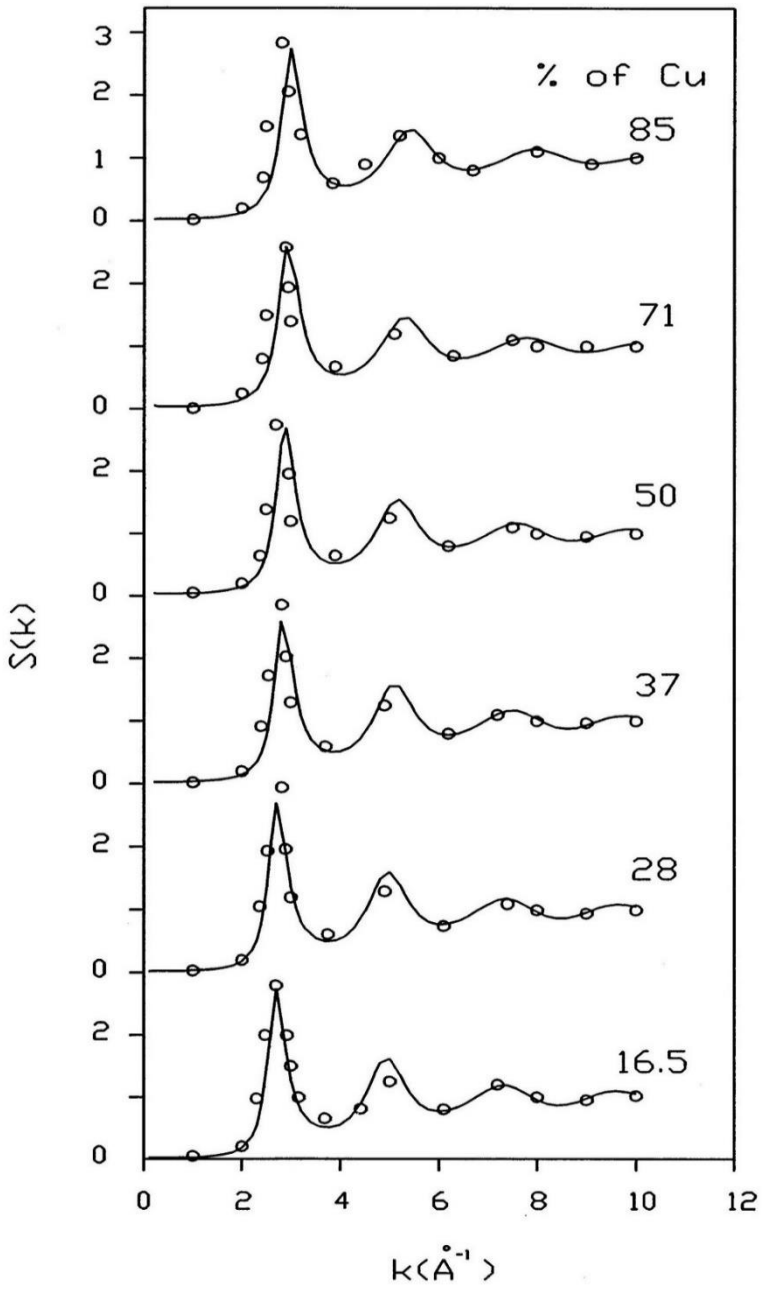

Fig. 4.7. S(k) versus k at different atomic percent of Cu in Ag-Cu alloys. (——) presents theoretical values, (o o o) experimental values.

We present the concentration dependent partial structure factor related to Cu-Cu atomic distribution i.e, $S_{11}(k)$, Ag-Ag atomic distribution i.e, $S_{22}(k)$ and Ag-Cu atomic distribution i.e, $S_{12}(k)$ in liquid Ag-Cu alloys at different concentrations ranging from

16.5 to 85 atomic percent of Cu in Figs. 4.8 to 4.10. It is observed that the peak positions and peak heights of $S_{11}(k)$ increases with increase in the concentration of Cu and it will come towards the pure Cu as mention in Chapter 2.

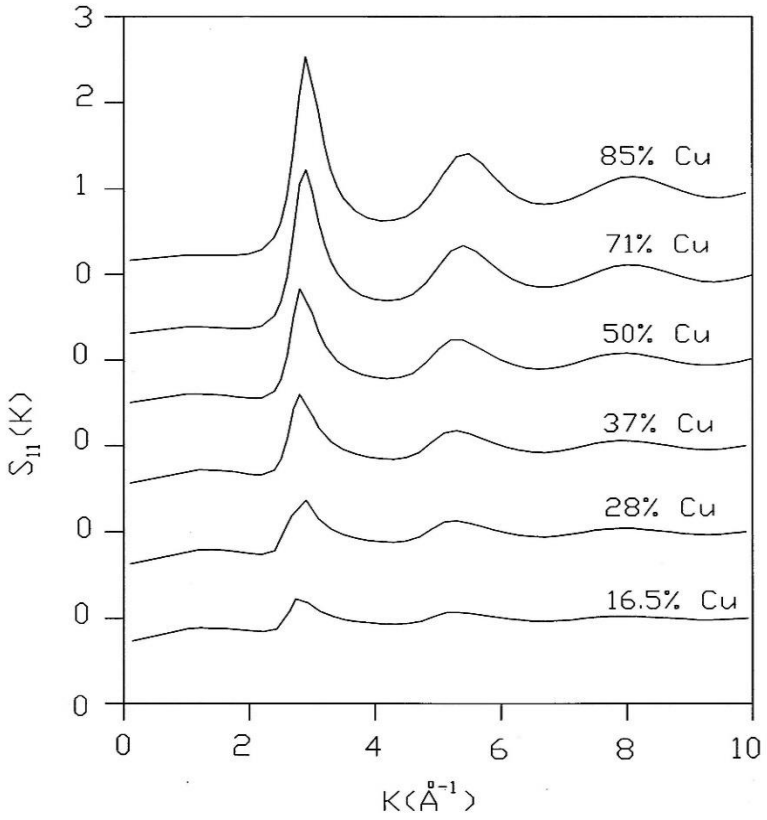

Fig. 4.8. $S_{11}(k)$ versus k at different atomic percent of Cu in Ag-Cu alloys.

One can see from Fig. 4.8 that the curvature of $S_{11}(k)$ i.e. the peak height increases with increasing concentration of Cu in lower k region. At low concentration of Cu, the tendency for complex formation of Ag in Ag-Cu is maximum which indicates low curvature in Cu-Cu correlation. As seen from Fig. 4.9 that the $S_{22}(k)$ curvature increases with increasing concentration of Ag and with increase in the concentration of Ag i.e, at 85 atomic percent of Cu only less curvature is seen as shown in Fig. 4.9.

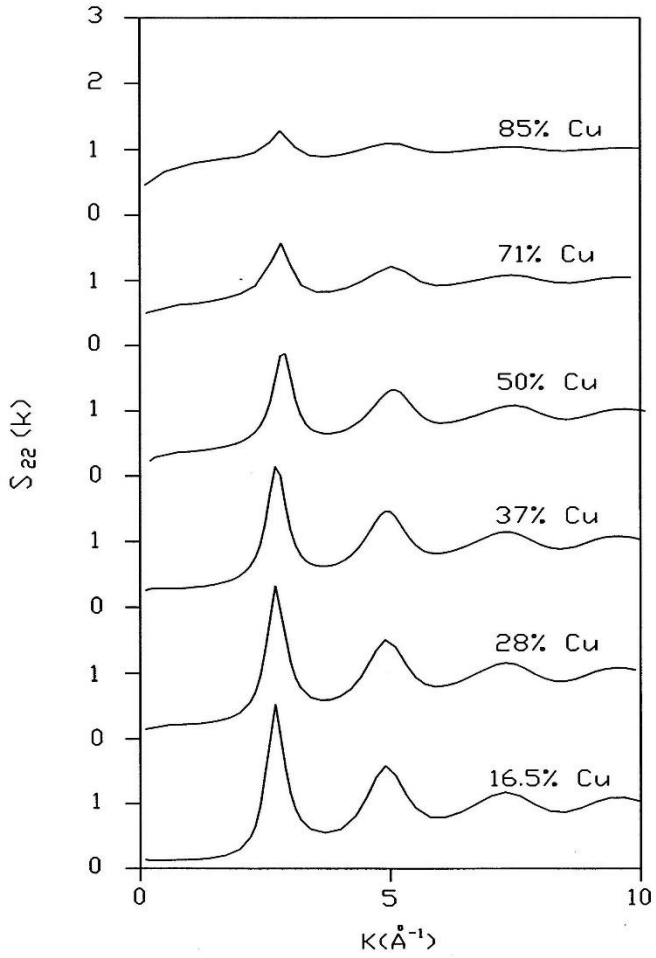

Fig. 4.9. $S_{22}(k)$ versus k at different atomic percent of Cu in Ag-Cu alloys

It can be seen from Fig. 4.9 that the $S_{22}(k)$ peak height decreases with increasing concentration of Cu. This decrease in curvature height in low k region beyond 50 atomic percent of Cu shows the complex formation tendency between Ag and Cu.

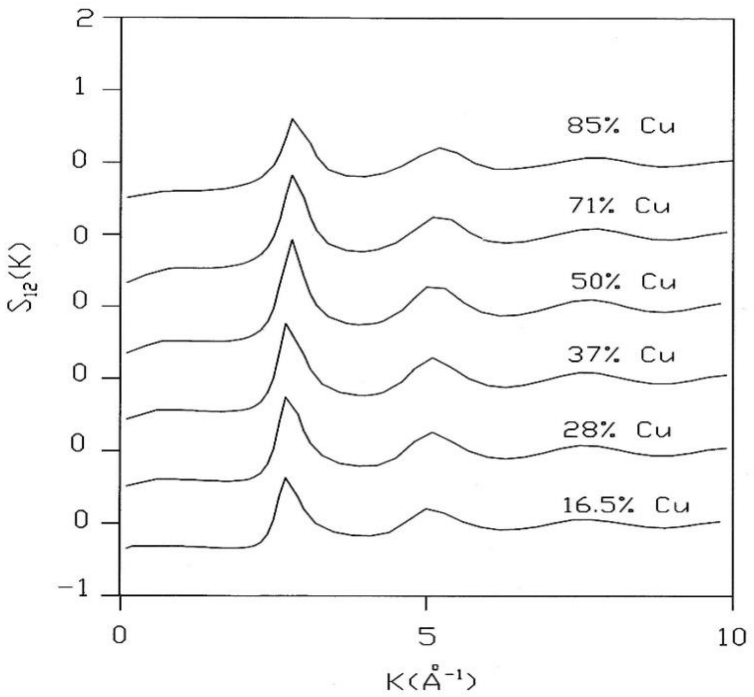

Fig. 4.10. $S_{12}(k)$ versus k at different atomic percent of Cu in Ag-Cu alloys.

As shown in Fig. 4.10, there is only small peak at lower k region in $S_{12}(k)$. Similar structures were obtained for liquid Ag-Sn alloys (Gopala Rao and Satpathy, 1990) and Ag-In alloys (Venkatesh et al., 2003). The peak height of $S_{12}(k)$ increases from 16.5 to 50 atomic percent of Cu and again decreases at higher atomic percent of Cu. This may be due to the segregation tendency of Cu atom in Ag-Cu melts. Such segregation tendency of Cu in binary melts has been discussed above and also explained by the computation of concentration fluctuation in the long wave length limit and chemical short range order parameter in Chapter 5.

4.3.2.2. *Partial and Total radial distribution functions in Ag-Cu alloys*:

The Fourier transform of the PSFs and TSFs give partial and total radial distribution functions in binary melts. The PRDFs, $g_{ij}(r)$ and total radial distribution

function, g(r) along with nearest neighbor distance between Cu-Cu (r_{11}), Ag-Ag (r_{22}) and Ag-Cu (r_{12}) are shown in Table 4.7. The peak positions of the partial radial distribution functions $g_{11}(r)$ and $g_{22}(r)$ are practically identical with those observed in pure Cu and Ag respectively which was also shown by Lukens and Wagner in their experiment on Ag-Cu alloys using X-ray diffraction (Lukens and Wagner, 1975). The inter-atomic distance (peak position of g(r)), r_{max} decreases from 2.77Å to 2.67Å with increase in concentration of Cu except 28% which is the eutectic compositions of the alloys. This may be the reason of Cu-Cu cluster formation in Ag-Cu melts. Ag-Ag separation is increasing with increasing Cu concentration shows that the shifting of $g_{22}(r)$ towards pure Ag radial distribution function. The position of the first maxima in g(r) of Ag-Cu alloys at different compositions of Cu are also lie in between that of the g(r) of pure Ag and Cu (i.e., in between 2.5 Å to 2.8 Å).

Table 4.7. Partial and total radial distribution function with first peak positions, *r* and peak heights g(r) of Ag-Cu alloys at different compositions of Cu.

% Cu in Ag-Cu	Temp K	r_{11}(Å)	$g_{11}(r)$	r_{22}(Å)	$g_{22}(r)$	r_{12}(Å)	$g_{12}(r)$	r_{max}(Å)	g(r)
16.5	1173	2.54	3.25	2.78	3.40	2.66	3.34	2.77	3.21
28	1138	2.67	3.54	2.86	3.74	2.70	3.13	2.83	3.23
37	1078	2.54	3.27	2.78	3.44	2.66	3.36	2.75	3.02
50	1123	2.67	3.45	2.76	3.76	2.69	3.12	2.72	3.13
71	1193	2.65	3.03	2.73	4.16	2.67	3.02	2.69	2.96
85	1273	2.64	2.89	2.72	5.12	2.66	2.98	2.67	2.86

The reduced distribution functions of Ag-Cu alloys are presented in Fig. 4.11 with their corresponding experimental values (Lukens and Wagner, 1975). It is obvious that the agreement between our computed values and the experimental values is satisfactory, which strengthened our present model calculations.

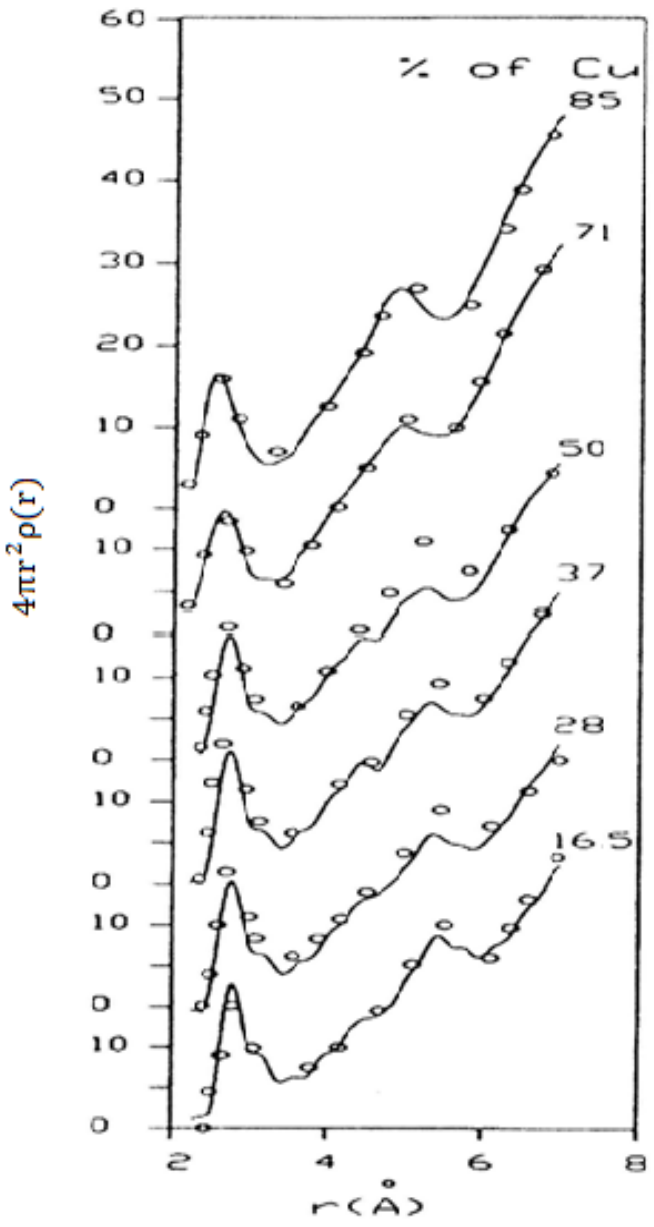

Fig. 4.11. Reduced radial distribution $4\pi r^2\rho g(r)$ versus r at different atomic percent of Cu in Ag-Cu alloys. (—) theoretical values, (o o o) experimental values.

4.3.2.3. *Partial and total coordination number of Ag-Cu alloys*:

The coordination number (partial and total) was obtained by integrating the partial and total radial distribution functions between two minima respectively. The partial coordination number related to Ag-Ag, Cu-Cu and Ag-Cu i.e, Z_{11}, Z_{22} and Z_{12} respectively are given in Table 4.8, the total coordination number, Z at different concentrations of Cu along with their corresponding experimental values are also listed ion Table 4.8. There is a good agreement between the computed values with the available experimental data (Lukens and Wagner, 1975).

Table 4.8. Partial and total coordination number of Ag-Cu alloys at different compositions of Cu.

% Cu in AgCu	Temp K	Z_{11}	Z_{22}	Z_{12}	Total coordination number, Z	
					theort.	expt.
16.5	1173	1.53	9.25	3.01	11.63	11.90
28	1138	1.86	8.78	3.65	12.26	12.25
37	1078	3.58	7.23	3.99	12.11	13.05
50	1123	5.30	6.34	4.32	12.16	13.00
71	1193	8.08	4.12	4.14	12.34	12.75
85	1273	10.07	2.43	3.43	12.35	12.35

The coordination number of Cu-Cu varies from 1.53 to 8.33 when the atomic percent of Cu increases from 16.5 to 85%, while the coordination number of Ag-Ag

decreases from 9.25 to 2.43. These variations support our calculation for separation between Ag-Ag and Cu-Cu in atomic dimension as above.

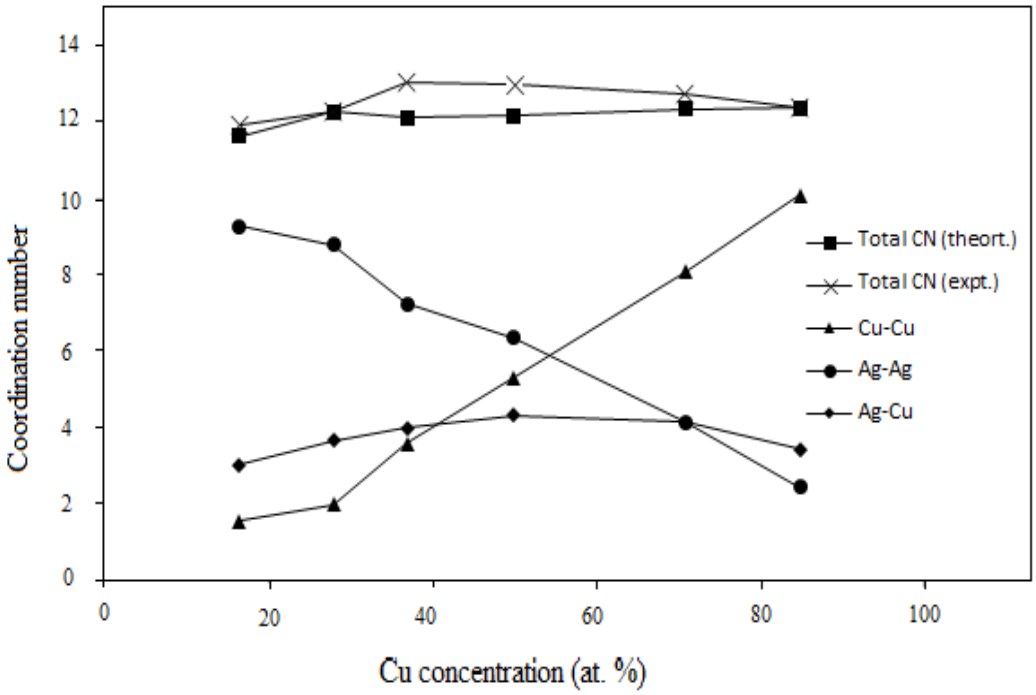

Fig. 4. 12. Partial and total coordination number of liquid Ag-Cu alloys at different atomic percent of Cu.

5. BHATIA - THORNTON FLUCTUATIONS AND ASSOCIATED PROPERTIES OF LIQUID ALLOYS

5.1. INTRODUCTION

The knowledge of the structural and thermodynamic properties is essential for understanding the nature of ordering in liquid alloys (Odusote, 2008). Liquid alloys are disordered materials which have short range order and it is more difficult to understand their complexities. Therefore, it requires extensive theoretical investigation to understand the complexities of liquid binary alloys (Koirala et al., 2014). Different theoretical models have been proposed to describe the concentration dependence of thermodynamic properties of liquid binary systems (Tribula et al., 2015).The well-known Bhatia-Thornton (BT) (Bhatia and Thornton, 1970) partial structure factors namely the number – number correlation function $S_{NN}(k)$, the concentration – concentration correlation function $S_{CC}(k)$, and the number-concentration correlation functions $S_{NC}(k)$ were determined in liquid Al-Cu and Ag-Cu alloys at various atomic percent of Cu using square well model of PSFs which are presented in Chapter 4. These functions in the binary mixture occur because of changes in number density and concentration of the constituent elements and characterize the different correlation between local density (N) and concentration (C) in it. BT correlation functions are linearly interrelated with Faber-Ziman and Ashcroft-Langreth partial structure factors (Venkatesh et al., 2003) and are of considerable importance to analyze the nature of interactions, particularly if the region of interest is of the order of atomic dimensions. Total structure factor of binary liquid can also be obtained using BT PSFs. Bhatia-Thornton mentioned in their paper that these number and concentration dependent fluctuation in

binary liquids decides various properties of liquids. The property of these fluctuations at long wavelength limit i.e., at k→0 is directly related to various thermodynamic properties. In long wavelength limit these PSFs are referred as $S_{NN}(0)$, $S_{CC}(0)$ and $S_{NC}(0)$ respectively (Bhatia and Thornton, 1970) and can be calculated directly from the thermodynamic properties of the alloys.

Mathematical representation of $S_{NN}(k)$, $S_{CC}(k)$ and $S_{NC}(k)$ as (Bhatia and Thornton, 1970).

$$S_{NN}(k) = \frac{1}{N} < N^*(k)N(k) > \tag{5.1}$$

$$S_{CC}(k) = N < C^*(k)C(k) > \tag{5.2}$$

$$S_{NC}(k) = Re < N^*(k)C(k) > \tag{5.3}$$

*represents the complex conjugate.

These number-concentration fluctuations have proved to be of great significance as they provide topological and chemical short range order in the system.

The Fourier transformations of $S_{NN}(k)$ and $S_{CC}(k)$ give radial number fluctuation, $4\pi r^2\rho_{NN}(r)$ and radial concentration fluctuations, $4\pi r^2\rho_{CC}(r)$ respectively, which describe the global or the topological short-range order and the Warren-Cowly short-range order parameters (Singh and Somer, 1997; Venkatesh et al., 2003).

The concentration-concentration fluctuation in the long wavelength limit $S_{CC}(0)$,is an important parameter to understand the structure and the binding of atoms at microscopic level. It is related to theordering effects in binary liquid alloys (Tribula et al., 2015).

The $S_{CC}(0)$ is an important parameter for the study of the thermodynamic properties (Trybula et al., 2015; Alblas and Vander lutg, 1982; Dahlborg et al., 2013; Ivanov and

Berezutski, 1996; Odusote, 2008), the glass formation tendency (Singh et al., 1991) and various transport properties (Novakovic et al., 2005; Cheng et al., 2009; Jakse and Pasturel, 2015; Singh and Somer, 2006) of the liquid alloys.

However, these PSFs in the long wavelength limit as $k \rightarrow 0$ can be given as

$$S_{NN}(0) = \frac{N}{V} k_B T \beta_T + \delta^2 S_{CC}(0) \tag{5.4}$$

$$S_{CC}(0) = N k_B T \left(\frac{d^2 G}{dC^2} \right)_{T,P,N} \tag{5.5}$$

$$S_{NC}(0) = -\delta' S_{CC}(0) \tag{5.6}$$

where β_T is the isothermal compressibility, G is the free energy, P is the pressure, and δ' is the dilation factor defined as

$$\delta' = \frac{v_1 - v_2}{c v_1 + (1-c) v_2} = \frac{N}{V}(v_1 - v_2) \tag{5.7}$$

where v_1 and v_2 are the partial molar volume per atom of the two species.

For $k \rightarrow \infty$, i.e. for completely uncorrelated system

$S_{NN}(k) \rightarrow 1, S_{CC}(k) \rightarrow C_A C_B$ and $S_{NC}(k) \rightarrow 0$

In this chapter, a detailed analysis of the BT correlation functions using square well (SW) model approach (Gopala Rao and Venkatesh, 1989; Venkatesh et al., 2003) for liquid Al-Cu alloys and Ag-Cu alloys at different atomic percent of Cu have been determined. The thermodynamically important concentration-concentration fluctuations, $S_{CC}(0)$ have also been theoretically evaluated unlike other workers who have computed this property for alloys through equations fitted with experimentally evaluated thermodynamic parameters and calculated back the same property or their derived properties (Singh and Somer, 1992;

Awe and Olawole, 2012). The microscopic function, the chemical short range order parameters (CSRO) α', which can be perceived from the $S_{CC}(0)$ gives information regarding the ordering and segregating in liquid alloys at atomic scale (Odusote, 2008). Further isothermal compressibility as a function of Cu concentration has been computed from the Kirkood-Buff formula (Venkatesh et al., 2003; Mishra and Venkatesh, 2008).

The concentration-concentration correlation function in the long wavelength limit, $S_{CC}(0)$, have been evaluated through model proposed by Venkatesh and Mishra (Venkatesh and Mishra, 2005; Mishra and venkatesh, 2008).

5.2. THEORY

The BT partial structure factors were calculated using AL type partial structure factors of Al-Cu and Ag-Cu liquid alloys.

The BT correlation functions in binary alloys are linearly related to the partial structure factors $S_{ij}(k)$ (Gopala Rao and Satpathy, 1990; Venkatesh et al., 2003) as follows

$$S_{NN}(k) = C_1 S_{11}(k) + C_1 S_{22}(k) + 2 (C_1 C_2)^{1/2} S_{12}(k)] \tag{5.8}$$

$$S_{CC}(k) = C_1 C_2 [C_2 S_{11}(k) + C_1 S_{22}(k) - 2 (C_1 C_2)^{1/2} S_{12}(k)] \tag{5.9}$$

$$S_{NC}(k) = C_1 C_2 S_{11}(k) - C_1 C_2 S_{22}(k) - (C_2 - C_1) (C_1 C_2)^{1/2} S_{12}(k)] \tag{5.10}$$

where C_1 and C_2 are the atomic fractions of the component 1 and 2 respectively.

The concentration fluctuation, $S_{CC}(0)$,which is an important parameter to understand the structure and the binding of atoms at the microscopic level, is related to ordering effects in binary liquid alloys (Singh, 1987; Singh, 1993). Further $S_{CC}(0)$ can be calculated through the computed PSFs in the long wavelength limits.

$$S_{CC}(0) = C_1C_2\,[C_2\,S_{11}(0) + C_1S_{22}(0) - 2\,(C_1C_2)^{1/2}\,S_{12}(0)] \tag{5.11}$$

The computed partial structure factors presented in Chapter 4 by Eqns. (4.25) to (4.27) of the considered alloys have been derived in the limit of $k \rightarrow 0$. Thus, $S_{11}(0)$, $S_{22}(0)$ and $S_{12}(0)$ are calculated in terms of direct correlation functions in the long wavelength limit i.e. $C_{11}(0)$, $C_{22}(0)$ and $C_{12}(0)$ as

$$S_{11}(0) = \left[\frac{[1-\rho_{11}C_{11}(0) - \rho_1\rho_2C_{12}^2(0)]}{1-\rho_2C_{22}(0)}\right]^{-1} \tag{5.12}$$

$$S_{22}(0) = \frac{[1-\rho_1C_{11}(0)]S_{11}(0)}{1-\rho_2C_{22}(0)} \tag{5.13}$$

$$S_{12}(0) = \frac{(\rho_1\rho_2)^{1/2}C_{12}(0)S_{11}(0)}{1-\rho_2C_{22}(0)} \tag{5.14}$$

Where

$$\rho_1C_{11}(0) = -24\eta_1\left[\frac{a_1}{3} + \frac{b_1\sigma_1}{4} + \frac{d\sigma_1^{\,3}}{6}\right] + \frac{8\eta_1\varepsilon_{11}(\lambda_{11}^3 - 1)}{k_BT} \tag{5.15}$$

$$\rho_2C_{22}(0) = -24\eta_2\left[\frac{a_2}{3} + \frac{b_2\sigma_2}{4} + \frac{d\sigma_2^{\,3}}{6}\right] + \frac{8\eta_2\varepsilon_{22}(\lambda_{22}^3 - 1)}{k_BT} \tag{5.16}$$

$$C_{12}(0) = -\frac{4\pi\varepsilon_{12}\sigma_{12}^3(\lambda_{12}^3 - 1)}{3k_BT} - \frac{4\pi a_1\sigma_{12}^3}{3} - 4\pi\sigma_1^3\left\{\frac{b(\sigma_1 + 2\sigma_2}{12} + \frac{\lambda d\sigma_1(3\sigma_1 + 5\sigma_2)}{10} + \frac{d\sigma_1^2(2\sigma_1 + 3\sigma_2)}{30}\right\} \tag{5.17}$$

Various parameters incorporated in Eqns. (5.12) to (5.17) have their usual notations, which are presented in Chapter 4 in detail.

Chemical short range order parameter, α' can be evaluated theoretically from the knowledge of $S_{CC}(0)$. An interesting relation between α' and $S_{CC}(0)$ for the first neighbor shell is given by

$$\alpha' = \frac{S_{CC}(0) - S_{CC}^{id}(0)}{Z\,S_{CC}(0) - S_1} = \frac{S_1}{Z\,S_{CC}(0) - S_1} \tag{5.18}$$

Here $S_{CC}^{id}(0) = C_1 \times C_2$ and S_1 is the deviation of the $S_{CC}(0)$ from its ideal value, Z is the total coordination number.

The concentration dependent isothermal compressibility β_T has been calculated through the Kirkwood-Buff's equation (Mishra and Venkatesh, 2008), which is given by

$$\rho k_B T \beta_T = [1 - c_1\rho_{11}\,C_{11}(0) + c_2\rho_{22}C_{22}(0) - 2\,C_1C_2(\rho_1\rho_2)^{1/2}\,C_{12}(0)]^{-1} \tag{5.19}$$

5.3. RESULTS AND DISCUSSION

The computations for the alloys were performed at different concentrations using potential parameters of the pure components. Thus the significance of the work is the evaluation of the thermodynamic and structural properties from the potential energy parameters of pure components.

5.3.1. Al-Cu Alloys

The potential parameters of the pure components for the evaluation of partial structure factors have shown in Table 4.1 in Chapter 4. The thermodynamically important correlation functions $S_{NN}(k)$, $S_{CC}(k)$ and $S_{NC}(k)$ are given in Figs. 5.1 to 5.3.

It can be seen from Fig. 5.1 that the peak position of $S_{NN}(k)$ at different concentration of Cu lies in between 2.70 $Å^{-1}$ and 2.80 $Å^{-1}$. $S_{NN}(k)$ varies in a similar manner

to the total structure factor S(k) and that is also similar in other cases as well (Venkatesh et al., 2003; Gopala Rao and Satpathy, 1990; Gopala Rao and Das Gupta; 1985). The peak maximum occurs at the same position as in the case of S(k) and the peak value increases as the atomic percent of Cu increases. The value of $S_{NN}(k)$ tends to one in higher k region. It may be noted that at all concentrations $S_{NN}(k)$ shows two conspicuous first and second peaks thus showing a strong number-number correlation in the momentum space (Mishra and Venkatesh, 2008).

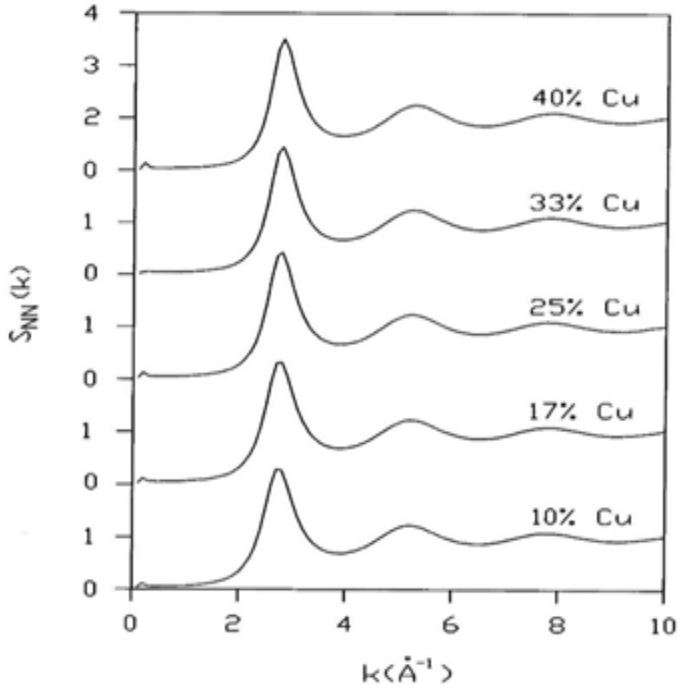

Fig. 5.1. $S_{NN}(k)$ against k for Al-Cu alloys at different atomic percent of Cu

The $S_{CC}(k)$ oscillates about the product of their atomic percent i.e. C_1C_2. There is a slight maximum around 2Å^{-1} at all compositions and this maximum increases with increasing concentration of Cu whereas become constant in higher k-region at all Cu% in Al-Cu melts. Thus the significant oscillation of $S_{CC}(k)$ was only observed in low k side

only. This increase in curvature of concentration fluctuation with increase in Cu% clearly shows a segregating behavior of the constituents of alloys.

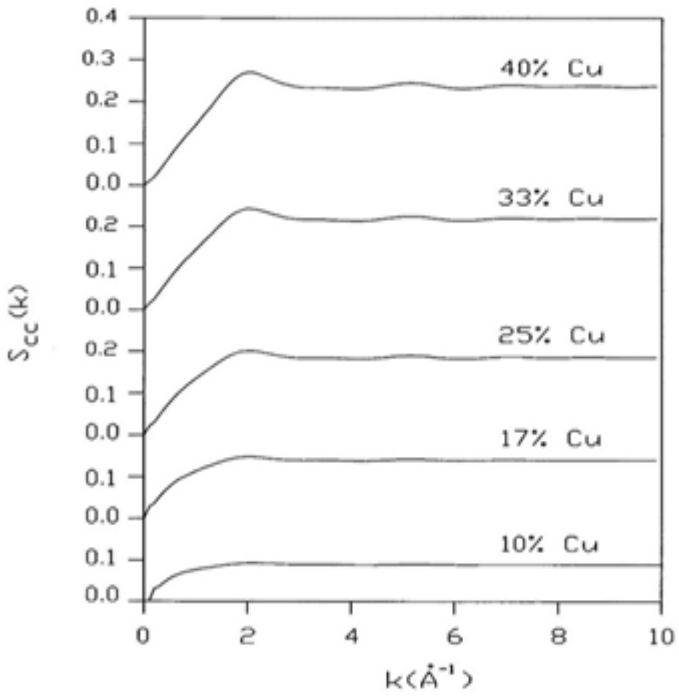

Fig. 5.2. $S_{CC}(k)$ against k for Al-Cu alloys at different atomic percent of Cu

The $S_{NC}(k)$ shown ion Fig. 5.3 oscillates around zero. There is a slight minimum at or near the peak point of S(k). The similar behavior was observed in Ag-Sn alloy (Gopala Rao and Satpathy, 1990), Ag-In alloy (Venkatesh et al., 2003) and Al-Si alloy (Mishra and Venkatesh, 2008). This minimum increases with increase in the atomic percent of Cu. At around 4Å^{-1} there is a slight maximum, which also increases with increase in atomic percent of Cu. In low k region, it may be noted that $S_{NN}(k)$ and $S_{NC}(k)$ varies inversely in magnitude and latter correlation function tends to zero as $k\rightarrow\infty$.

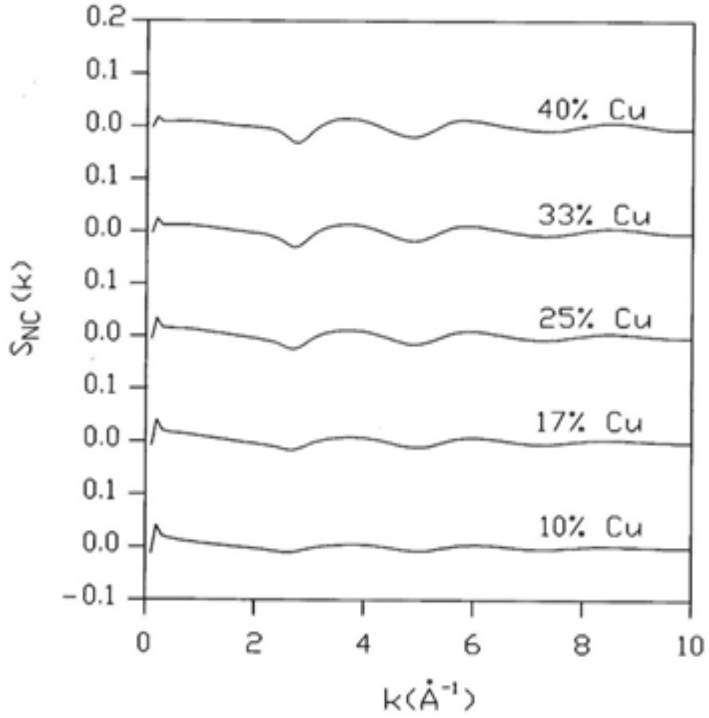

Fig. 5.3. $S_{NC}(k)$ against k for Al-Cu alloys at different atomic percent of Cu

The computed values of $S_{CC}(0)$ as a function of atomic fraction of Cu for liquid Al-Cu alloys along with the ideal values, $S_{CC}^{id}(0)$ are given in Table 5.1. The values of the coordination number of Al-Cu at different compositions were taken from Chapter 4. It may be observed from Table 5.1 that there is a slight positive deviation of $S_{CC}(0)$ from its corresponding ideal values at all compositions taken under investigation.

The deviation of $S_{CC}(0)$ from its ideal value is an important factor for the description of the nature of atomic interactions in the mixture. $S_{CC}(0)<S_{CC}^{id}(0)$ shows the presence of chemical ordering while $S_{CC}(0)>S_{CC}^{id}(0)$ shows segregation in the melts (Singh, 1987; Singh, 1993).

Table 5.1. The concentration-concentration fluctuation at the long wavelength limit $S_{CC}(0)$ and its ideal value, $S^{id}_{CC}(0)$, Co-ordination number, *Z* and Chemical short range order parameter, α' of Al-Cu alloys at different compositions of Cu.

% of Cu in Al-Cu alloys	$S_{CC}(0)$	$S^{id}_{CC}(0)$	Co-ordination number, *Z*	α'
10	0.0991	0.0900	11.16	0.00797
17	0.1576	0.1411	11.99	0.00881
25	0.2201	0.1875	12.78	0.01236
33	0.2698	0.2211	13.06	0.01402
40	0.3004	0.2400	13.32	0.01533

The chemical short-range order parameter, α' at different atomic percent of Cu was given in the same table. This ordering parameter, α' can used to quantify the ordering or segregation effects in the melts. For liquid binary alloy, α' is foundto be within the range of -1 to +1. Negative value means ordering in the melts and positive value of indicates the segregation nature (Singh and Somer, 1997).

For more clear understanding the nature of alloys in entire range of concentrations, $S_{CC}^{id}(0)$, $S_{CC}(0)$ vs concentration of Cu and α'vs concentration of Cu were presented in Fig. 5.4 and Fig. 5.5 respectively.

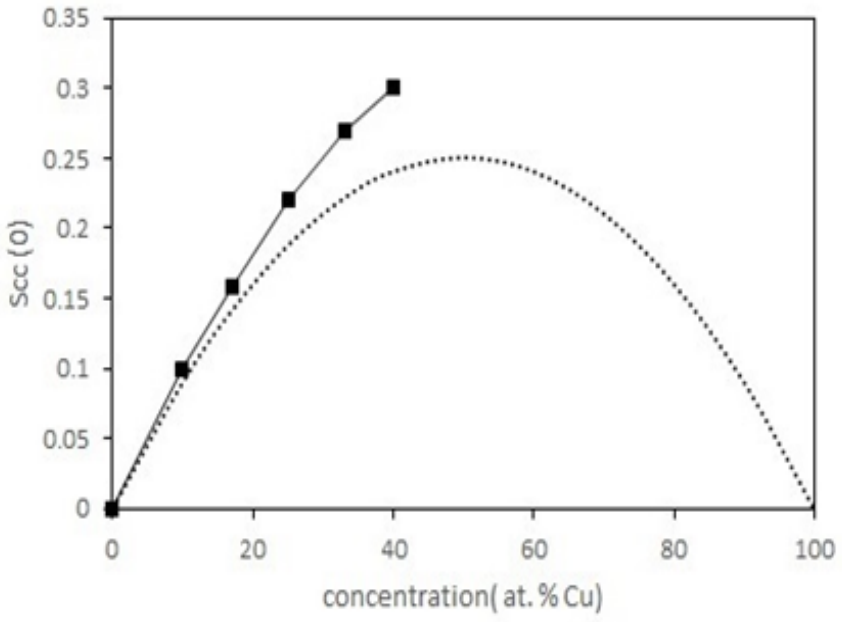

Fig. 5.4. Scc(0) versus atomic percent of Cu in Al-Cu alloys, (-----) represents ideal value and (——) theoretical

The negative deviation of $S_{CC}(0)$ from the ideal value informs the complex formation and the positive deviation of $S_{CC}(0)$ from the ideal value shows segregation in the alloy. The computed values of $S_{CC}(0)$ show a positive deviation from its ideal values at all concentrations, which means there is the segregation tendency in Al-Cu alloys. Further the computed values of chemical short range order parameter, α' is also given in Table 5.1 as well as in Fig. 5.5. The values of α' at different atomic percent of Cu has positive values ranges from 0.008 to 0.015 indicating segregation of the constituents atoms.

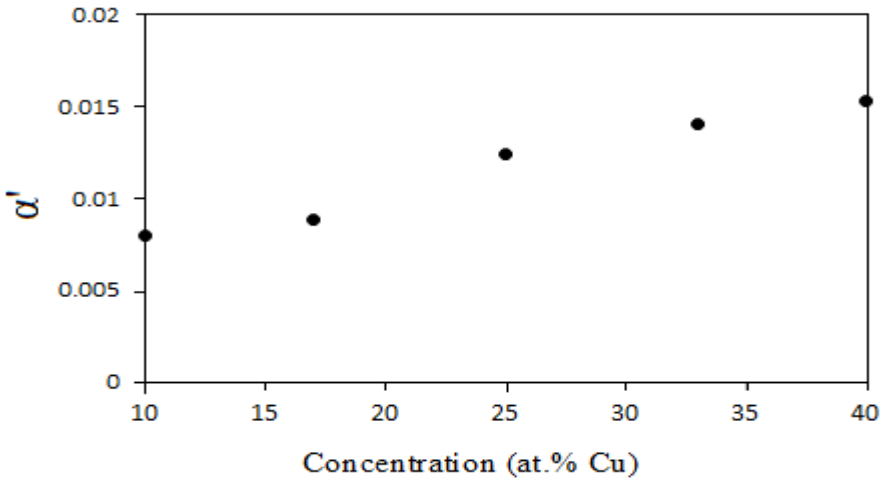

Fig. 5.5. The chemical short range order parameter, α' versus atomic percent of Cu in Al-Cu alloys

The partial structure factors in the long wavelength limit $S_{11}(0)$, $S_{22}(0)$, $S_{12}(0)$ were employed to obtained the concentration dependent isothermal compressibility, β_T in the melts and these values are presented in Table 5.2.

Table 5.2. $S_{11}(0)$, $S_{22}(0)$ and $S_{12}(0)$ and isothermal compressibility, β_T ($10^{-11}m^2\ N^{-1}$) of Al-Cu alloys at different compositions of Cu.

% of Cu in Al-Cu alloys	$S_{11}(0)$	$S_{22}(0)$	$S_{22}(0)$	$\beta_T \times 10^{-11}$ ($m^2\ N^{-1}$)
10	0.984	0.128	-0.284	6.53
17	0.964	0.194	-0.377	6.06
25	0.919	0.289	-0.477	5.81
33	0.859	0.392	-0.548	4.63
40	0.792	0.488	-0.594	4.16

The computed values of β_T at different compositions of Cu have been computed by Eqn. (5.13) and the values are found to decrease with increasing atomic percent of Cu. The computed values of isothermal compressibility of pure liquid Al and Cu are 5.91 (10^{-11} m^2 N^{-1}) and 2.00 (10^{-11} m^2 N^{-1}) respectively, which are given in Chapter 3. The compressibility of Al-Cu alloys was found to decreasewith increase in concentration of Cu as expected. This model calculation gives good result for the calculation of thermo physical properties of liquid binary alloys.

5.3.2. Ag-Cu Alloys

The potential parameters used for the calculations of correlation functions in Ag-Cu alloys are given in Table 4.5 of Chapter 4. The thermodynamically important BT correlation functions $S_{NN}(k)$, $S_{CC}(k)$ and $S_{NC}(k)$ for Ag-Cu alloys at different atomic percent of Cu are given in Figs. 5.6 to5.8.

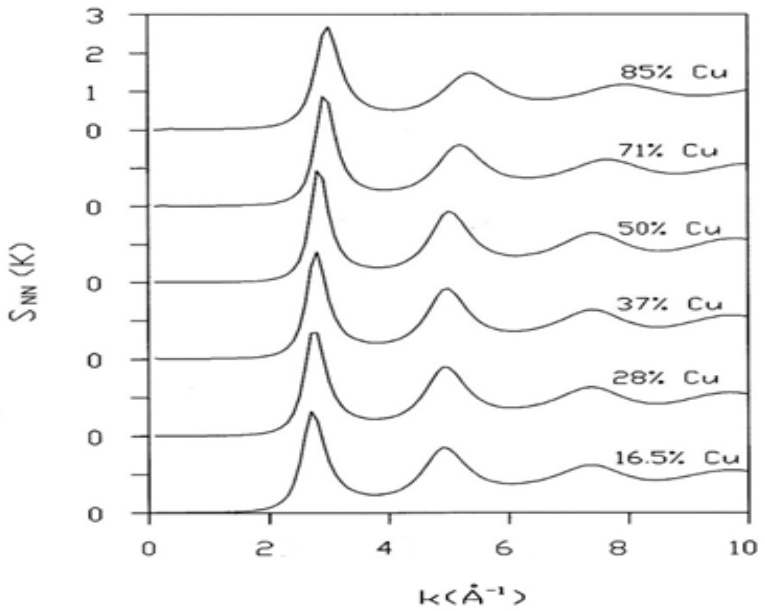

It can be seen from Fig. 5.6 that the $S_{NN}(k)$ of Ag-Cu alloys at different atomic percent of Cu shows a great first peak in low k-region and peak position shifts from 2.7$Å^{-1}$ to 3.0$Å^{-1}$ and the peak become weaker and broader at higher k-region. Thus the oscillation of the $S_{NN}(k)$ similar to that of S(k) that is also similar in other cases as well (Venkatesh et al., 2003; Gopala Rao and Satpathy, 1990; Gopala Rao and Das Gupta; 1985). The presence of strong second peak at all compositions is due to strong number-number correlation in the melts.

The computed values of $S_{CC}(k)$ are shown in Fig. 5.7. It was observed that $S_{CC}(k)$ oscillates about the product of their atomic percent i.e. C_1C_2.

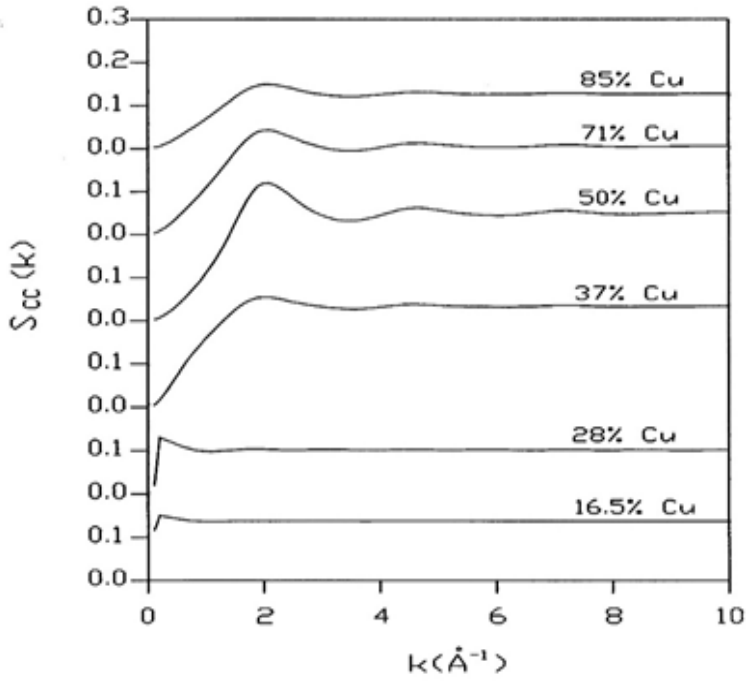

Fig. 5.7. $S_{CC}(k)$ against k for Ag-Cu alloys at different atomic percent of Cu.

It can be observed from Fig. 5.7 that there is a small peak at low concentrations of Cu i.e.at 16.5% and 28% Cu in Ag-Cu alloys near 0.2$Å^{-1}$. At higher concentrations of Cu,

i.e., from 37% Cu to 85%, there is a maximum at 2.1Å^{-1} and this maximum in $S_{CC}(k)$ graph decreases as the atomic percent of Cu increases. This concentration fluctuations showthe segregating tendency of the constituents of the alloys.

It can be observed from Fig. 5.7 that the $S_{CC}(k)$ is only short-ranged correlation in this alloy. The cross correlation function, $S_{NC}(k)$ of Ag-Cu alloys is also shown in Fig. 5. 8.

The computed values of the $S_{NC}(k)$ shown in Fig. 5.8 oscillate around zero. There is a slight maximum at or near the peak point of S(k) i.e., around 2.7Å^{-1}. This maximum increases as the atomic percent of Cu is increases. It can be seen that there is small second peak at higher concentration of Cu.

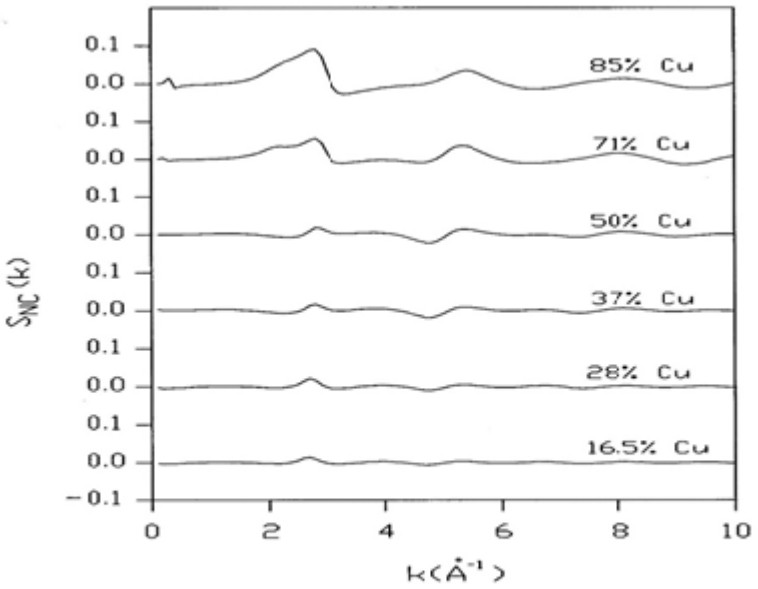

Fig. 5.8. $S_{NC}(k)$ against k for Ag-Cu alloys at different atomic percent of Cu.

The computed values of $S_{CC}(0)$ at different atomic percent of Cu in liquid Ag-Cu alloys are given in Table 5.3 and are also shown in Fig. 5.9 along with their ideal values. The coordination number of Ag-Cu at different compositions was taken from Chapter 4.

This coordination number were employed in the calculation of α' through Eqn. 5.18. It can be seen from Table 5.3 that the values of α' for Ag-Cu alloys at all compositions show positive values which indicates segregating tendency in the alloys.

Table 5.3. The concentration-concentration fluctuation at the long wavelength limit, $S_{CC}(0)$ and its ideal value, $S_{CC}^{id}(0)$, Co-ordination number, Z and Chemical short range order parameter, α' of Ag-Cu alloys at different compositions of Cu.

% of Cu in Ag-Cu alloys	$S_{CC}(0)$	$S^{id}_{CC}(0)$	Z	α'
16.5	0.1383	0.1378	11.63	0.00031
28	0.2029	0.2016	12.26	0.00052
37	0.2352	0.2331	12.11	0.00070
50	0.2531	0.2500	12.16	0.00101
71	0.2127	0.2059	12.34	0.00259
85	0.1319	0.1275	12.35	0.00271

It can be seen from the Table 5.3 that the computed values of $S_{CC}(0)$ is greater than the corresponding ideal values i.e., $S_{CC}(0) > S_{CC}^{id}(0)$ which shows segregation in the melts. This tendency is also supported by the computed CSRO (α') parameter which is given in Fig. 5.10 (Pasturel and Jakse, 2015).

It can be observed from Fig. 5.9 that the deviation of $S_{CC}(0)$ from $S_{CC}^{id}(0)$ increases with increase in atomic percent of Cu up to 71 atomic percent and then it decreases.

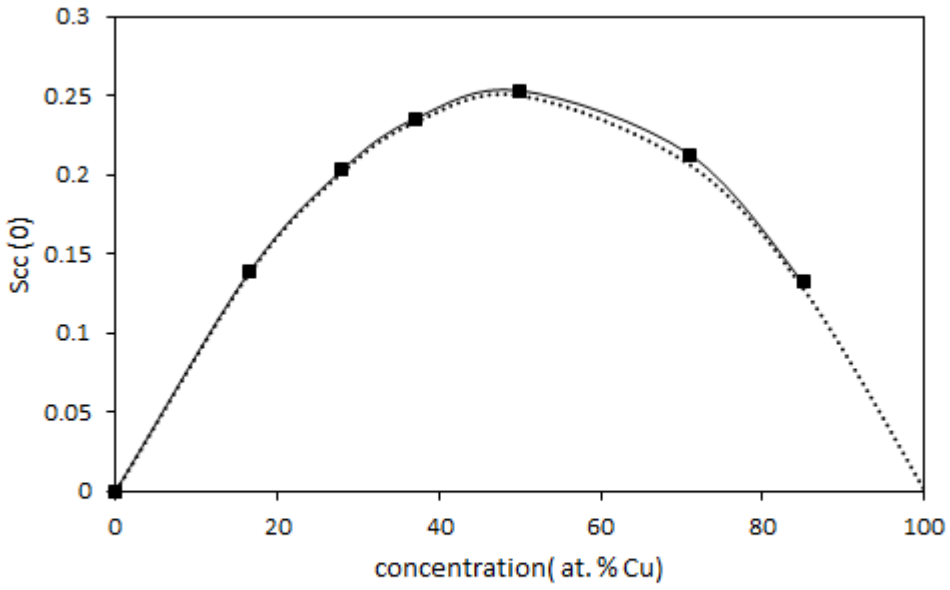

Fig. 5.9. $S_{CC}(0)$ versus atomic percent of Cu in Ag-Cu alloys, (-----) represents ideal value and (——) theoretical

The computed value of $S_{CC}(0)$ has slightly higher value than that of the ideal value at all compositions. Therefore, the alloy is of a weakly interacting nature and the positive value of $S_{CC}(0)$ from its ideal value which is shown in Fig. 5.9 also confirms the segregation in the melts. The positive value of α' also supports the segregating nature.

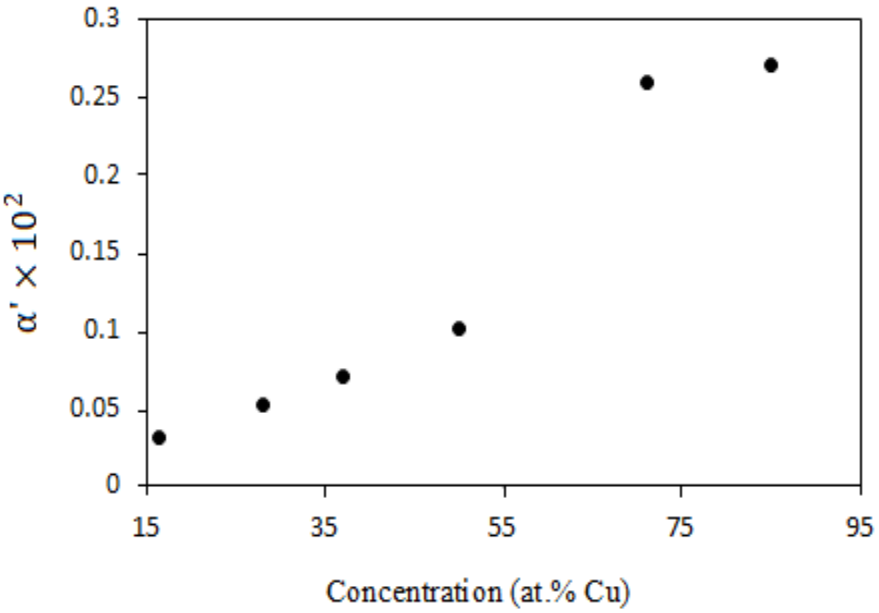

Fig. 5.10. The chemical short range order parameter, α' versus atomic percent of Cu in Ag-Cu alloys

The isothermal compressibility, β_T at different compositions of the melts has been obtained from the well-known Kirkwood-Buff's equation using long wavelength limit of PSFs. The computed values of $S_{11}(0)$, $S_{22}(0)$,$S_{12}(0)$ and β_T are shown in Table 5.4. β_T values are found to decrease with increase in atomic percent of Cu. This shows that as the concentration of Cu increases, the void space between the particles decrease or the existence of compact nature of the alloys is indicated.

Table 5.4. $S_{11}(0)$, $S_{22}(0)$ and $S_{12}(0)$ and isothermal compressibility, β_T ($10^{-11} m^2 N^{-1}$) of Ag-Cu alloys at different compositions of Cu at 1373K.

% Cu in Ag-Cu	$S_{11}(0)$	$S_{22}(0)$	$S_{12}(0)$	$\beta_T \times 10^{-11}$ ($m^2 N^{-1}$)
16.50	0.8962	0.12657	-0.3148	1.447
21.65	0.8603	0.1638	-0.3570	1.459
28.00	0.8134	0.2132	-0.3999	1.463
37.00	0.7417	0.2876	-0.4472	1.453
39.76	0.7184	0.3116	-0.4589	1.447
50.00	0.6223	0.4111	-0.4921	1.466
63.43	0.4862	0.5479	-0.5022	1.447
71.00	0.4123	0.6415	-0.4985	1.578
85.00	0.2383	0.8172	-0.4221	1.471
86.38	0.2189	0.8334	-0.4074	1.447
97.39	0.0562	0.9681	-0.1959	1.206

Further, Ag being a soft metal is segregated from Cu and as the concentration of Cu increases the compressibility decreases which it should as pure Ag is soft and is used to harden by alloying with Cu.The compressibility of pure Ag and Cu are 2.5 (10^{-11} m^2 N^{-1}) and 2.0 (10^{-11} m^2 N^{-1}) respectively, the computed results for alloys throughout the concentrations is less than 2. From Table 5.4 one can see that compressibility is decreases at higher composition of Cu. Hence the magnitudes of compressibility are definitely of right order.

6. TRANSPORT, SURFACE AND SCALING PROPERTIES IN LIQUID BINARY ALLOYS.

6.1. INTRODUCTION

In recent years considerable efforts have been made to determine the temperature and concentration dependent atomic transport properties (diffusion coefficient and viscosity) in liquid binary alloys (Novakovic, et al.,2005; Vardeman and Gezelter, 2001; Brillo et al., 2008; Zhang, et al., 2010; Cheng et al., 2009; Singh and Somer, 1997; Dahlborg et al, 2013; Venkatesh et al, 2003; Mishra and Venkatesh, 2008; Echendua et al., 2010; Wang et al., 2009; Pasturel and Jakse, 2015; Wang et al., 2015; Cao et al., 2016). The concentration dependent self, intrinsic and mutual diffusion coefficients were determined in Al-Cu and Ag-Cu melts over a wide composition range. The knowledge on the basic laws of mass, momentum and energy transport in materials is the subject of interest and an important topic for scientists and engineers. A detail understanding of the momentum transport (viscous flow), energy transport (heat conduction, convection and radiation), mass transport (diffusion), electron transport (conductivity) has become one of the biggest challenge in the field of science and technology, and are the interesting subject to investigate. The transport properties like diffusion coefficients are also among the basic parameters for materials design from the melts. The dynamical properties like self-diffusion coefficients of a liquid binary system can be calculated by several methods (Hansen and McDonald, 1986; Shimoji and Itami, 1986; Nath and Joarder, 2005; Venkatesh and Mishra, 2005; Brillo et al., 2008; Jakse and Pasturel 2016). The diffusion coefficient D, in a binary

mixture A-B mixture is defined by Fick's law which correlates the flow of the component A (per unit area), J_A and its concentration gradient ∇C_A is given by

$$J_A = -D_{AB} \nabla C_A \tag{6.1}$$

Another transport coefficient, i.e. the shear viscosity coefficient η of a fluid is a proportionality constant between the shearing force F_S and the velocity gradient ∇V. Thus if the fluid motion is in the x – direction then it is written as

$$F_S = \eta \left(\frac{\partial V_x}{\partial V_y}\right) \tag{6.2}$$

Further, χ, the coefficient of thermal conduction, which is also proportionality constant between thermal flux q and temperature gradient ∇T is given by

$$q = -\chi \nabla T \tag{6.3}$$

and the electrical conductivity, (reciprocal of resistivity) σ_e is related to the electrical current density J_e and the electric field E (i.e. the potential gradient $-\nabla\varphi_e$) is given by

$$J_e = \sigma_e E = -\sigma_e \nabla \varphi_e \tag{6.4}$$

The simultaneous occurrence of two or more phenomenon results in cross phenomenon caused by interference. For example we have thermoelectric effect Q' produced by placing metal junctions at different temperatures. Thus, the thermoelectric power Q' is defined by

$$Q' = -\frac{\nabla \varphi_e}{\nabla T} \tag{6.5}$$

Another example of interference phenomenon in condensed phases is the so called Soret effect caused by diffusion coupled with heat conduction (thermal diffusion). Here the concentration gradient is formed as a result of temperature gradient.

These cross effects can be described by Onsager relations (Peng et al., 2015; Jakse and Pasturel, 2015; Zhang et al., 2010).

In the present chapter an investigation on mass transport i.e. diffusion coefficient is considered in detail. It may be noted that the transport coefficients of dense classical fluids is extremely complex. The transport properties, together with structural and thermodynamic properties, provide important basis for theories of liquid state. At this juncture, it may be pointed out that the structural calculations of liquids using model potentials generate a set of potential parameters, which are useful for the evaluation of transport properties like diffusion coefficient, shear viscosity, bulk viscosity etc. Many theories, which are related to the simple translational movements of the species in liquids, giving reasonable agreement with experiment, have been studied to describe diffusion of simple liquids (Rice and Gray, 1963; Gopala Rao and Das Gupta, 1985; Shimoji and Itami, 1986; Venkatesh and Mishra, 2005; Chen et al., 2014; Dubinin et al., 2014; Jakse and Pasturel, 2016).

The composition dependent self-diffusion coefficients, D_i in binary liquid alloys were determined by incorporating the partial and total correlation functions in the force auto correlation function (Venkatesh et al., 2003; Gopala Rao and Das Gupta, 1985; Gopala Rao and Satpathy, 1990) and function was solved by using Helfand's prescription extended by Davis and Polyvos (Davis and Polyvos, 1967). The inter or mutual diffusion coefficients D_m, in binary liquid alloys were determined by incorporating the thermodynamic correction factor through $S_{CC}(0)$ (Cheng et al., 2009; Pasturel and Jakse, 2015) in Darkens relation.

New sets of equations were formulated in the evaluation of the temperature derivative of diffusion coefficients and these equations were applied in the computation of the activation energy of diffusion of both the alloys considering like others (Wang et

al., 2015; Peng et al., 2015; Cheng et al., 2009; Wax et al., 2000) that the self-diffusion obeyed the Arrhenius law.

$$D = D_0 \, e^{-\frac{Q}{RT}} \tag{6.6}$$

where R is the gas constant (R=8.314 $JK^{-1}mol^{-1}$), 'Q' is the activation energy for diffusion corresponding to the height of the energy barrier required in jumping and D_0 is the temperature independent pre-exponential factor whose detailed expression is referred to the literature (Glasstone et al., 1951).

Further we evaluate the concentration dependent surface tension γ, excess scaling entropy S_E and activation energy of diffusion Q of liquid Al-Cu and Ag-Cu alloys using their diffusion data and temperature derivative of diffusion coefficient.

The theory by Enskog (Thiele, 1963) considers binary collisions only and ignores the attractive forces between the particles. This theory involves the derivation of the transport properties of hard spheres and it works above the critical temperatures when the potential depth is small. Molecular dynamical calculations for rigid sphere transport coefficients were calculated by Alder, Gass and Wainwright (Alder et al., 1970). Enskog theory is extended by Thorne (Bajaras et al., 1973) to binary hard sphere mixtures. Tham and Gubbins (Tham and Gubbins, 1971) have worked with multi-component theory. For liquids it is important to mention that the square well model is preferable for it takes into account the attractive forces between molecules. Davis with his co-workers (Davis and Polyvos, 1967; Davis et al., 1961) developed the theory for obtaining the transport properties by solving modified Boltzmann's integro-differential equation

$$\frac{\partial f_1}{\partial t} + \bar{u}_1 \frac{\partial f_1}{\partial \bar{r}_1} = \int_{u_2} \int_{b} \int_{\psi=0}^{2\pi} (f_1' f_2' - f_1 f_2) \, wb \, db \, d\bar{u}_2 \, d\psi \tag{6.7}$$

where f′ is the time dependent distribution function, b is an impact parameter, ψ, the angle in polar coordinates defined relative to a fixed axis, w is the relative velocity at large separation. Further f′ = f (r, u′) and f = f (r, u) where u and u′ are the velocities before and after collision. The subscript 1 and 2 on f specify whether it is the position and momentum of molecule 1 or 2 that are referred to while the primed quantities are evaluated with velocities after collision.

One of the most important and widely used approaches is to relate the movement of particles in the fluid to the Brownian motion. The best known theory is due to Kirkwood (Kirkwood, 1946) and is similar to the distribution function approach to the equilibrium theory. The basic idea used is the introduction of time interval chosen to isolate a fundamental dynamical event, which is independent of period event and this procedure is known as "coarse graining".

To describe the classical non-equilibrium process in dense fluids by extending the Brownian motion concepts (Lado, 1971), the coefficient of friction ξ in the Einstein formula of diffusion coefficient D is given by

$$D = \frac{k_B T}{\xi} \tag{6.8}$$

The friction coefficient ξ as expressed by Kirkwood in terms of time integral of force autocorrelation function is given by

$$\xi = \frac{1}{3} k_B T \left[\int_0^{\tau} d\vec{S} < \vec{F}(t) \,.\, \vec{F}(t+s) > \right] \tag{6.9}$$

where $\vec{F}(t)$ and $\vec{F}(t+s)$ are the molecular forces on a particle at time t and (t + s) respectively.

Ross (Ross, 1956) originally introduced the linear trajectory approximation using perturbation theory and Fokker Plank equation. Helfand (Helfand, 1961) evaluated the friction coefficient and Rice and Allnat (Rice and Gray, 1963) evaluated the soft potential contribution to the kinetic equations. The linear trajectory approximation states that for the purpose of calculating the time integral of certain auto correlation functions, one can replace the actual trajectories of interacting molecules with linear trajectories. In this chapter, we give only the important points of Helfand (Helfand, 1961) and of Davis and Polyvos (Polyvos and Davis, 1957) as the method is very well known.

The static structural and atomic dynamics in Al-Cu and Ag-Cu have been investigated experimentally by cold neutron scattering (Dahlborg et al., 2013), X-ray diffractometer (Murdy et al., 2008, Lukens and Wagner, 1975). The surface tension of both the alloys has been investigated experimentally using electromagnetic levitation (Schmitz et al., 2009; Brillo et al., 2014). Therefore, it is interesting to formulate a new way to investigate how the static structural behavior could influence the dynamical, surface and transport properties like self and mutual diffusion coefficients, surface tension and viscosity as a function of concentration of one component in binary alloys.

The knowledge of diffusion coefficients plays an important role in design of metallurgical and solidification process such as in casting industry (Dalgic and Colakogullari, 2006), nucleation, crystallization and glass-formation (Zhang and Griesche, 2009; Shimoji and Itami, 1986). The self-diffusion describes the motion of a tagged particle at long times, inter-diffusion or mutual diffusion originates from collective concentration fluctuations among different species (Hansen and McDonald, 1986).

6.2. THEORY

6.2.1. EVALUATION OF DIFFUSION COEFFICIENTS IN ALLOYS

The mutual or inter-diffusion coefficient in binary melts were determined by calculating self-diffusivity of the constituting atoms by incorporating thermodynamic factor in Darken's relation as determined by other workers for various alloys with different approaches (Peng et al., 2015; Jakes and Pasturel, 2015; Zhang et al., 2010).

In binary system the intrinsic diffusion coefficient, D_{id} (Novakovic et al., 2004; Jakes and Pasturel, 2015; Awe and Olawole, 2012; Singh and Somer, 1997; Singh and Somer, 1992), which is referred as Onsager coefficient (Peng et al., 2015; Jakes and Pasturel, 2015; Zhang et al., 2010) can be derived from the self-diffusion coefficient through the Darken's thermodynamic equation for the diffusion (Cheng and Lu, 2009)

$$D_{id} = C_i D_j + C_j D_i \tag{6.10}$$

The mutual or inter-diffusion coefficients in binary liquids can be related to self-diffusion coefficients D_i and D_j as (Hansen and McDonald, 1986; Cheng and Lu, 2009; Zang et al., 2010)

$$D_m = (C_i D_j + C_j D_i)\,\phi S \tag{6.11}$$

Where, S is the manning factor (Cheng et al., 2009) which measures the departure of the Darkens law due to cross correlation contribution to intrinsic diffusion coefficient. In a crystalline substance S is referred to as manning factor (Manning, 1961). In the case all the cross correlation contribution are negligible (S=1), since Darkens relation is recovered if S=1. Thus mutual diffusion coefficient can be defined as

$$D_m = (C_i D_j + C_j D_i)\,\phi \tag{6.12}$$

Thermodynamic driving factor, ϕ is related to second derivative of Gibb's free energy of mixing and therefore the concentration-concentration correlation in long wavelength limit (Novakovic et al., 2004; Jakes and Pasturel, 2015; Awe and Olawole, 2012; Singh and Sommer, 1997; Singh and Sommer, 1992) as

$$\phi = \frac{S_{CC}^{id}(0)}{S_{CC}(0)} = \frac{S_{CC}^{id}(0)}{k_B T} \frac{\partial^2 G}{\partial C_i \partial C_j} \tag{6.13}$$

where G is the Gibbs free energy, k_B is the Boltzmann constant, and $S_{CC}(0)$ is the long wavelength limit of the concentration-concentration structure factor in the Bhatia-Thornton formalism (Bhatia and Thornton,1970).

The Onsager coefficient can be estimated from Darken's equation, which is linearly related to self-diffusivity of constituting elements. The self-diffusivity D_i in binary melts can be determined from well-known Einstein's equation, $D_i = \frac{k_B T}{\xi_i}$, where ξ_i is the friction coefficient of the i^{th} species in a binary mixture and can be given as

$$\xi_i = \xi_i^H + \xi_i^S + \xi_i^{SH} \tag{6.14}$$

Here, ξ_i^H, ξ_i^S and ξ_i^{SH} are the friction coefficients due to hard sphere, soft and soft-hard part respectively (Gopala Rao and Satpathy, 1990; Gopala Rao and Venkatesh, 1989). The friction coefficients arise due to hard and soft part of the force under SW interaction were solved under linear trajectory principle (Helfand, 1961).

Thus the interparticle pair potential $U_{ij}(r)$ for model potential is assumed to be separable into two parts (Gopala Rao and Das, 1987; Mishra and Venkatesh, 2008) i.e. as a pair potential for hard spheres and the other for the attractive part (soft part).

$$U_{ij}(r) = U_{ij}^H(r) + U_{ij}^S(r) \tag{6.15}$$

where $U_{ij}^{H}(r)$ is the contribution from the hard spheres and $U_{ij}^{S}(r)$ from the soft part. These are represented as

$$U_{ij}^{H}(r) = \begin{cases} \infty & ; \quad r < \sigma_{ij} \\ 0 & ; \quad r > \sigma_{ij} \end{cases} \tag{6.16}$$

and

$$U_{ij}^{S}(r) = \begin{cases} 0 & ; \quad r < \sigma_{ij} \\ U_{ij}(r) & ; \quad r > \sigma_{ij} \end{cases} \tag{6.17}$$

Similarly, the force can also be divided into two parts.

(a) F_H, the hard sphere contribution

(b) F_S, the soft potential contribution

Thus,

$$\xi_i^{H} = \sum_{j=1}^{2} \frac{8}{3} \sigma_{ij}^2 \; g_{ij}(\sigma_{ij}) \rho_j (2\pi \mu_{ij} k_B T)^{1/2} \tag{6.18}$$

The contribution from the soft part is given by (Shimoji and Itami, 1986; Rao and Satpathy, 1982; Polyvos and Davis, 1967)

$$\xi_i^{S} = -\sum_{j=1}^{2} \frac{\rho_j}{3} \left[\frac{2\pi \mu_{ij}}{k_B T} \right]^{1/2} \frac{1}{(2\pi)^2} \int_0^{\infty} k^3 U_{ij}^{S}(k) \, h_{ij}(k) dk. \tag{6.19}$$

while ξ_i^{SH}, the cross contribution (Polyvos and Davis,1967) is given by

$$\xi_i^{SH} = -\sum_{j=1}^{2} \frac{2\rho_j}{3} \; g_{ij}(\sigma_{ij}) \; [\frac{2\mu_{ij}}{\pi k_B T}]^{1/2} \int_0^{\infty} [k\sigma_{ij} \cos(k\sigma_{ij}) - \sin(k\sigma_{ij})] \; U_{ij}^{S}(k) \, dk \tag{6.20}$$

Here ρ_j is the number density of the j^{th} species $h_{ij}(k)$ and $U_{ij}(k)$ are the Fourier transforms of the total correlation function $h_{ij}(r)$ and the soft part of the potential $U_{ij}^{S}(r)$ respectively. Further μ_{ij} is the reduced mass and is given by

$$\mu_{ij} = \frac{m_i\, m_j}{m_i + m_j} \tag{6.21}$$

The quantities $h_{ij}(k)$ and $U_{ij}(k)$ are given by

$$h_{ij}(k) = [S_{ij}(k) - \delta_{ij}]\,(\rho_i\, \rho_j)^{-1/2} \tag{6.22}$$

and

$$U_{ij}^{S}(k) = \frac{4\pi\varepsilon_{ij}}{k^3}[A_{ij}\, k\sigma_{ij}\cos(A_{ij}k\sigma_{ij}) - \sin(A_{ij}k\sigma_{ij}) - k\sigma_{ij}\cos(k\sigma_{ij}) + \sin(k\sigma_{ij})] \tag{6.23}$$

Here δ_{ij} is the Kronecker delta function already defined in Chapter 2. σ_{ij}, ε_{ij} and A_{ij} are the cross correlation due to hard core diameter, depth and breadth of the square well potential. The mixed parameters are discussed in Chapter 4. The partial structure factors which were already discussed in Chapter 4 for Al-Cu and Ag-Cu alloys are used in the evaluation of the friction coefficients.

Therefore the self-diffusion coefficient D_i can be written as

$$D_i = \frac{k_B T}{\xi_i^H + \xi_i^S + \xi_i^{SH}} \tag{6.24}$$

Thus D_m can be rewritten through Eqns.(6.11) to (6.13) as

$$D_m = D_{id} \times \frac{S_{CC}^{id}(0)}{S_{CC}(0)} \tag{6.25}$$

where $S_{CC}^{id}(0)$ is ideal value of $S_{CC}(0)$, given by $S_{CC}^{id}(0) = C_i \times C_j$ (Zhang and Griesche, 2010; Cheng and Lu, 2009; Odusote, 2008).

6.2.2. EVALUATION OF SURFACE TENSION IN LIQUID BINARY ALLOYS

Prasad et al. considered the existence of layer structure near the surface of binary liquid alloys in their statistical mechanical formalism (Prasad et al., 1998; Prasad

et al., 1991). They also pointed out that the surface of binary liquid alloys is in thermodynamically equilibrium with the bulk and surface properties are influenced by thermodynamic properties of the bulk.

Detailed studies of the surface properties of condensed matter help in understanding their metallurgical processing. The surface tension, γ for series of liquid metals has been studied by statistical mechanical approach under zeroth order approximation and given in Chapter 3. It is further extended for binary alloys. In present work, γ in binary melts has been computed by using mutual diffusion coefficient values at different concentrations.

The Surface tension with respect to bulk concentration of Cu in liquid binary Al-Cu and Ag-Cu alloys is defined as in pure metals (Chapter 3) and can be given as

$$\gamma_{Alloy} = \frac{15}{16}\left(\frac{k_B T}{\mu_{ij}}\right)^{1/2} \times \frac{k_B T}{2\pi\sigma D_m}. \qquad (6.26)$$

Where μ is the reduced mass, which is shown in Eqn. (6.21).

6.2.3. EVALUATION OF ACTIVATION ENERGY OF DIFFUSION IN LIQUID BINARY ALLOYS

The activation energy of diffusion, Q in binary alloys were obtained through temperature derivative of diffusion coefficients, which can be given as

$$\frac{d\ln D_i}{dT} = \frac{1}{T} - \frac{1}{\xi_i}\frac{d\xi_i}{dT} \qquad (6.27)$$

Hence to evaluate the above quantity we must evaluate the temperature derivative of the friction coefficients of the i^{th} constituent. Thus

$$\frac{d\xi_i^H}{dT} = \frac{\xi_i^H}{2T} + \frac{8}{3}\left(\frac{2\pi k_B}{N_0}\right)^{1/2}\left[\sigma_{ii}^2(T\mu_{ii})^{1/2}\left\{\rho_{ii}\left(\frac{dg_{ij}(r)}{dT}\right)_{r=\sigma_{ii}} + g_{ij}(\sigma_{ij})\frac{d\rho_{ii}}{dT}\right\}\right.$$
$$\left. + \sum_{j\neq i}\sigma_{ij}^2(T\mu_{ij})^{1/2}\left\{\rho_{jj}\left(\frac{dg_{ij}(r)}{dT}\right)_{r=\sigma_{ij}} + g_{ij}(\sigma_{ij})\frac{d\rho_{ij}}{dT}\right\}\right.$$

(6.28)

$$\frac{d\xi_i^S}{dT} = -\frac{\xi_i^S}{2T} - \frac{1}{12\pi^2}\left(\frac{2\pi}{k_B N_0}\right)^{1/2}\left[\left(\frac{\mu_{ii}}{T}\right)^{1/2}\left\{\left(\frac{d\rho_{ii})}{dT}\right)\int_0^\infty k^3 U_{ii}^S(k)h_{ii}(k)dk\right.\right.$$
$$\left.\left. + \rho_{ii}\frac{d}{dT}\int_0^\infty k^3 U_{ii}^S(k)h_{ii}(k)dk\right\} + \sum_{j\neq i}\left(\frac{\mu_{ij}}{T}\right)^{1/2}\left\{\left(\frac{d\rho_{jj})}{dT}\right)\int_0^\infty k^3 U_{ij}^S(k)h_{ij}(k)dk\right.$$
$$\left. + \rho_{ii}\frac{d}{dT}\int_0^\infty k^3 U_{ii}^S(k)h_{ii}(k)dk\right.$$

(6.29)

$$\frac{d\xi_i^{SH}}{dT} = -\frac{\xi_i^S}{2T} - \frac{2}{3}\left(\frac{2}{\pi k_B N_0}\right)^{1/2}\left[\left(\frac{\mu_{ii}}{T}\right)^{1/2}\int_0^\infty k\sigma_{ii}\cos(k\sigma_{ii})\sin(k\sigma_{ii})U_{ii}^S(k)dk\right.$$
$$\left.\left(g_{ij}(\sigma_{ii})\frac{d\rho_{ii}}{dT} + \rho_{ii}\left(\frac{dg_{ij}(r)}{dT}\right)_{r=\sigma_{ii}}\right)\right\} + \sum_{j\neq i}\left(\frac{\mu_{ij}}{T}\right)^{1/2}$$
$$\left.\int_0^\infty (k\sigma_{ij}\cos(k\sigma_{ij})\sin(k\sigma_{ij})U_{ij}^S(k)dk\left(g_{ij}(\sigma_{ij})\frac{d\rho_{ij}}{dT} + \rho_{ij}\left(\frac{dg_{ij}(r)}{dT}\right)_{r=\sigma_{jj}}\right)\right\}\right]$$

(6.30)

$$\frac{dS_{ij}(k)}{dT} = \kappa_{ij}\,[S_{ij}(k)]\left\{[1 - S_{ij}(k)] + \frac{24\eta_{ij}\,S_{ij}(k)}{(k\sigma)^6}\,[\frac{4\mu_1\,\alpha_{ij}\,\eta_{ij}\,(2+\eta_{ij})}{(1+2\,\eta_{ij})\,(1-\eta_{ij})}\right.$$
$$\left. + \frac{\mu_2\,(\eta_{ij}^{\,2} + 9\eta_{ij} + 2)}{(2+\eta_{ij})\,(1-\eta_{ij})} + \frac{\mu_3\,\gamma\,(2\eta_{ij}^{\,2} + 9\eta_{ij} + 1)}{(1+2\,\eta_{ij})\,(1-\eta_{ij})} - \frac{\varepsilon_{ij}\,\mu_4}{\kappa\,k_B T^2}]\right\}$$

(6.31)

$$\mu_1 = (k\sigma_{ij})^3\left[\sin(k\sigma_{ij}) - k\sigma_{ij}\cos(k\sigma_{ij})\right] \quad (6.32)$$

$$\mu_2 = (k\sigma_{ij})^2\,[2k\sigma_{ij}\sin(k\sigma_{ij}) - (k^2\sigma_{ij}^{\,2} - 2)\cos(k\sigma_{ij}) - 2] \quad (6.33)$$

$$\mu_3 = (4k^3\sigma_{ij}^{\,3} - 24k\sigma_{ij})\sin(k\sigma_{ij}) - (k^4\sigma_{ij}^{\,4} - 12k^2\sigma_{ij}^{\,2} + 24)\cos(k\sigma_{ij}) + 24 \quad (6.34)$$

$$\mu_4 = (k\sigma_{ij})^3\left[\sin(\lambda_{ij}k\sigma_{ij}) - \lambda_{ij}k\sigma_{ij}\cos(\lambda_{ij}k\sigma_{ij}) + k\sigma_{ij}\cos(k\sigma_{ij}) - \sin(k\sigma_{ij})\right] \quad (6.35)$$

The rest of the symbols have their usual connotation which is given in details in Chapter 4 thus no need to repeat here.

6.2.4. SCALING PROPERTIES IN LIQUID BINARY ALLOYS

The dimensionless diffusion coefficient in a binary liquid alloys in terms of self diffusion coefficients of the constituting atoms can be given as (Hoyt et al., 2000)

$$D^* = \left(\frac{D_i}{\chi_i}\right)^{C_i}\left(\frac{D_j}{\chi_j}\right)^{C_j} \quad (6.36)$$

χ_i and χ_j are the scaling factors (Hoyt et al., 2000) which are modified for real liquids under the SW interaction in present computation. The hard sphere diameter σ and $g_{ij}(\sigma)$ in the original equation given by many authors (Hoyt et al., 2000; Samanta et al., 2004; Pasturel and Jakse, 2015) are replaced by the first peak position of partial pair correlation functions and their corresponding values respectively, which are computed under the SW interaction.

$$\chi_i = 4(r_{ii}^{max})^4 \rho_i C_i g_{ii}(r^{max}) \sqrt{\frac{\pi k_B T}{m_i}} + 4(r_{ij}^{max})^4 \rho_i C_j g_{ij}(r^{max}) \sqrt{\frac{\pi(m_i + m_j)k_B T}{m_i m_j}}. \quad (6.37)$$

$$\chi_j = 4(r_{jj}^{max})^4 \rho_j C_j g_{jj}(r^{max}) \sqrt{\frac{\pi k_B T}{m_j}} + 4(r_{ij}^{max})^4 \rho_j C_i g_{ij}(r^{max}) \sqrt{\frac{\pi(m_i + m_j)k_B T}{m_i m_j}}. \quad (6.38)$$

In Eqns. (6.37) and (6.38), r_{ii}^{max} is the first peak position of the corresponding PRDFs, $g_{ij}(r^{max})$ and m_i and m_j are the atomic masses, these generalized scaling parameters are the collision rate in a mono-atomic hard sphere liquids of diameter σ and mass, m given by the Enskog theory i.e., $\Gamma = 4\sigma^2 \rho g(\sigma)\sqrt{\pi k_B T/m}$, used by Dzugutov in his original scaling law (Dzugutov, 1996) and so $D^*=D/\Gamma\sigma^2$.

Within this approach the reduced diffusion coefficients given by Eqn. (6.36) is proportional to the $\exp(S_2)$, here S_2 is excess entropy which can be approximated by two body contribution (Dzugutov, 1996; Hoyt et al., 2000). The normalized diffusion coefficient, D^* as a function of two body excess entropy S_E as presented by Yokoyama and coworker (Yokoyama, 1998; Yokoyama and Tsuchiya, 2002) for binary alloys can be written as (Dzugutov, 1996; Hoyt et al., 2000)

$$D^* = a\, e^{k_B/S_E} \quad (6.39)$$

6.3. RESULTS AND DISCUSSION

6.3.1. Al-Cu ALLOYS

6.3.1.1. *Friction coefficients and Diffusion coefficients of Al-Cu alloys*

Various friction coefficients (ξ^H, ξ^S and ξ^{SH}) in Al-Cu melts as a function of composition at 1373 K were computed through Eqns. (6.18) to (6.20) and are given in Table 6.1.

Table 6.1. Concentration dependent friction coefficients of Al-Cu alloys at 1373K.

% Cu in Al-Cu alloys	$\xi^H \times 10^{-3}$(Kg/s)		$\xi^S \times 10^{-3}$(Kg/s)		$\xi^{SH} \times 10^{-3}$(Kg/s)	
	Al	Cu	Al	Cu	Al	Cu
10	6.74	7.79	1.49	1.91	1.07	1.79
17	7.34	8.45	1.24	1.68	0.93	1.71
25	8.07	9.41	1.75	1.37	1.38	2.37
33	8.71	10.25	1.88	2.57	1.56	2.70
40	9.37	11.16	2.01	2.76	1.73	3.07

The friction coefficients of this liquid alloys were calculated by using PSFs, PRDFs and SW parameters at 1373K. This temperature was chosen for the study of dynamic properties because experimental results were available at this temperature only. Further, correlation functions were also computed at 1373K in order to obtain self and mutual diffusion coefficient in Al-Cu alloys at 1373K.

It can be observed from Table 6.1 that at all compositions the hard sphere part dominates. ξ^H is more than 50% in all cases as ξ^H depends on hard sphere repulsive part of the SW potential which dominates in structural functions also. Even though Cu is a noble metal and melts at higher temperature than Aland ξ^H(Cu) is more than ξ^H(Al). This may be due to the formation of Cu cluster in the melts. Also ξ^S and ξ^{SH} of Cu is

more than that of Al. this may be due to segregation and formation of small clusters of Cu atoms (Venkatesh et al., 2003).

The concentration dependent self-diffusion coefficients and mutual diffusion coefficients of the melts have been calculated by using computed friction coefficients at 1373K and the results are shown in Table 6.2. The self-diffusion coefficients of Cu were compared with experimental values (Dahlborg et al., 2013) as given in Table 6.2. A satisfactory agreement is found between the computed and experimental results. The self-diffusion coefficient of Al i.e, D_{Al} has a larger value than D_{Cu} at all compositions and both decreases with increase in Cu concentration while the ratio D_{Cu}/D_{Al} remains constant (0.8) at all compositions. The D_m of liquid Al-Cu alloys was computed at the different atomic percent of Cu using D_{id} and ϕ values. It can be seen, from Table 6.2 that D_m is also decreasing with increase in Cu concentration. To best of our knowledge there are no experimental data for D_{Al} and D_m parameters to compare our theoretical values at these working compositions.

Table 6.2. Theoretical and experimental values of concentration dependent self and mutual diffusion coefficients of liquid Al-Cu alloys at 1373K.

% Cu in AlCu	$D_{Cu}\times10^{-9}(m^2/s)$		$D_{Al}\times10^{-9}$	$D_m\times10^{-9}$	D_{Cu}/D_{Al}
	theort.	expt.	(m^2/s)	(m^2/s)	
10	15.47	16.02	19.39	14.06	0.8
17	15.00	13.80	18.12	13.90	0.8
25	13.39	12.52	16.90	12.15	0.8
33	12.21	-	15.60	10.92	0.8
40	11.16	-	14.45	9.97	0.8

The decrease in diffusivity with increase in Cu content is also observed experimentally (Dahlborg et al., 2013). The D_m/D_{id} value is less than one at all compositions, which indicates the phase separation over the whole concentration range (Novakovic et al., 2005). This decrease in self and mutual diffusion coefficient with increasing concentration of Cu may be due to segregation of Al and Cu cluster. The $S_{CC}(0)$ data presented in Chapter 5 also support this findings.

Further the temperature dependent friction coefficients and diffusion coefficients were also determined at 18.7% of Cu in Al-Cu melts to verify the model calculation with available mutual diffusion coefficient values at different temperatures (Zhang et al., 2009). The computed values of friction coefficients at different temperatures are presented in Table 6.3.

Table 6.3. Temperature dependent friction coefficients of Al-Cu alloys at 18.7% Cu.

Temp	$\xi^H \times 10^{-3}$(Kg/s)		$\xi^S \times 10^{-3}$(Kg/s)		$\xi^{SH} \times 10^{-3}$(Kg/s)	
(K)	Al	Cu	Al	Cu	Al	Cu
1177	6.38	7.37	1.71	2.34	1.24	2.06
1075	6.11	7.04	1.81	2.51	1.30	2.16
870	5.53	6.33	2.09	2.95	1.45	2.39

The values temperature dependent friction coefficients at 18.7% Cu were used for the calculation of self and mutual diffusion coefficients of the melts and are listed in Table 6.4. Since, the experimental data for the temperature dependent D_m is available (Zhang et al., 2009) at 18.7% Cu in melts thus the temperature dependent friction coefficients and diffusion coefficients were determined and these results are shown in Table 6.4.

Table 6.4. Theoretical and experimental values of temperature dependent self and mutual diffusion coefficients of Al-Cu at 18.7% Cu in Al-Cu alloys.

Temp K	$D_{Cu}\times10^{-9}(m^2/s)$	$D_{Al}\times10^{-9}(m^2/s)$	$D_m\times10^{-9}(m^2/s)$		D_{Cu}/D_{Al}
			theort.	expt	
870	10.28	13.42	8.8	7.5	0.8
1075	12.67	16.06	11.4	11.0	0.8
1177	13.79	17.41	12.6	14.5	0.8

As can be seen from Table 6.4, both D_i and D_m values increases with increase in temperature from 870K to 1177K. The computed values of D_m were compared with the available experimental results (Zhang et al., 2009). There is a satisfactory agreement between the computed and experimental results. The computed values of D_{Al}, D_{Cu}, D_m and D_{id} are also presented in Fig.6.1.

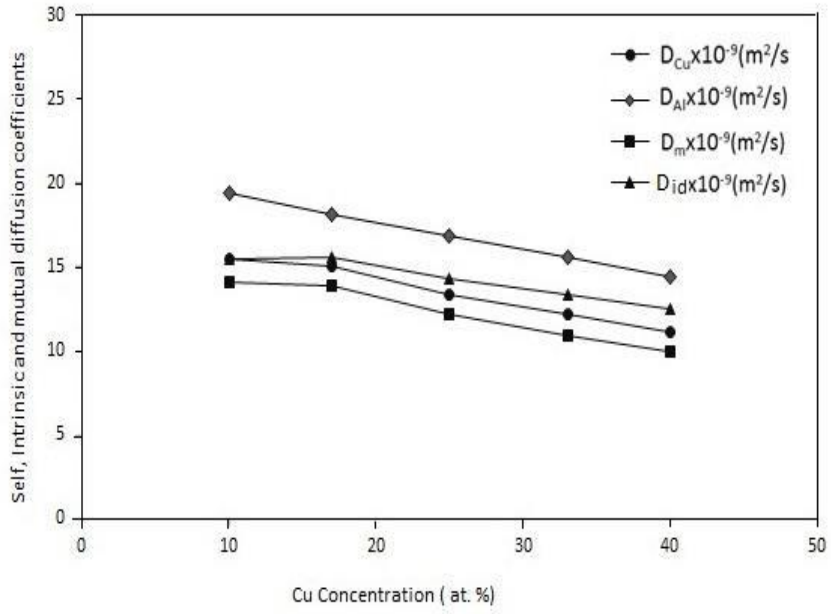

Fig. 6.1. Self, intrinsic and mutual diffusion coefficients of Al-Cu alloys at different atomic percent of Cu

In a binary mixture the self-diffusion coefficient of heavier component generally increases with increasing concentration of lighter one (Ali et al., 2001; Van den Berg and Hoheisel, 1990). The results presented in Figs. 6.1 and 6.2. For self and mutual diffusion of Al, Cu and Al-Cu at different atomic percent of Cu support this finding.

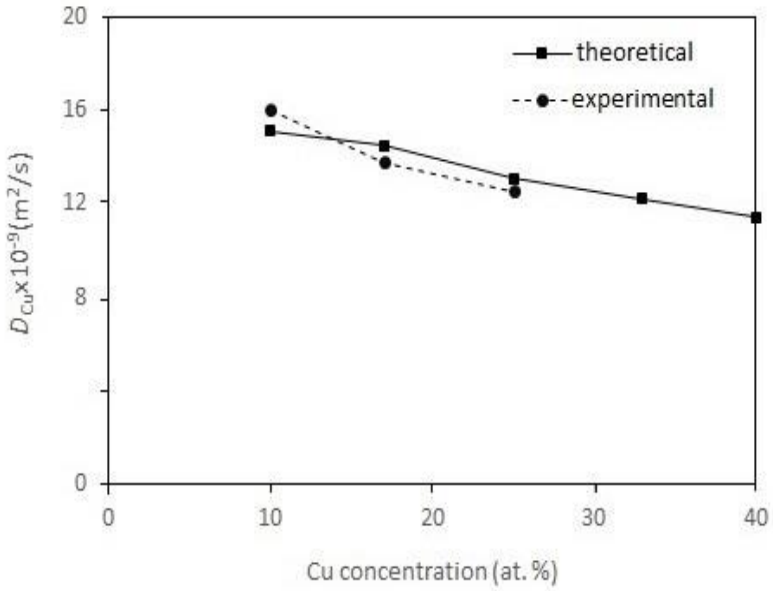

Fig. 6. 2. Theoretical and experimental values of self-diffusion coefficients of Cu in liquid Al-Cu alloys at different atomic percent of at 1373K.

6.3.1.2. *Surface tension and Activation energy of Al-Cu alloys*

The computed values of diffusion data were successfully employed to determine surface tension in these alloys. The computed values of the concentrated dependent surface tension for liquid Al-Cu alloys along with their experimental data (Schmitz et al., 2009) are present in Table 6.5.

Table 6.5. Surface tension, $\gamma_{Al\text{-}Cu}$ (N m^{-1}) of Al-Cu alloys at different compositions of Cu at 1373K.

% Cu in AlCu	$\gamma_{Al\text{-}Cu}$ (N m^{-1})	
	theort.	expt.
10	0.61	0.81
17	0.62	0.86
25	0.70	-
33	0.78	-
40	0.86	0.97

The surface tension of Al-Cu alloys increases with increase in Cu concentration, the similar trend was obtained by Schmitz et al. in their experiment on liquid Al-Cu alloys (Schmitz et al., 2009). The surface tension of pure liquid Al and Cu were found to be 0.8 and 1.03 Nm^{-1} respectively which have been shown in Chapter 3. Hence obtained surface tension for liquid binary alloys through SW model gives satisfactory results. The surface tension is related with self-diffusion coefficients of liquids. Since self-diffusion coefficients of liquids are determined using microscopic structural functions along with SW potential and hence computed γ_{ST} is also related to microscopic structure of liquids.

The D_i in binary melts obey Arrhenius law as can be seen from Eqn. (6.6), which is also reported by other authors (Venkatesh and Mishra,2005; Dahlborg et al., 2013; Cheng et al., 2009; Wang et al., 2009). It was pointed out that Al-Cu alloy shows a non-Arrhenius behavior at high concentration of Cu (Ali and Samanta, 2001). Concentration dependent activation energy of diffusion is obtained in liquid Al-Cu

alloys through temperature derivative of self-diffusion coefficient (Eqns. 6.27 to 6.33). In this analytical temperature differentiation of diffusion coefficient the pre exponential, D_0 is taken as independent of temperature. The activation energy for diffusion in liquid Al-Cu alloys are in the range 19.3 to 21.6 $KJmol^{-1}$ which are quite close to the values obtained by others at some of the composition (Dahlborg et al., 2013; Cheng et al., 2009; Wang et al., 2009).

6.3.2. Ag-Cu ALLOYS

6.3.2.1 *Friction coefficients and Diffusion coefficients of Ag-Cu alloys*

The friction coefficients of Ag-Cu melts at various concentrations of Cu were calculated by using PSFs, PRDFs and SW values at corresponding concentrations at 1373K. The computed values of various friction coefficients (ξ^H, ξ^S and ξ^{SH}) of Ag-Cu alloys are listed in Table 6.6. The self-diffusion coefficients and mutual diffusion coefficients of the melts have been calculated at 1373K since the experimental values of surface tension is available at this for some compositions of Ag-Cu alloys.

It can be observed from Table 6.6 that ξ^H is contributing more than ξ^S and ξ^{SH} in this alloy at all compositions**.** In this alloy both the constituents atoms are noble metal, the melting point of Ag being 1235.08K is slightly lower than that of Cu (1353K) but surprisingly ξ^H(Ag) is more than ξ^H(Cu), this may be due to the existence of Ag in amorphous form (where packing will not be compact) or due to the segregation of the constituents. Further, ξ^S and ξ^{SH} of Ag is more than that of Cu

Table 6.6. The computed values of the friction coefficients in Ag-Cu alloys at 1373K.

% Cu in Ag-Cu alloys	$\xi^{H}\times10^{-3}$ (Kg/s)		$\xi^{S}\times10^{-3}$ (Kg/s)		$\xi^{SH}\times10^{-3}$ (Kg/s)	
	Ag	Cu	Ag	Cu	Ag	Cu
16.50	20.11	17.09	12.70	1.72	9.99	6.66
21.65	20.21	17.21	12.65	1.67	9.93	6.64
28.00	20.34	17.36	12.59	1.61	9.85	6.62
37.00	20.53	17.59	12.50	1.53	9.74	6.59
39.76	20.59	17.66	12.47	1.50	9.70	6.58
50.00	19.02	17.70	13.98	1.40	8.64	6.44
63.43	17.42	18.47	15.13	1.32	7.46	6.47
71.00	15.36	19.34	17.64	1.09	6.60	6.74
85.00	15.29	19.98	17.32	0.64	6.04	6.67
86.38	15.27	20.00	17.33	0.62	5.99	6.66
97.39	15.50	20.30	17.43	0.46	5.85	6.53

The composition dependent self and mutual diffusion coefficients of the alloy are given in Table 6.7. Unfortunately we could not find the experimental value of diffusion coefficients for Ag-Cu alloy for comparing our results.

The self-diffusion coefficient of Cu i.e, D_{Cu} has a larger value than D_{Ag} at all compositions. D_{Cu} decreases from $7.44\text{x}10^{-9}(m^2/s)$ to $6.93\text{x}10^{-9}(m^2/s)$ with increase in Cu concentrations while D_{Ag} increases from $4.43\text{x}10^{-9}(m^2/s)$ to $4.95\text{x}10^{-9}(m^2/s)$ as the atomic percent of Cu increases in the melts.

Table 6.7. Theoretical and experimental values of concentration dependent self and mutual diffusion coefficients of liquid Ag-Cu alloys at 1373K.

% Cu in AgCu	$D_{Cu}\times10^{-9}$ (m^2/s)	$D_{Ag}\times10^{-9}$ (m^2/s)	$D_m\times10^{-9}$ (m^2/s)	D_{Cu}/D_{Ag}
16.50	7.44	4.43	6.92	1.7
21.65	7.42	4.43	6.75	1.7
28.00	7.39	4.43	6.53	1.7
37.00	7.37	4.43	6.25	1.7
39.76	7.36	4.44	6.16	1.7
50.00	7.31	4.55	5.89	1.6
63.43	7.21	4.73	5.58	1.5
71.00	6.97	4.78	5.27	1.5
85.00	6.95	4.89	5.05	1.4
86.38	6.94	4.90	5.03	1.4
97.39	6.93	4.95	4.97	1.4

As can be seen from Table 6.7, D_m is also decreasing with increase in Cu concentrations. This decrease in self diffusion coefficients of Cu and mutual diffusion coefficient with increasing concentration of Cu may be due to formation Cu-Cu clusters in this melts which leads to segregation. The important microscopic function CSRO parameter calculated in Chapter 5 also supports segregating nature in this alloy at all compositions. To our knowledge there is no experimental work on self and mutual diffusion coefficients for this alloy. With these self-diffusion coefficients intrinsic

diffusion coefficients (Onsager coefficient) of the alloys were calculated through $D_{id} = C_i D_j + C_j D_i$. The thermodynamic contribution was incorporated with intrinsic diffusion coefficients for calculating the mutual diffusion coefficients of the melts as presented by many workers (Novakovic, et al.,2005; Vardeman and Gezelter, 2001; Brillo et al., 2008; Zhang, et al., 2010; Cheng et al., 2009; Singh and Somer, 1997; Dahlborg et al, 2013; Wang et al., 2009). The results on self, mutual and intrinsic diffusion coefficients are also given in Fig. 6.3.

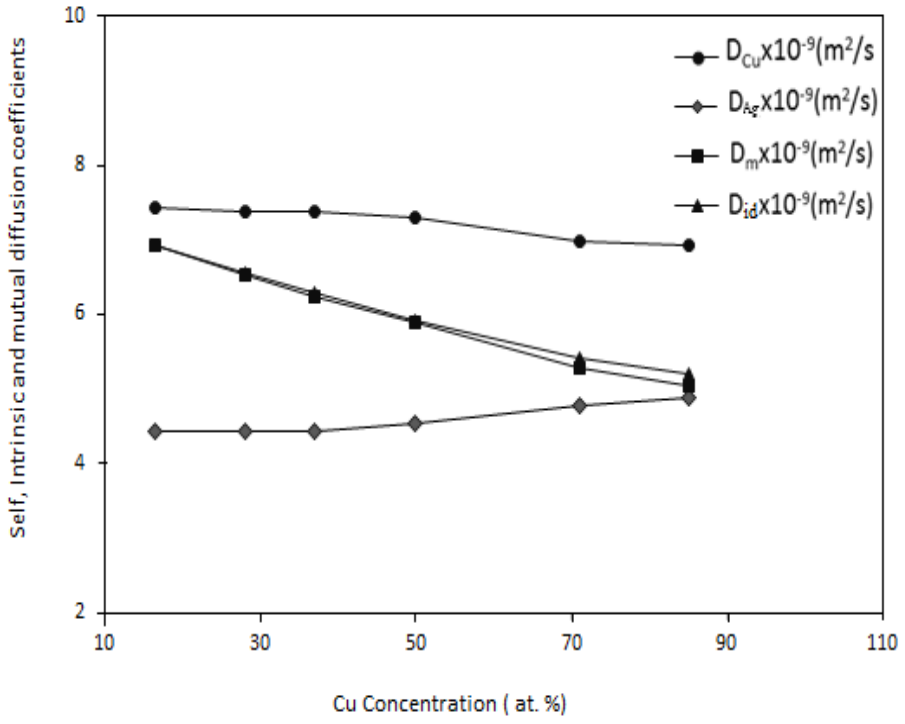

Fig. 6. 3. Self, intrinsic and mutual diffusion coefficients of Ag-Cu at different atomic percent of Cu

6.3.2.2. *Surface tension and Activation energy of Ag-Cu alloys*

The surface tension of Ag-Cu melts was computed at various atomic percent of Cu through the diffusion data which is shown in Table 6.7. The diffusion data were successfully employed to determine surface tension values and the results were given in Table 6.8 along with their experimental data (Novakovic et al., 2005).

Table 6.8. Surface tension, $\gamma_{Ag\text{-}Cu}$(N m^{-1})of Ag-Cu alloys at different compositions of Cu at 1373K.

% Cu in AgCu	$\gamma_{Ag\text{-}Cu}$ (mN m^{-1})	
	theort.	expt
16.50	796.5	-
21.65	841.5	906.0
28.00	845.4	-
37.00	882.8	-
39.76	895.4	937.0
50.00	930.3	-
63.43	997.4	995.0
71.00	981.9	-
85.00	1114.6	-
86.38	1123.2	1132.0
97.39	1163.7	1262.0

The surface tension of liquid Ag-Cu melts was found to increase with increase in atomic percent of Cu. The same trend was observed by Novakovic et al. using the pinned-sessile drop method (Novakovic et al., 2005). It can be seen from find from Table 6.7 that there is a satisfactory agreement between theory and experimental results.

The computed value of concentration dependent activation energy for diffusion through Eqns. (6.27) to (6.35) in Ag-Cu alloys was obtained in the range 17.6 to 19.7

KJ mol^{-1}. To the best of our knowledge we do not find activation energy calculation for liquid Ag-Cu either experimentally or theoretically.

6.3.3. SCALING PROPERTIES IN LIQUID BINARY ALLOYS

A quantitative structure-dynamic relationship was explored with the SW potential by considering Dzugutov's scaling law, which correlates the reduced diffusion coefficients of a liquid with its excess entropy. Dzugutov approximated the excess entropy under two body approximation (Dzugutov, 1996), which was extended and examined by many researchers with different model calculations (Hoyt et al., 2000; Samanta et al., 2004; Pasturel and Jakse, 2015) for binary alloys, which is also examined under the SW interaction in present study. Thus, the excess entropy can be defined as

$$S_2 = -2\pi\rho_{ij}\sum_{i,j=1}^{2} C_i C_j \int_0^{\infty}\{g_{ij}(r)\ln[g_{ij}(r)] - [g_{ij}(r)-1]\}\, r^2 dr \qquad (6.40)$$

ρ_{ij} is the number densities of the components in the alloys which were determined from those of the pure components assuming ideal law of mixing to hold (Gopala Rao and Das Gupta, 1985).

$$\rho_{11} = C_1\rho_{11}^0\rho_{22}^0 / C_1(\rho_{22}^0 - \rho_{11}^0) + \rho_{11}^0 \qquad (6.41)$$

$$\rho_{22} = (1-C_1)\rho_{11}^0\rho_{22}^0 / C_1(\rho_{22}^0 - \rho_{11}^0) + \rho_{11}^0 \qquad (6.42)$$

$$\rho_{12} = \sqrt{\rho_{11}\times\rho_{22}} \qquad (6.43)$$

Yokoyama and co-worker (Yokoyama, 1998; Yokoyama and Tsuchiya, 2002) presented S_2 as S_E, which can be given in terms of partial molar entropy and thus the Eqn. (6.40) can be written as (Pasturel and Jakse 2015);

$$S_E = c_i \times S_E^i + c_j \times S_E^j \qquad (6.44)$$

Here S_E^i is the partial molar entropy of i^{th} component in binary mixture. S_E^i can be obtained through self-diffusion coefficients of the constituents under Dzugutov scaling law as

$$S_E^i/k_B = \log\frac{D_i}{0.049\,\chi_i} \tag{6.45}$$

$$S_E^j/k_B = \log\frac{D_j}{0.049\chi_j} \tag{6.46}$$

Where χ_i and χ_j are the scaling factor (Samanta et al., 2004; Hoyt et al., 2000; Pasturel and Jaske, 2015) presented in Eqns. (6.37) and (6.38).

The composition dependent χ_i and χ_j were obtained through Eqns. (6.37) and (6.38) and the values were employed in Eqns. (6.45) and (6.46) to obtain partial molar entropies in binary alloys. The excess entropies in both the alloys were calculated at different compositions of Cu through Eqn. (6.44).

Table 6.9. Scaling factors, D^*, partial and total excess entropy of liquid Al-Cu alloys at different compositions of Cu at 1373K.

% Cu in Al-Cu	χ_{Cu} ($10^{-6}m^2/s$)	χ_{Al} ($10^{-6}m^2/s$)	D^*x10^{-3}	$-S_E^{Cu}/k_B$	$-S_E^{Al}/k_B$	$-S_E/k_B$
10	0.33	2.81	8.35	0.059	1.959	1.769
17	0.57	2.86	8.07	0.621	2.046	1.804
25	0.94	2.96	7.18	1.236	2.148	1.920
33	1.29	2.84	6.57	1.642	2.189	2.009
40	1.61	2.72	5.91	1.957	2.221	2.115

The computed values of S_E as a function of Composition as well as S_E^{Cu} and S_E^{Al} calculated at 1373K are given in Table 6.9. The scaling factor (χ_{Cu} and χ_{Al}), the dimensionless diffusion coefficients, $D^*$of liquid Al-Cu alloys at different compositions of Cu at 1373K are also given in Table 6.9

The partial excess entropies correlate to Chemical Short Range Order (CSRO) parameter, α' (Paturel and Jakse, 2015) which has been mentioned in Chapter 5. It can be seen from Table 6.9 that the both the partial and total excess entropies (S_E^{Cu}, S_E^{Al} and S_E) are found to increase with increase in Cu concentration at the same time α' also increase with increasing Cu concentration. Further, the obtained values of excess entropy (in k_B unit) of liquid Al-Cu alloys were plotted against dimensionless diffusion coefficients and presented in Fig. 6.4.

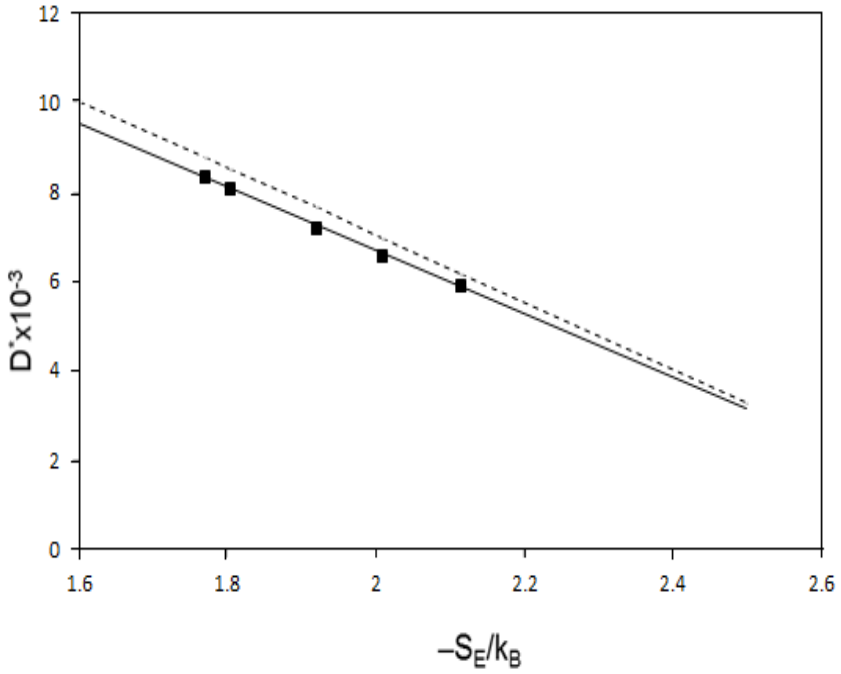

Fig. 6.4. D^* versus S_E for liquid Al-Cu alloys; the dashed line is Dzugutov's law.

It can be seen from Fig. 6.4 that there is a linear relationship between reduced diffusion coefficients and excess entropy at different compositions of Cu in Al-Cu

alloys. The computed result was compared with the Dzugutov's hypothesis and it is found that the computed results are compatible with Dzugutov's law (Dzugutov, 1996) and close to that found by Pasturel and Jakse (Pasturel and Jakse, 2015) on their work on Al-Ni alloys. The obtained partial excess entropies for constituting atoms in binary liquid alloys, described by their two body contribution, are valuable structural indicators and able to measure the evaluation of local structuring as a function of composition (Paturel and Jakse, 2015).

The partial and total excess entropies as a function of compositions in Ag-Cu alloys were computed at 1373K and the results are given in Table 6.10. The scaling factor (χ_{Cu} and χ_{Ag}) and the dimensionless diffusion coefficients, D^*as a function of atomic percent Cu are given in Table 6.10.

Table 6.10. Scaling factors, D^*, partial and total excess entropy of liquid Ag-Cu alloys at different compositions of Cu at 1373K.

%Cu in Ag-Cu	χ_{Cu} (10^{-6} m^2/s)	χ_{Ag} (10^{-6} m^2/s)	D^*x10^{-3}	$-S_E^{Cu}/k_B$	$-S_E^{Ag}/k_B$	$-S_E/k_B$
16.5	0.66	2.51	2.39	1.463	3.324	3.021
28.0	1.11	2.34	2.69	1.992	3.253	2.899
37.0	1.45	2.15	2.87	2.264	3.171	2.835
50.0	1.91	1.83	3.10	2.536	2.982	2.759
71.0	2.45	1.15	3.11	2.847	2.471	2.757
85.0	2.79	0.64	2.95	2.979	1.853	2.810

It can be seen from Table 6.10 that in Ag-Cu alloys, the partial excess entropy of Cu i.e., $-S_E^{Cu}$ increases, while the partial excess entropy of Ag i.e., $-S_E^{Ag}$ decreases with increase in atomic percent of Cu in the melts. Total excess entropy, S_E of the melts decreases with increasing atomic percent of Cu up to 71% and then slightly increases at 85% Cu. The same trend is also observed in Al-Ni melts (Pasturel and Jakse, 2015).

The obtained values of excess entropy (in k_B unit) for Ag-Cu alloys were plotted against dimensionless diffusion coefficients and presented in Fig. 6.5.

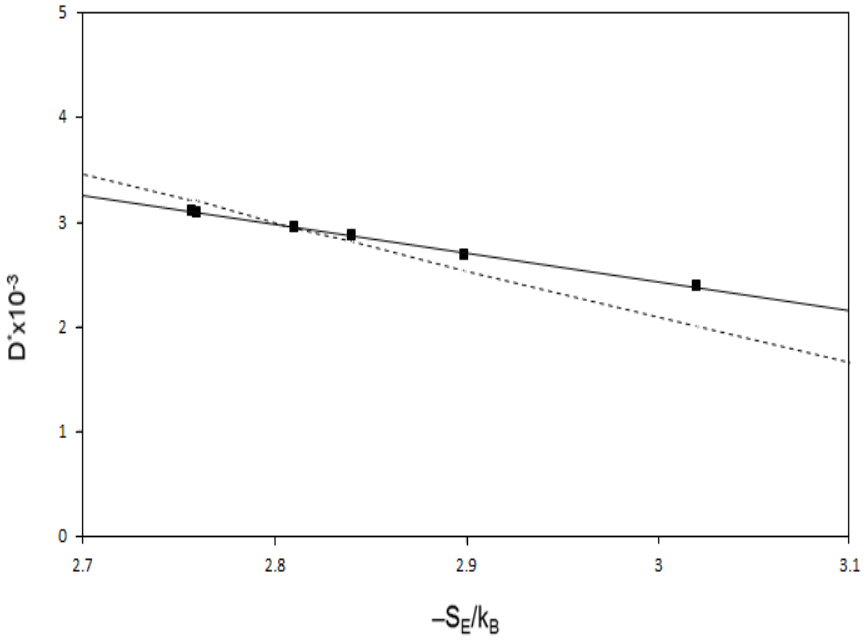

Fig. 6.5. D^* versus S_E for liquid Ag-Cu alloys; the dashed line is Dzugutov's law.

The plot of dimensionless diffusion coefficients versus excess entropy as a function of composition of Cu in Ag-Cu alloys was shown in Fig. 6.5. A linear relation was found for Ag-Cu alloys which fulfill the scaling law hypothesis. A good correlation between excess entropy and dimensionless diffusion coefficients was obtained as demonstrated from the comparison with Dzugutov's law (Dzugutov, 1996).

7. CONCLUSIONS

The structure factor is shown to play a major role in obtaining both equilibrium and non-equilibrium properties of liquids. Thus, various microscopic structural functions and derived associated properties of liquid metals and binary liquid alloys have been theoretically investigated and discussed in this thesis.

We give a detailed survey of literature which includes the integral equations proposed as Born – Green – Yvon (BGY), hyper-netted chain (HNC), and the Percus – Yevick (PY) which relate the potential function with the radial distribution function. In addition we give equations connecting radial distribution function (RDF) and thermodynamic quantities like compressibility, surface properties etc. Hence an understanding of liquid is possible if the distribution function is clearly perceived. The various correlation functions and the OZ equation are presented in diagram form for more clear understanding to viewers.

The applicability of square well potential as a perturbation over the result of the hard sphere solution of PY integral equation obtained by Wertheim and Thiele (Wertheim, 1963; Thiele, 1963) has been discussed in introduction of the thesis. We use the mean spherical model approximation (MSMA) to obtain the direct correlation function (DCF) outside the core. We emphasize that square well potential gives analytical expressions in which numerical computations are used and hence even other potentials, if attempted to solve structure and associated properties we feel that analytical expressions are more appropriate and hence the applicability of square well potential to be more superior than the rest especially for liquid metals and alloys.

The theory connecting scattering intensities and the structure factor is given. Finally the transport properties related to surface properties and the connected equations have been briefly given.

The Square well model was applied to a sample of liquid metals to compute the microscopic structural functions like structure factor, radial distribution function, coordination number. Transport properties eg. diffusion coefficients and shear viscosity of liquid metals were also presented. The computed results were found in good agreement with experimental values for most of the liquids. The discrepancy in some cases was discussed in the result and discussion section of the concerned chapters.

The transport properties of liquids together with structural and thermodynamic information provide an important base for theories of the liquid state especially when applied with success by computing the derived properties and comparing them with the available literature values.

Thus diffusion coefficient data were employed to determine the Debye temperature, surface tension and surface entropy in all the considered liquid metals. Further, newly developed scaling law for diffusion given by Dzugutov (Dzugutov, 1996) was extended and examined for the SW liquids as in order to confidently label the universal scaling law, the hypothesis must be tested with different form of the inter atomic potential. This study demonstrates that the Dgututov's scaling law is valid for SW liquid metals under MSMA.

We have shown how the detailed partial structure of alloys can be obtained from Lebowitz solution of hard sphere mixtures (Lebowitz, 1964) with a square well perturbing tail. These computed partial structure factors are incorporated in the calculations of totals structure factors of Al – Cu and Ag – Cu alloys at different atomic percent of Cu. The SW model has been treated under MSMA to compute the total and

partial direct correlation functions in the attractive and repulsive regions of the interacting potential in both alloys (Al-Cu and Ag-Cu) at different atomic fraction of Cu. Thus the different partial DCFs $C_{ij}(r)$ are Fourier transformed to obtain $C_{ij}(k)$, from which the partial structure factors are computed.

It is important to point out that in the present calculations no experimental data of the alloys is used to generate the partial and total structure factors. The potential parameters were those obtained for pure metals fitted with the peak positions of the structure factors of pure constituents. With these potential parameters (the partial and total) structure factors were evaluated, and then Fourier transformed to get the partial and total radial distribution functions. In all the cases it is gratifying to note that the computed theoretical structure factors are found to be in excellent agreement with the experimental values. We also obtained total and partial coordination numbers from partial and total pair correlation functions respectively.

This indicates that the alloys structure factors can be computed completely using theoretical methods without taking any experimental values of the alloys.

At this juncture it is important to note that with one total structure factor it is not possible to calculate the three partial structure factors. Of course it is possible to do different experiments with different isotopic substitution. Hence the present detailed model calculations are of immense help and important.

The Bhatia - Thornton fluctuations (Bhatia and Thornton, 1970) namely the number - number, concentration - concentration, and number - concentration correlation functions have been shown to be related to the partial structure factors linearly and hence these thermodynamically important quantities are also computed from the partial structure factors at various compositions of alloys in the entire momentum space with special emphasis on the values at long wave limit from which we evaluate the chemical

short range order parameter (CSRO) to comprehend the segregating and compound formation tendencies in binary melts.

Thermodynamically concentration-concentration correlation function in the long wavelength limit $S_{CC}(0)$ has been evaluated and discussed in chapter 5. This function helps to understand the complexities of binary liquid alloys and various thermodynamic functions as well.

Further isothermal compressibility has been calculated as a function of Cu composition in Al - Cu and Ag - Cu alloys by incorporating long wavelength of structure factor in Kirkwood-Buff's equation.

The self and mutual diffusion coefficients along with Onsager's coefficient, D_{id} were calculated by incorporating thermodynamic factor due to $S_{CC}(0)$ in Darken's equation. The theoretically calculated partial and total structure factors were employed to derive the self and mutual diffusion coefficients in Al - Cu and Ag - Cu alloys at different compositions of Cu. For this we use the Helfand's linear trajectory principle generalized by Davis and Polyvos (Davis and Polyvos, 1967) for a binary mixture. The self - diffusion coefficient of i^{th} constituent in a binary system is calculated through the Einstein's equation given by

$$D_i = \frac{k_B T}{\xi_i} \tag{7.1}$$

The friction coefficient of the i^{th} constituent ξ_i is a contribution from three parts given by

$$\xi_i = \xi_i^H + \xi_i^S + \xi_i^{SH} \tag{7.2}$$

Here, ξ_i^H, ξ_i^S and ξ_i^{SH} are respectively the hard sphere, soft and cross coefficient of the friction constants respectively. The equations connected with these have been applied to evaluate the total friction constant for the alloys. It is found that the hard

sphere contribution to friction constant, as expected, is predominant. However, it is found in both the alloys the soft part is also considerable.

Further in both the alloys, it is found that the ratio of the self-diffusion coefficients of the constituents for all concentrations is constant. This implies that both the alloys form regular solutions.

New equations have been formulated for the temperature dependence of diffusion coefficient for binary mixture. These equations are extended to Al-Cu and Ag-Cu alloys at different concentrations of Cu for evaluating the activation energy of diffusion. The computed value of activation energy of diffusion obeys Arrhenius law are in good agreement with available literature values.

Recently developed Dzugutov's scaling law for diffusion (Dzugutov, 1996) has been examined by using square well form of inter particle interaction for pure liquid metals and binary liquid alloys as well. The excess entropy, S_E per atom in liquid metal is defined as (Dzugutov, 1996; Yokayama, 1998)

$$S_E = -2\pi\rho_{ij}\sum_{i,j=1}^{2} C_i C_j \int_0^{\infty}\{g_{ij}(r)\ln[g_{ij}(r)] - [g_{ij}(r)-1]\}r^2 dr \qquad (7.3)$$

and thus the modified scaling diffusion coefficient for SW interaction is given as $D^*=D/\Gamma r^2_{max}$. Further, the concept is extended for SW binary liquids in terms of scaling factor obtained through correlation functions of the considered binary liquid alloys.

$$D_i = \frac{k_B T}{\xi_i} \qquad (7.4)$$

The Dzugutov's universal scaling law is an important function among many scaling laws, which links the dynamic behavior of a liquid particle with microscopic correlation functions. This new piece of work opens the path for formulation of new scaling law for different transport properties in liquids with SW potential.

Thus, in all the calculations of structural, transport and thermodynamic properties the potential parameters of the pure constituents only have been used and no experimental data of the alloys have been employed.

Thus, in this thesis we present

(1) TSFs and g(r) of liquid metals (Na, K. Cs, Mg, Al, In, Pb, Ag, Cu and Au) were determined. The computed structural parameters were employed to derive transport, thrmophysical and surface properties in the considered liquid metals.

(2) Partial and total structure factors, partial and total radial distribution functions and coordination numbers in Al - Cu and Ag - Cu alloys at different concentrations of Cu.

(3) Bhatia – Thornton correlation functions in the entire momentum space with special emphasis on the values at long wave limit i.e. $S_{CC}(0)$, chemical short range order parameter and compressibility of the same alloys at different concentrations.

(4) The self and mutual diffusion coefficients have been calculated for the constituents of the same alloys through the use of Helfand linear trajectory principle at various concentrations. Extension of equations for the computation of activation energy in binary mixtures has been given.

(5) The universal scaling law was tested with the SW interaction in one component liquid metals to binary liquid alloys.

It may be concluded that models of liquid state must be judged according to the success with which they account for the kinetic and equilibrium properties of liquids.

Future immediate work and improvement that can be done on these studies:

(1) The calculated and computed structural and transport properties can be used for calculating various other properties of monatomic and binary liquids such as electrical conductivity, thermal conductivity, thermal radiation, bulk viscosity etc.

(2) The activity coefficient of pure constituent in a binary mixture can be calculated theoretically without using any experimental data from concentration – concentration fluctuation in the long wave limit i.e. through $S_{CC}(0)$ and free energy calculations.

(3) Pressure derivative of diffusion coefficients can be formulated, which can be employed to determine the Grüneisen parameters in liquid metal and alloys. This thermophysical property can be used to calculate various mechanical and thermodynamic properties of liquids.

(4) The scaling viscosity can be formulated for the SW model of liquids.

We finally believe that the structure factor is the most important and unifying property in deriving static, dynamic, elastic, equilibrium and non-equilibrium properties of liquids.

LIST OF PUBLICATIONS

A. Journals

International Journals

1. Raj Kumar Mishra, **R. Lalneihpuii**, Raghvendu Pathak. Investigation of structure, thermodynamic and surface properties of liquid metals using square well potential. *Chemical Physics*, 457 (2015), 13-18. ISSN: 0301-0104 [IF: 1.758]
2. Raj Kumar Mishra, **R. Lalneihpuii.** Test of the universal scaling law for square well liquid metals. *Journal of Non-Crystalline solids*, 444 (2016), 11-15. ISSN: 0022-3093 [IF: 1.825]

National Journals

3. **R. Lalneihpuii**, Raj Kumar Mishra. Transport and surface properties of liquid metals using their diffusion data. *Science and Technology Journal*, 4:2 (2016), 123-126. ISSN:2321-3388

Book chapters

4. Raj Kumar Mishra, **R. Lalneihpuii**, R Pathak. Concentration-Concentration Correlation in Long Wavelength Limit and Short Range Order in Binary Alloys. *Basic and Applied Physics,* 175-182. ISBN 978-81-8487-517-1, Narosa Publication, New Delhi.
5. R Pathak, **R. Lalneihpuii**, Raj Kumar Mishra. Statistical mechanical Studies of liquid metals.*Green Chemistry for Greener Environment*.135-141.ISBN 978-81-928823, Educreation Publication, New Delhi,

Communicated Papers

1. Bhatia-Thornton characteristics structure factors, dynamic and ordering in liquid Al-Cu alloys within the Square well model (Communicated).
2. Concentration dependent structural, transport surface and scaling properties in liquid Al-Cu alloys (Communicated).

B. Paper presented in Conferences / Symposia

1. **R**. **Lalneihpuii**, Raj Kumar Mishra, R. Pathak. Statistical mechanics of liquids. National Seminar on "Green Chemistry for Greener Environment", 26^{th} – 27^{th} November, 2012. Organized by Department of Chemistry, Pachhunga University College, Aizawl, Mizoram, India.

2. Raj Kumar Mishra, **R. Lalneihpuii**, R Pathak. Concentration-Concentration Correlation in Long Wavelength Limit and Short Range Order in Binary Alloys. 8^{th} National Conference of the Physics Academy of North East, 17^{th} – 19^{th} December, 2012. Organized by Department of Physics, Mizoram University, Aizawl, Mizoram, India.

3. **R. Lalneihpuii,** Raj Kumar Mishra.Theoretical and Computational studies on liquid Al-Cu alloys. 8^{th} Mid-year CRSI National Symposium in Chemistry, 10^{th} – 12^{th} July, 2014. Organized jointly by CSIR-North East Institute of Science and Technology, JorhatandTezpur University, Tezpur.

4. **R. Lalneihpuii,** Raj Kumar Mishra.Comparision of experimental X-ray scattering with theoretical model for liquids. Orientation workshop on Radiation - Its applications in Chemical, Physical and Life Sciences. 29^{th} – 31^{st} October, 2014. Organized jointly by UGC-DAE Consortium for Scientific Research, Kolkata Centre and Department of Chemistry, Mizoram University, Aizawl.

5. **R. Lalneihpuii**, Raj Kumar Mishra.Static and Dynamic properties of Al-Cu melts. 18^{th} CRSI National Symposium in Chemistry, 5^{th} – 7^{th} February, 2016. Organized by Institute of Nano Science and Technology and Panjab University, Chandigarh, India.

6. Raj Kumar Mishra, **R. Lalneihpuii**. Calculation of diffusion coefficient of liquid metals. National Conference on Application of Mathematic, 25^{th} – 26^{th} February, 2016. Organized by Department of Mathematics and Computer Science, Mizoram University, Aizawl, Mizoram, India.

7. **R. Lalneihpuii,** Raj Kumar Mishra. Structure, thermodynamic and surface properties of liquid metals investigated by square well potential. Condensed Matter Days-2016, National Conference, 29^{th} – 31^{st} August, 2016. Organized by Department of Physics, Mizoram University,Aizawl, Mizoram, India.

Chemical Physics 457 (2015) 13–18

Contents lists available at ScienceDirect

Chemical Physics

journal homepage: www.elsevier.com/locate/chemphys

Investigation of structure, thermodynamic and surface properties of liquid metals using square well potential

Raj Kumar Mishra [a,*], R. Lalneihpuii [a], Raghvendu Pathak [b]

[a] Department of Chemistry, School of Physical Sciences, Mizoram University, Aizawl 796 004, India
[b] Department of Chemistry, Pachhunga University College, Aizawl 796 001, India

ARTICLE INFO

Article history:
Received 12 December 2014
In final form 11 May 2015
Available online 19 May 2015

Keywords:
Square well potential
Structure factor
Diffusion coefficient
Coordination number
Surface tension

ABSTRACT

In the present paper surface tension, Debye temperature, coordination numbers along with microscopic correlations of ten liquid metals are determined using square-well model of correlation functions. Wertheim's solution of the fundamental statistical mechanical equation given by Percus and Yevick for hard spheres is invoked with a square well attractive part as a perturbation tail to get exact solution of the direct correlation function, $C(k)$ in momentum space and the analytical expressions are obtained for structure factor, $S(k)$. These expressions are then used to predict static structure factors for ten liquid metals, leading to fair agreement with experimental data. Radial distribution function $g(r)$ is obtained by Fourier analysis of computed $S(k)$, from which the coordination numbers and the nearest neighbor distances of liquid metals are evaluated. Computed coordination numbers and surface properties of liquid metals using such a simple technique are in good agreement with experimental results.

1. Introduction

The auto correlation function, $S(k)$ (where $k = \frac{4\pi}{\lambda}\sin\theta$) and its Fourier component $g(r)$, pair correlation function (PCF) are important quantities characterizing the structure of a liquid. Experimentally these quantities have been determined using neutron or X-rays scattering intensities. PCF is obtained by Fourier analysis of experimental $S(k)$, which is a laborious and costly procedure. The analysis of results on structure and thermodynamic properties of liquid metals and alloys enable us to understand their structural ordering and complexities [1–4]. Hence, a detailed knowledge of the $S(k)$ or $g(r)$ is essential for a quantitative understanding of the structure of liquids and is also sufficient to determine numerous other equilibrium and transport properties [4–7].

The subject of statistical mechanics has been successfully applied in various fields including the prediction of the microscopic function, $S(k)$ of liquid metals [8–10]. Wertheim [11] and Thiele [12] (WT) solved Percus–Yevick's (PY) equation for hard sphere fluids to obtain the hard sphere direct correlation function $C_{hs}(r)$. Liquid metals static structure factors behave like hard sphere fluids and calculations of thermo-physical and thermodynamic properties with this reference system have been found to be reasonable in many cases [13]. However, we believe with other researchers that hard sphere reference system lacks realistic properties because thermodynamics and the relation between thermodynamics with $S(k)$ or $g(r)$ are different for hard sphere and real fluids [14]. Hence, it is important to include attraction between the particles in deriving structure factors of liquids. It must be mentioned that the hard sphere repulsive forces act up to a short-range and primarily determine the structure peak of a liquid and the relatively long-range uniform attractive part of the potential brings atoms in short-range order. Further, it is pointed out that the success of any theoretical model depends on its experimental confirmation [15,16]. Thus in the present work the square-well (SW) attractive tail has been perturbed over a hard sphere reference system to evaluate the direct correlation function $C(k)$ in momentum space, in deriving the structure factors of liquid metals. The analytical solution of the SW model with the mean spherical model approximation was introduced by Rao et al. [17–19]. The model is applied to a number of liquid metals to obtain microscopic structural characteristics with their application in the determination of various properties of the considered systems. Present work has been devoted to study the structure, thermodynamic and surface properties of liquid metals within Mean Spherical Model Approximation (MSMA) ranging from alkali metals to more complex metals of the periodic table.

The SW potential includes both repulsive and attractive parts and is easy to solve numerically and hence it is most suitable for different theoretical techniques, such as integral equations or

* Corresponding author. Tel.: +91 9774379665.
E-mail address: rkmishramzu@yahoo.com (R.K. Mishra).

http://dx.doi.org/10.1016/j.chemphys.2015.05.006
0301-0104/

perturbation theories. The SW potential has been successfully applied for metallic liquids [17–20], colloidal particles [21,22], hetro-chain molecules [23,24] and complex systems [25,26].

Here we consider that the multi-particle interactions are due to the sum of pair wise interactions.

The study of coordination number, Debye temperature and surface tension of melts is of fundamental importance and the better understanding of these properties is helpful in material processing technology. The coordination number of liquid metals is determined from their $g(r)$ curves using square well parameters. Several authors have reported that the surface properties of liquids are largely dependent on their bulk microstructural characteristics and their transport properties.

In the present paper self diffusion coefficients data of several liquid metals were employed to determine their surface tension, which is recently published by many authors with different approaches [27,28]. Lu et al. [27] reported that surface tension, γ_{ST} values are not well known experimentally even for many simple metals.

2. Theoretical formalism

2.1. Evaluation of static structure factor and coordination number

The SW is an extension of the hard sphere potential that retains hard sphere repulsive properties but also allows the particles to attract one another and the interaction energy $U(r)$ between the two square well particles separated by a distance r is given by

$$\beta U(r) = \begin{cases} \infty; & r < \sigma \\ -\varepsilon; & \sigma < r < \lambda\sigma \\ 0; & r > \lambda\sigma \end{cases} \tag{1}$$

where σ is the hard core diameter, σ $(\lambda - 1)$ and ε (<0) are the breadth and depth of the potential well, $\beta = 1/k_BT$.

An important model system is the MSMA, first proposed by Lebowitz and Percus [29], which expressed $g(r)$ and the direct correlation function $C(r)$ as

$$\left.\begin{array}{ll} g(r) = 0; & r < \sigma \\ C(r) = -U(r)/k_BT; & r > \sigma \end{array}\right\} \tag{2}$$

We write the Ornstein–Zernike direct correlation function (DCF) of a square well fluid in momentum space under MSMA as

$$C(k) = C_{hs}(k) + C_{sw}(k). \tag{3}$$

With

$$\begin{aligned} \rho\, C_{hS}(k) = -[24\eta/(x)^6][\alpha(x)^3\{\sin(x\sigma) - x\cos(x)\} \\ + \beta(x)^2\{2x\sin(x) - (x^2-2)\cos x - 2\} \\ + \gamma\{(4x^3 - 24x)\sin(x) \\ - (x^4 - 12x^2 + 24)\cos x - 24\}]. \end{aligned} \tag{4}$$

Table 1
Input parameters of liquid metals with σ as the diameter, ε/k_B as the depth, λ as the breath of the square well potential and ρ as the number density.

Metals	Temperature (K)	σ (nm)	ε/k_B (K)	λ	ρ (10^{25} m^{-3})
Sodium	378	0.330	111.60	1.65	2430
Potassium	343	0.411	96.14	1.65	1276
Cesium	303	0.481	109.5	1.70	0813
Magnesium	953	0.275	127.82	1.43	3900
Aluminum	943	0.245	160.00	1.30	6459
Indium	433	0.283	173.76	1.70	3686
Lead	613	0.297	70.00	1.4	3099
Silver	1273	0.260	500.00	1.75	5159
Copper	1423	0.225	300.00	1.68	7408
Gold	1373	0.260	600.00	1.73	5271

Table 2
Theoretical and experimental values of first positions (k) and peak heights $S(k)$; first peak positions (r) and peak heights $g(r)$ of liquid metals.

Metals	First peak of $S(k)$				First peak position $g(r)$			
	Theoretical		Experimental		Theoretical		Experimental	
	k (nm^{-1})	$S(k)$	k (nm^{-1})	$S(k)$	r (nm)	$g(r)$	r (nm)	$g(r)$
Na	20.0	2.7	20.0	2.7	0.36	3.24	0.37	2.42
K	16.0	2.6	16.0	2.6	0.45	2.80	0.46	2.35
Cs	14.0	2.5	14.0	2.7	0.50	3.61	0.51	2.58
Mg	25.0	2.5	24.0	2.5	0.29	2.84	0.31	2.46
Al	27.0	2.4	27.0	2.4	0.27	2.47	0.28	2.83
In	23.0	2.4	23.0	2.5	0.30	2.64	0.31	2.66
Pb	23.0	2.5	23.0	2.5	0.32	2.34	0.32	2.98
Ag	26.0	2.3	26.0	2.5	0.28	2.98	0.28	2.58
Cu	30.0	2.4	30.0	2.7	0.25	2.35	0.25	2.75
Au	26.0	2.4	26.0	2.5	0.28	2.68	0.28	2.77

$$\rho\, C_{SW}(k) = [24\eta\varepsilon/k_BT](x)^3[\sin(\lambda x) - \lambda x\cos(\lambda x) + x\cos(x) - \sin(x)]. \tag{5}$$

where $x = k\sigma$, ρ is the number density and the other terms that enter in Eq. (4) are given by following expressions [30].

$$\alpha = \frac{(1+2\eta)^2}{(1-\eta)^4} \tag{6}$$

$$\beta = -\frac{6\eta(1+\eta/2)^2}{(1-\eta)^4} \tag{7}$$

$$\gamma = \frac{\eta\alpha}{2} \tag{8}$$

where η is the packing fraction i.e. volume occupied by the atoms divided by total volume and is given by

$$\eta = \frac{\pi\rho\sigma^3}{6}. \tag{9}$$

The $S(k)$ of one component liquid can be given in terms of $C(k)$ as

$$S(k) = [1 - \rho\, C(k)]^{-1}. \tag{10}$$

Experimentally obtained $g(r)$ provides limited information about the short range order of liquids but the nearest-neighbor coordination number ψ can be obtained by integrating the $g(r)$ function between the first two minimum i.e. the left edge of the first peak to the first minimum on the right hand side of the first peak, r_{min}. ψ characterizes several types of short-range order present in the liquids [2].

The Fourier inversion of $S(k)$ gives the radial distribution function, $g(r)$.

$$g(r) = 1 + \frac{1}{2\pi^2\rho}\int_0^\infty k^2[S(k) - 1]\frac{\sin(kr_{nm})}{kr_{nm}}dk. \tag{11}$$

The microstructure of liquids can also be characterized by ψ, which is obtained by integration over the whole area between the beginning and first minimum values of radial distance.

$$\psi = 4\pi\rho\int_0^{r_{\min}} g(r)r^2dr. \tag{12}$$

Here r_{min} is the first minimum of the radial distribution function.

Further self diffusion coefficients for the liquid metals examined using the well known Einstein's formula $D = \frac{k_BT}{\xi_H+\xi_S+\xi_{HS}}$. Here ξ_H, ξ_S and ξ_{HS} are the friction coefficients due to hard, soft and hard-soft part of the potential function respectively and are obtained in line with Ref. [20] under Helfand's linear trajectory principle, using a SW tail as a soft perturbation over hard sphere reference system, and can be given as follows

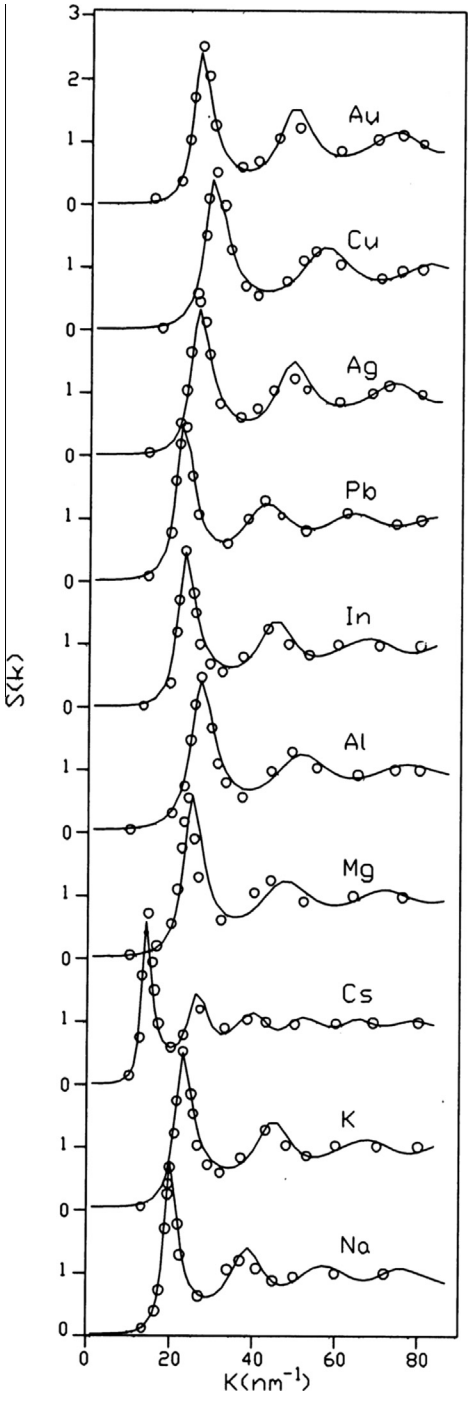

Fig. 1. $S(k)$ against k for liquid metals, (———) present calculated results; (○○○) experimental results.

$$\xi_H = \frac{8}{3}\rho\sigma^2(\pi m k_B T)^{1/2} g^{HS}(\sigma) \tag{13}$$

$$\xi_S = -\frac{1}{3}\frac{\rho}{4\pi^2}\left(\frac{\pi m}{k_B T}\right)^{1/2}\int_0^\infty \frac{1}{\rho}k^3 U^{SW}(k)[S(k)-1]dk. \tag{14}$$

$$\xi_{HS} = -\frac{1}{3}\rho g^{HS}(\sigma)\left(\frac{m}{\pi k_B T}\right)^{1/2} \times \int_0^\infty [k\sigma\ cos(k\sigma) - \sin(k\sigma)]U^{SW}(k)dk. \tag{15}$$

Here $U^{SW}(k)$ is the Fourier transform of the SW potential

$$U^{SW}(k) = \frac{4\pi\varepsilon}{k^3}[Ak\sigma\ \cos(Ak\sigma) - \sin(Ak\sigma) - k\sigma\ \cos(k\sigma) + \sin(k\sigma)] \tag{16}$$

2.2. Relation of self diffusion coefficient in bulk liquid metals to surface properties and Debye temperature

Detailed studies of the surface properties of condensed matter help in understanding their metallurgical processing.

The surface tension of elemental liquids can be given by statistical mechanical approach under zeroth order approximation as [31]

$$\gamma_{ST} = \frac{\pi\rho^2}{8}\int_0^\infty \frac{dU(r)}{dr}g(r)r^4 dr. \tag{17}$$

Born and Green [32] derived the coefficient of viscosity of liquid metals using statistical mechanical approach as

$$\eta_V = \frac{2\pi\rho^2}{15}\left(\frac{m}{k_B T}\right)^{1/2}\int_0^\infty \frac{dU(r)}{dr}g(r)r^4 dr. \tag{18}$$

Here m is the atomic mass of the liquid metals. Eqs. (17) and (18) were derived on a strong scientific basis for hard sphere model but it is not easy to get the numerical solution of the integral equations. As we know that the statistical mechanics also provides various useful relationships between structure and thermodynamic properties of liquids.

A striking result can be obtained by using Eqs. (17) and (18) with the well-known Stokes–Einstein relation, $\eta_V = k_B T/(2\pi\ aD)$, here a, the nearest neighbor distance, can be taken as first peak position of $g(r)$ for real liquids [33] as

$$\gamma_{ST} = \frac{(k_B T)^{3/2}}{m^{1/2}}\frac{15}{32\pi a D}. \tag{19}$$

Since, D can be evaluated from well-known Einstein's relation using the SW long range interaction and hence the surface tension of liquid metals is obtained through Eq. (19).

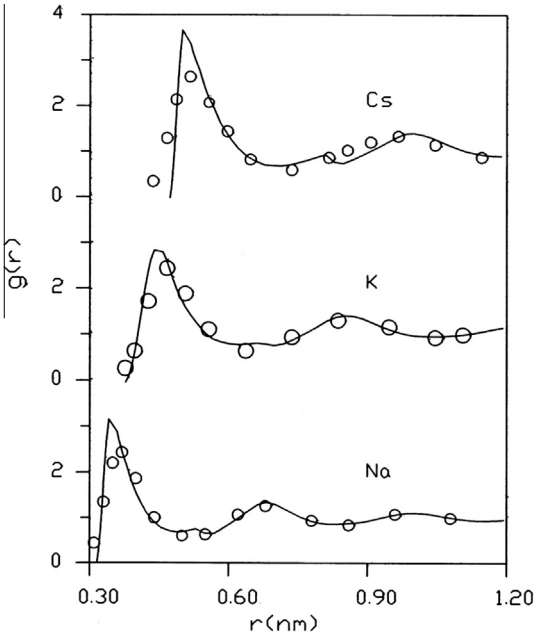

Fig. 2a. $g(r)$ against r for liquid metals, (———) present calculated results; (○○○) experimental results.

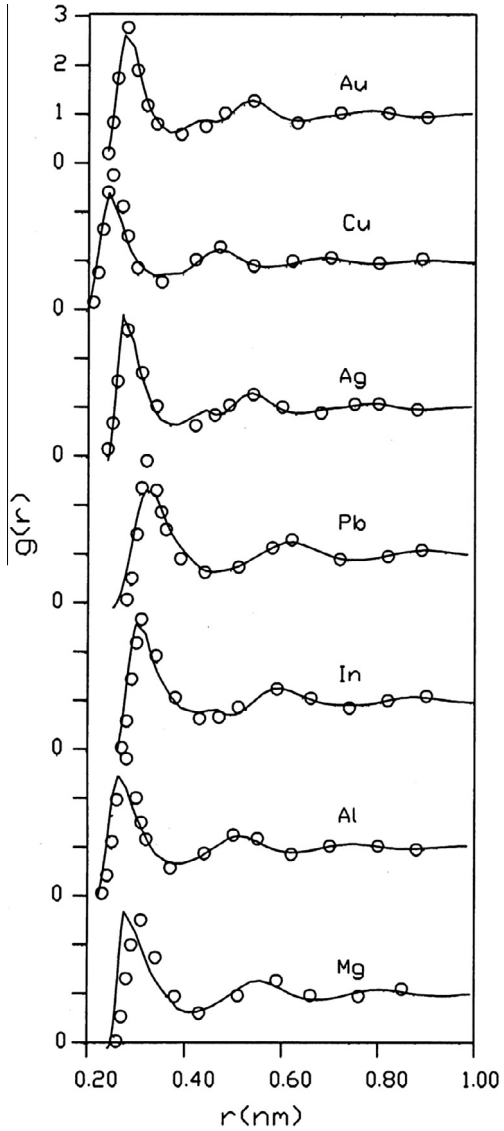

Fig. 2b. $g(r)$ against r for liquid metals, (———) present calculated results; (○○○) experimental results.

Recently Singh and Ali [34] presented the Debye temperature, θ_D, for a number of liquid metals, which is an important characteristic of melts. This is well-known fact that metallic glasses show some features of liquid metals [2,35] and hence computed diffusion coefficients were verified by calculating θ_D, using the equation obtained by Lal and Singh [36]

$$\theta_D = \frac{96Dh}{k_B a^2}. \tag{20}$$

Here h is Planck's constant, k_B is Boltzmann's constant, a is the nearest-neighbor distance in $g(r)$ and D is the self diffusion coefficient of liquid metals.

3. Results and discussion

Wertheim's solution [11] of PY hard sphere fluid perturbed with the SW potential within MSMA was solved numerically using temperature, T, atomic density, ρ, and the SW parameters as input data. Using the molar volumes of liquid metals as given by Singh and Sommer [37] number densities were calculated. The input parameters of liquid metals are listed in Table 1.

The peak positions and peak heights of the computed $S(k)$ and $g(r)$ for all the considered liquid metals are presented in Table 2 together with their experimental values, which give detailed information regarding the principal peak and structural characteristics of the metals. From Table 2, it is seen that the agreement between our computed $S(k)$ and the experimental results [38] around the first peak appears to be very good. But in the case of Cs, Ag and Cu the peak heights from the calculation are slightly lower than that from the experiment but the peak positions are same. It is pointed out that the principal peak dominates in evaluating transport properties of real liquids. A similar trend is observed by Rao and Murthy [17–19] while calculating $S(k)$ for four liquid metals using the SW model under the random phase approximation. The difference in peak heights for these three metals may be due to existence of some small atomic cluster in these liquids which is not signifying by this model. However, other properties obtained with the same parameter are in fair agreement with the experimental values.

The calculated results for $S(k)$ of these metals at their respective temperatures together with their experimental values in entire momentum space are depicted in Fig. 1. The agreement between our computed results and the experimental results [38] is good throughout the k regions. We find from Fig. 1 that structure factors of all the considered metals become constant around one in high k region. It shows the presence of short range order in liquid materials. Further, it may be noted that the simulation result with different approaches [1,7,16] for the peak height and position of $S(k)$ of number of liquid metals did not agree well with experiment. However, *ab initio* molecular dynamic simulation for the study of the structure and dynamic properties of liquids has been widely considered by the research community [39].

The peak positions and peak heights of the $g(r)$, computed from Eq. (11), for all the considered metals with their experimental values are listed in Table 2 and are also presented in Fig. 2(a) and Fig. 2(b). The ratio of the positions of the first and second peaks of the calculated and the experimental $g(r)$ for all the liquids taken

Table 3
First minimum position of computed $g(r)$; theoretical and experimental values of first coordination number (ψ) of liquid metals.

Metals	First minimum position of $g(r)$	ψ_{Computed}	$\psi_{\text{Experimental}}$
Na	0.49	10.5	10.4
K	0.62	10.8	10.5
Cs	0.70	11.4	–
Mg	0.42	10.2	10.9
Al	0.39	11.2	11.5
In	0.43	11.4	11.6
Pb	0.45	10.5	10.9
Ag	0.38	10.6	11.3
Cu	0.34	10.7	11.3
Au	0.37	10.3	10.9
		Average = 10.76	11.03

Table 4
Friction coefficients of liquid metals due to hard sphere ξ_H, square well ξ_S and hard sphere- square well interaction ξ_{HS}.

Metals	$\xi_H \times 10^{-13}$ (kg/s)	$\xi_S \times 10^{-13}$ (kg/s)	$\xi_{HS} \times 10^{-13}$ (kg/s)
Na	7.41	1.56	1.94
K	7.55	1.12	1.58
Cs	7.56	1.50	1.89
Mg	11.78	1.36	1.19
Al	11.98	1.76	1.07
In	18.14	4.39	5.38
Pb	25.59	2.04	1.75
Ag	42.28	8.25	12.56
Cu	31.96	2.78	4.53
Au	62.19	11.05	18.65

Table 5
Theoretical and experimental values of diffusion coefficient, D, Debye temperature, θ_D and surface tension, γ_{ST} of liquid metals.

Metals	$D_{Computed}$ (10^{-9} m^2/s)	$D_{Experimental}$ (10^{-9} m^2/s)	$\theta_{DComputed}$ (K)	$\theta_{DLiterature}$ (K)	$\gamma_{STComputed}$ (Nm^{-1})	$\gamma_{STExperimental}$ (Nm^{-1})
Na	4.70	4.23	167.34	97.20	0.176	0.200, 0.197
K	4.28	3.76	97.37	59.20	0.096	0.110, 0.112
Cs	2.18	2.31	40.17	–	0.082	0.069, 0.070
Mg	5.23	5.63	286.51	–	0.418	0.557, 0.583
Al	4.93	4.87	311.53	294.00	0.801	0.867, 1.070
In	2.10	2.60	107.48	–	0.251	0.561
Pb	2.87	2.19	129.12	81.00	0.211	0.457, 0.462
Ag	2.61	2.55	152.77	164.10	1.026	0.925, 0.910
Cu	4.85	3.97	357.51	244.40	1.030	1.310, 1.320
Au	2.10	–	123.38	121.60	1.200	1.145, 1.138

under investigation is about 0.51 and 0.53 respectively. This suggests that our model calculation of $g(r)$ gives the structural properties of real liquids fairly well.

The deviation of $g(r)$ from unity is a measure of the local order around the reference atoms. There are few maxima and minima in the $g(r)$ which rapidly damped around unity, where the first maximum corresponds to the position of the nearest neighbors around an origin atom.

The nearest-neighbor distance, a, and the first coordination numbers (ψ) were obtained by using Eq. (12), for liquid metals and the computed values are presented with their corresponding experimental results [40] in Table 3. In all cases the first peak and first minimum of computed $g(r)$ lie between σ to $\lambda\sigma$. The computed values of ψ lie between 10.3 and 11.4 and that of the experimental values lie between 10.4 and 11.6. It is worth to mention here that the variation in values of ψ even for simple liquids depends on the theoretical approach of the computation [40]. Detailed study of the first cell coordination number in liquid and crystalline form of the metals helps to understand the local structure in two phases [2].

Table 3 illustrates that the computed values of ψ are in good agreement with the experimental data. The computed average ψ of the ten liquid metals is 10.76 and is closed to the experimental average ψ of the considered metals which is 11.03. This shows that the theoretical and computational method presented in this work is suitable for the determination of coordination number of liquid metals. Computed values of friction coefficients ξ_H, ξ_S and ξ_{HS} are presented in Table 4. ξ_H is dominating in all cases however ξ_S and ξ_{HS} also contribute significantly in the case of all the considered liquid metals. All the three components of friction coefficients has lower values for Cu compared to those of Ag and Au however working temperature of Cu is higher than these two liquid metals. This may be due to the existence of some amorphous characteristics in liquid Cu at 1423 K.

The diffusivity in liquid metals has been evaluated under LT principle as mentioned in Ref. [20] using well known Einstein equation for coefficient of diffusion [41]. Computed results are compared with available experimental results [33] and presented in Table 5.

Lal and Singh [39] proposed a relationship between Debye temperatures, θ_D with self diffusion coefficient for metallic glasses. Since it has been established that metallic glasses may be considered as super cooled liquids [2,35] hence this relationship is tested for all the considered liquid metals using square well model of diffusion. θ_D is an important parameter concerning the bonding and structural deformation of metals. Computed values for θ_D are summarized in Table 5 and compared with recently calculated and published values by Singh et.al [34]. The agreement can be considered satisfactory, for the reasons mentioned already.

The surface tension is related with self-diffusion coefficients of liquids. Since, self diffusion coefficients of liquids are determined using microscopic structural functions along with SW potential, and hence computed γ_{ST} are also related to the microscopic structure of liquids.

Computed values of γ_{ST} with their experimental values taken from Ref. [27] are also presented in Table 5 and we find satisfactory agreement between them.

4. Conclusions

In the present work, we present results of a microstructural study of ten liquid metals. The SW potential is analytically solved and successfully applied for computing static structure factor, coordination number and thermodynamic properties of the considered liquids which are important information for metallurgical industry. Our results indicate that the SW model leads to a good agreement between computed and experimental results of structure factors and derived associated properties and hence increase our confidence in present model. This model calculation provides an option to use the SW potential in the framework of the MSMA to derive the various thermo-physical and thermodynamic properties of liquid metals without using any adjusting parameter.

Coordination number calculated with number density and square well parameters are important findings to understand phase change at the microscopic level.

Perturbation theory with hard sphere reference system is a good first approximation for the study of static and dynamic properties of liquid metals. The correlation between D and γ_{ST} finds successful application for the estimation of γ_{ST}. Debye temperatures of liquid metals are calculated using diffusion data obtained through square well model.

Conflict of interest

I did not declare any conflict of interest in this paper.

Acknowledgments

R K Mishra acknowledges the financial support from the Department of Science and Technology, Govt. of India, New Delhi under Fast Track Project (SR/FT/CS-021/2008) and R. Lalneihpuii to the University Grant commission, New Delhi for awarding Rajiv Gandhi National Fellowship.

References

[1] J.F. Wax, R. Albaki, J.L. Bretonnet, Phys. Rev. B 62 (2000) 14818.
[2] G.X. Li, Y.F. Lang, Z.G. Zhu, C.S. Liu, Al. J. Phys.: Condens. Matter. 15 (2003) 2259.
[3] R.K. Mishra, R. Venkatesh, Chem. Phys. 354 (2008) 112.
[4] S.K. Lai, O. Akinlade, M.P. Tosi, Phys. Rev. A 41 (1990) 5482.
[5] R. Stadler, D. Alfe, G. Kresse, A. de Wijs, M.J. Gillan, J. Non-Cryst. Solids 82 (1999) 250.
[6] U. Balucani, A. Torcini, R. Vallauri, Phys. Rev. B 47 (6) (1993) 3011.
[7] J.N. Herrera, P.T. Cummings, H.R. Estrada, Mol. Phys. 96 (1999) 835.
[8] R.C. Gosh, A.Z. Ziauddin Ahmed, G.M. Bhuiyan, Eur. Phys. J. B 56 (2007) 177.
[9] M.P. Taylor, J.L. Strathmann, J.E.G. Lipson, J. Chem. Phys. 114 (2001) 5654.
[10] R.V. Gopala Rao, R. Venkatesh, Phys. Rev. B 39 (1989) 3563.
[11] M.S. Wertheim, Phys. Rev. Lett. 10 (1963) 321.
[12] E. Thiele, J. Chem. Phys. 39 (1963) 474.

[13] F. Zalid, G.M. Bhuiyan, S. Sultana, M.A. Khaleque, R.I.M.A. Rashid, S.M.M. Rahman, Phys. Stat. Sol. (b) 215 (1999) 987.
[14] S. Ravi, M. Kalidoss, R. Srinivasanmoorthy, J. Amoros, Fluid Phase Equilibr. 178 (2001) 33.
[15] S.G. Prakash, R. Ravia, R.P. Chhabra, Chem. Phys. 302 (2004) 149.
[16] M. Boulahbak, N. Jakes, J.F. Wax, J.L. Bretonnet, J. Chem. Phys. 108 (1998) 2111.
[17] R.V. Gopala Rao, A.K. Murthy, Phys. Stat. Sol. (b) 66 (1974) 703.
[18] R.V. Gopala Rao, A.K. Murthy, Phys. Lett. 51A (1975) 3.
[19] R.V. Gopala Rao, A.K. Murthy, Z. Natur Forsch 30a (1975) 619.
[20] R. Venkatesh, R.K. Mishra, J. Non-Cryst. Sol. 351 (2005) 705.
[21] N. Asherie, A. Lomakin, G.B. Bendek, Phys. Rev. Lett. 77 (1996) 4832.
[22] M.G. Noro, Di Frenkel, J. Chem. Phys. 113 (2000) 2941.
[23] E. Zaccarelli, G. Foffi, K.A. Dawson, F. Sciortino, P. Tartaglia, Phys. Rev. E 63 (2001) 031501.
[24] J. Cui, J.R. Elliot, J. Chem. Phys. 114 (2001) 7283.
[25] Y. Zhou, M. Karplus, K.D. Ball, R.S. Berry, J. Chem. Phys. 116 (2002) 2323.
[26] Y. Zhou, M. Karplus, J.M. Wichert, C.K. Hall, J. Chem. Phys. 107 (1997) 10691.
[27] H.M. Lu, Q. Jiang, J. Phys. Chem. B 109 (2005) 15463.
[28] S. Blairs, J. Colloid Interface Sci. 302 (2006) 312.
[29] J.L. Lebowitz, J.K. Percus, Phys. Rev. 144 (1966) 251.
[30] R. Block, J.B. Suck, W. Freyland, F.Hansel, W. Glaser, in: Proceedings of 3rd International Conference on Liquid Metals, The Institute of Physics, Bristol, London (1977) 126.
[31] R.H. Fowler, Proc. R. Soc. A 159 (1937) 229.
[32] M. Born, H.S. Green, A General Kinetic Theory of Liquids, University Press, Cambridge, 1949.
[33] M. Shimoji, T. Itami, Diffusion and Defect Data, Atomic Transport in Liquid Metals, Trans Tech Publication, Switzerland, 1986.
[34] R.N. Singh, I. Ali, Int. J. Appl. Phys. Math. 3 (2013) 275.
[35] P.P. Mishra, M. Milanarun, N. Jha, A.K. Mishra, J. Alloys Compd. 340 (2002) 108.
[36] M. Lal, D.P. Singh, Indian J. Phys. A67 (1993) 445.
[37] R.N. Singh, F. Sommer, Rep. Prog. Phys. 60 (1997) 57.
[38] Y. Waseda, The Structure of Non-Crystalline Materials, McGraw-Hill, New York, 1980.
[39] U. Dahlborg, M. Besser, M.J. Kramer, J.R. Morris, M. Calvo-Dahlborg, Phys. B 412 (2013) 50.
[40] D.P. Tao, Metall. Mater. Trans. A 36A (2005) 3495.
[41] B.J. Berne, R. Pecora, Dynamics of Light Scattering: With Application to Chemistry, Biology and Physics, 3rd ed., Dover Publication, New York, 2000.

Journal of Non-Crystalline Solids 444 (2016) 11–15

Contents lists available at ScienceDirect

Journal of Non-Crystalline Solids

journal homepage: www.elsevier.com/locate/jnoncrysol

Test of the universal scaling law for square well liquid metals

Raj Kumar Mishra *, R. Lalneihpuii

Department of Chemistry, School of Physical Sciences, Mizoram University, Aizawl 796 004, India

ARTICLE INFO

Article history:
Received 2 November 2015
Received in revised form 6 April 2016
Accepted 10 April 2016
Available online xxxx

Keywords:
Square well model
Pair correlation function
Excess entropy
Surface entropy
Isothermal compressibility

ABSTRACT

A universal scaling law relating the dimensionless diffusion coefficient with excess entropy of a liquid [M. Dzugutov, Nature (London), 381 (1996), 137] is tested for liquid noble metals due to their fundamental importance both in society and industry. The square well form of interatomic potential is used to study liquid noble metals because it possesses the basic nature of real liquids. The radial distribution function (RDF), $g(r)$ and self diffusion coefficient, D of liquid noble metals were derived using statistical mechanical square well (SW) model under random phase approximation, which was proposed by Rao and Murthy [R. V. Gopala Rao and A. K. Murthy, Physics Letters A, 51 (1975), 3]. $g(r)$ and D data of liquid noble metals were employed to compute excess entropy, S_E using scaling law, surface entropy, S_V through temperature derivative of D under linear trajectory principle and microscopic reducing parameter; Enskog collision frequency, Γ. Further new equations have been derived from equation of state (EOS) for the SW potential and verified them to compute structure factor in the long wavelength limit. The results obtained were compared with available experimental results and we find there is fair agreement between theoretical and experimental values. Present study shows the applicability of the Dzugutov scaling law for square well liquids.

1. Introduction

The study of transport coefficients such as diffusion and viscosity of liquid metals and alloys is important for metallurgical, industrial and biophysical processes [1,2]. Statistical mechanics provides numerical relations between structures, dynamic and thermodynamic properties of liquid metals and alloys [3]. In recent years different scaling laws relating the equilibrium thermodynamic properties, excess entropy with dimensionless transport coefficients have been reported by many authors [2,4–6]. The Dzugutov universal scaling law [4] is very important function among many scaling laws, which links the dynamic behavior of a liquid particle with pair correlation function, $g(r)$, microscopic reducing parameter Γ and excess entropy. Dzugutov in his original work approximated the excess entropy per particle by two body approximations, which is denoted as S_2 and defined by

$$S_2 = -2\pi\rho\int_0^\infty \{g(r)\ln[g(r)] - [g(r)-1]\}r^2 dr. \quad (1)$$

Here ρ is the number density. Yokoyama has modified Dzugutov's two body approximation by the term S_E [7]. The S_E per atom in liquid metals is the difference between the total thermodynamic entropy and that of the equivalent ideal gas.

In last two decades a considerable efforts have been made using molecular dynamics simulation to verify the Dzugutov universal scaling law by other researchers with embedded atom method (EAM) or Stillinger-Weber scheme or Tersoff potential or glue potential or second-moment approximation of tight-binding scheme for several liquid metals and alloys [1,2,5–9], by Dzugutov himself with Lennard-Jones and hard sphere potential functions. Recently, Ma et al. tested the scaling law in colloidal monolayers using optical microscopy and particle tracking techniques [3].

Three non-radioactive members of group-11 of the periodic table: copper, silver and gold have held great importance in societies throughout history, both symbolically and practically. They have been chosen as currency for so long because they are durable and they do not readily react with many other materials and therefore designated as noble metals. Noble metals are generally not oxidizing in air, malleable, ductile, good conductors and they have anti-corrosion properties. Extensive computer simulations with different interatomic potentials [10–21] and experimental studies [22–25] on the structure, transport, thermophysical and thermodynamic properties of liquid noble metals have been reported by many researchers.

The square well (SW) fluid is basic one possessing all characteristics of real liquid and the SW potential has been successfully applied for studying of various liquids for long time [26–34]. The authors have recently shown that the thermophysical and surface properties of liquid metals can be computed through diffusion data, which was derived by square well model [35]. Study of thermophysical and thermodynamic properties of liquids and their relation with microscopic structure

* Corresponding author.
E-mail address: rkmishramzu@yahoo.com (R.K. Mishra).

http://dx.doi.org/10.1016/j.jnoncrysol.2016.04.016
0022-3093/

Table 1
Input parameters of liquid metals (Au, Ag, Cu) with σ as the diameter, ε/k_B as the depth, λ as the breath of the square well potential and ρ as the number density.

Metals	Temperature (K)	σ (nm)	ε/k_B (K)	λ (nm)	ρ (10^{25}m^{-3})
Gold	1423	0.260	600	1.73	5271
Silver	1273	0.260	500	1.75	5159
Copper	1423	0.225	300	1.68	7408

functions are of long interest [36–40]. Surface tension, γ and its temperature derivatives, S_V of condensed matter are important and informative parameters for understanding the material processing technology [36,40–42].

We agree with other workers that the Dzugutov's hypothesis for dimensionless quantities must be tested with different form of inter atomic interactions [1]. Thus in this paper we report microscopic function $g(r)$ through Fourier transform of the auto correlation function, $S(k)$ and Brownian diffusion using the SW formalism as given in Refs. [10] and [31] and test the universal scaling law by estimating the excess entropy of liquid noble metals as function of reduced diffusion. Technologically important surface properties like γ and its temperature derivative i.e. surface entropy, S_V ($S_V = -\frac{d\gamma}{dT}$) are studied through D and its temperature derivatives. Computed $g(r)$ were employed to obtain Γ. This paper may be considered as an extension of the previous contributions [31,35].The calculations on shear viscosity, η_V for noble liquids is limited in the literature, which is calculated by using D with the Stokes-Einstein relation under the slipping boundary condition [8], which is an important dynamic properties to decide cooling rate of a liquid.

Further, new equations have been derived through equation of state of the SW potential [43] and employed them to compute long wavelength limit of $S(k)$ i.e. $S(0)$ in liquid Cu, Ag and Au. $S(0)$ can be related with various thermophysical and thermodynamic properties of liquids [11].

2. Theory

We used mean spherical model approximation (MSMA) for the determination of $S(k)$, the direct correction function (DCF) under MSMA with three parameters SW is

$$C(r) = \begin{cases} C_{hs}(r) & ; \quad 0 < r \le \sigma \\ -\beta U(r) & ; \quad \sigma \le r \le \lambda\sigma \\ 0 & ; \quad r > \lambda\sigma \end{cases} \tag{2}$$

Here $\beta = 1/k_BT$ and $U(r)$, the pair interaction potential, can be given as

$$U(r) = \begin{cases} \infty & ; \quad r \le \sigma \\ -\varepsilon & ; \quad \sigma < r \le \lambda\sigma \\ 0 & ; \quad r > \lambda\sigma \end{cases} \tag{3}$$

where ε and $\sigma(\lambda - 1)$ are the depth and width of the potential well. In case of atomic liquids DCF in momentum space for SW model can be given as

$$C(k) = C_{hs}(k) + C_{SW}(k). \tag{4}$$

Here $C_{hs}(k)$ stands for hard sphere DCF, obtained by Wertheim [44] from Percus-Yevick's equation for hard sphere mixtures and $C_{SW}(k)$ due to SW tail in momentum space [10].

The Fourier transform of the attractive part of SW potential is [31]

$$U(k) = \frac{4\pi\varepsilon}{k^3}[\sin(k\lambda\sigma) - \sin(k\sigma) - k\lambda\sigma\cos(k\lambda\sigma) + k\sigma\cos(k\sigma)]. \tag{5}$$

The analytical expression for $S(k)$ for SW model with hard sphere reference system under random phase approximation (RPA) is given by

$$S(k) = \frac{1}{1 - \rho C_{hs}(k) + \beta\rho U(k)}. \tag{6}$$

Here ρ is the number density of atoms.

The Fourier inversion of $S(k)$ gives the radial distribution function, $g(r)$

$$g(r) = 1 + \frac{1}{2\pi^2\rho}\int_0^\infty k^2[S(k) - 1]\frac{\sin(kr_{nm})}{kr_{nm}}dk. \tag{7}$$

Evaluation of thermodynamic properties of liquids through microscopic structural functions $S(k)$ and $g(r)$ is of fundamental importance for their better understanding [1,35]. In order to test the Dzugutov scaling law for diffusion for noble metals, we compute the collision frequency and excess entropy with SW model under RPA. Rosenfeld [5] defines the reduced transport coefficients in terms of reducing by macroscopic parameters, density and temperature, however, microscopic reducing parameters like hard sphere collision frequency, Γ and inter atomic distance σ (hard sphere diameter) according to Enskog theory [45] were chosen for deriving normalized diffusion. This concept was also extended by Li et al. for defining the reduced viscosity [2]. Further, reduced transport coefficients were scaled by exponential of excess entropy with different values of pre-exponential factors [1–7].

As we have already mentioned that SW liquids posses all characteristics of real liquids. Thus we define the Γ for SW liquids in terms of $g(r)$ from Eq. (7)

$$\Gamma = 4r_{max}^2 g(r_{max})\rho\left(\frac{\pi k_B T}{m}\right)^{1/2}. \tag{8}$$

Here, r_{max} and $g(r_{max})$ are first peak position and value of pair correlation function respectively, m is the mass of diffusing species in atomic unit, ρ is the number density of atoms and other symbols have their usual meanings. Dzugutov [4] defined the reduced diffusion coefficient, and we modified for SW liquids

$$D^* = \frac{D}{\Gamma r_{max}^2}. \tag{9}$$

Table 2
Theoretical and experimental values of first peak positions (r_{max}) and peak heights $g(r_{max})$, first minimum positions (r_{min}) and peak heights $g(r_{min})$ and collision frequency, τ (10^{12}s^{-1}) of liquid metals.

Metals	Temperature (K)	First peak position				First minimum position				Γ (10^{12} s^{-1})
		Theort.		Expt.		Theort.		Expt.		
		r_{max} (nm)	$g(r_{max})$	r_{max} (nm)	$g(r_{max})$	r_{min} (nm)	$g(r_{min})$	r_{min} (nm)	$g(r_{min})$	
Au	1423	0.28	2.68	0.28	2.78	0.37	0.62	0.39	0.60	12.979
Ag	1273	0.28	2.98	0.28	2.58	0.37	0.62	0.41	0.60	16.083
Cu	1423	0.25	2.35	0.25	2.75	0.38	0.70	0.35	0.56	21.931

There are various universal relations for different dimensionless physical parameters proposed for simple metals on the basis of corresponding state theory using characteristics parameters of different ionic potentials [46].

The Dzugutov scaling law [4] modified by Yokoyama [7,8] can be given as

$$D^* = a\, e^{S_E/k_B} \tag{10}$$

where a is a constant taken from Dzugutov scaling law [2,4]. S_E is the excess entropy per atom. Results of S_E for liquid noble metals can be represented as

$$S_E/k_B = log\frac{D}{0.049\Gamma r_{max}^2}. \tag{11}$$

Since D is evaluated from the well known Einstein's formula of self diffusion coefficient, $D = \frac{k_B T}{\xi}$, here ξ is the friction coefficient experiences by the atoms of same kind. We feel that the pair wise interaction would have significant role in the determination of D and hence ξ of liquid noble metals has been computed on the basis of Helfand-Rice-Nachtrieb approach [47] using square well model. Methods have been fully explained [31] previously and they are not to be repeated here.

The surface tension, γ for series of liquid metals has been studied [35] however its temperature derivative is obtained by temperature coefficient of D [35]

$$\gamma = \frac{15}{32\,\pi}\left(\frac{k_B}{m}\right)^{1/2} T^{1/2} \times \frac{\xi}{\sigma}. \tag{12}$$

dD/dT has been given previously [31] so will not be repeated here.

$$\frac{d\,\gamma}{dT} = \gamma\left[\frac{1}{T} - \frac{1}{\sigma}\frac{d\sigma}{dT} + \frac{1}{\xi}\frac{d\xi}{dT}\right] \tag{13}$$

$$\frac{d\,\xi}{dT} = \frac{d\xi^H}{dT} + \frac{d\xi^S}{dT} + \frac{d\xi^{SH}}{dT} \tag{14}$$

The surface entropy of pure liquid at constant volume is defined as [36]

$$S_V = -\frac{d\gamma}{dT}. \tag{15}$$

The shear viscosity coefficient, η_V is obtained under the SW model with the Stokes-Einstein relation

$$\eta_V = \frac{k_B T}{2\,\pi r_{max} D}. \tag{16}$$

In the last section of this manuscript we derive the structure factor in long wavelength limit, $S(0)$,which is an important parameter to evaluate various properties of liquid state [48], through equation of state in random phase approximation for SW fluids [43]

$$\frac{PV}{RT} = \frac{1+\eta+\eta^2}{(1-\eta)^3} - \frac{4\varepsilon\,\lambda\left(\lambda^3-1\right)}{k_B T} \tag{17}$$

$$\left[\frac{V}{RT} + \frac{P}{RT}\frac{dV}{dP}\right]_T = \frac{d}{dP}\left(1+\eta+\eta^2\right) \times \frac{1}{(1-\eta)^3} - \left(1+\eta+\eta^2\right) \times \frac{(-3)}{(1-\eta)^4}(-1)\frac{d\eta}{dP} - \frac{4\varepsilon\,\lambda\left(\lambda^3-1\right)}{k_B T}\frac{d\eta}{dP} \tag{18}$$

$$\text{here,} \frac{d\eta}{dP} = \frac{\pi\sigma^3}{6}\frac{d\rho}{dP} = \frac{\pi\sigma^3}{6}\rho\beta_1 = \eta\beta_1 \quad \beta_T = -\frac{1}{V}\frac{dV}{dP} \tag{19}$$

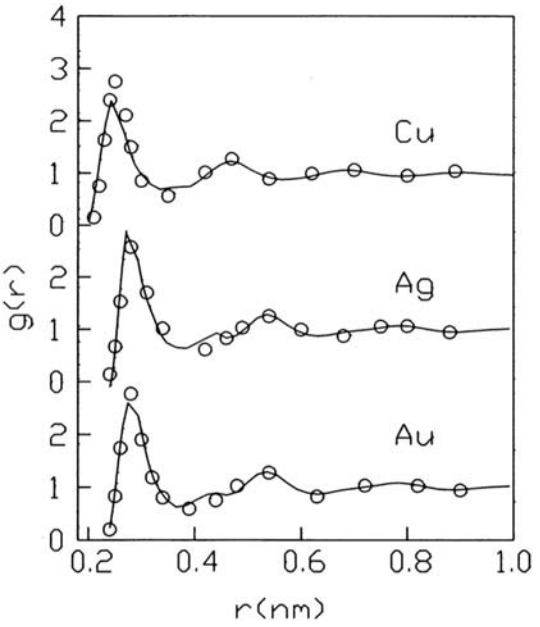

Fig. 1. $g(r)$ against r for liquid metals, (——) present calculated results; (o o o) experimental values.

$$\frac{V}{RT} = \beta_T\left\{\frac{4\eta^2+4\eta+1}{\eta\,(1-\eta)^4} - \frac{8\,\varepsilon}{k_B T}\left(\lambda^3-1\right)\right\} \tag{20}$$

$S(0)$ is related to isothermal compressibility, β_T as [49]

$$S(0) = \rho\, k_B T\, \beta_T \tag{21}$$

$$S(0) = \frac{1}{\left[\frac{(2\eta+1)^2}{(1-\eta)^4} - \frac{8\,\varepsilon\,\eta}{k_B T}\left(\lambda^3-1\right)\right]} \tag{22}$$

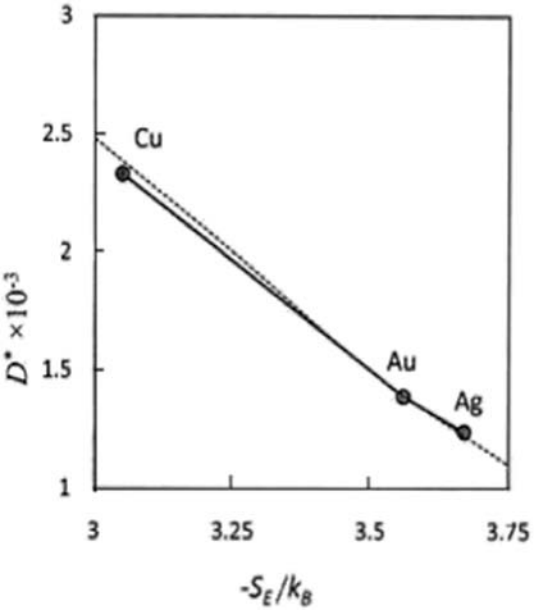

Fig. 2. The scaled diffusion coefficient, D^* vs the excess entropy, S_E of liquid metals. The dashed line is the relationship found in original work of Dzugutov.

Table 3
Theoretical and experimental values of the scaled diffusion coefficient, D^*, excess entropy, S_E/k_B and shear viscosity coefficient, η_V (mPa s) of liquid metals.

Metals	Temperature (K)	$D^* \times 10^{-3}$	$-S_E/k_B$		η_V (mPa s)	
			Theort.	Expt.	Theort.	Expt.
Au	1423	1.39	3.56	–	5.3	4.3
Ag	1273	1.24	3.67	–	3.8	3.7
Cu	1423	2.33	3.05	3.44	2.6	3.5

where η is called packing fraction i.e. volume occupied by the atoms divided by total volume and is given by $\eta = \frac{\pi\rho\sigma^3}{6}$.

3. Result

The Wertheim's [44] solutions of PY hard sphere fluid were perturbed with SW potential and solved numerically for liquid metals [10] using temperature, T, ρ, and three parameters of SW potential. The input parameters of noble metals are listed in Table 1. The peak positions and height of the radial distribution function computed by Fourier transformation of structure factor are given in Table 2. The calculated values of $g(r)$, are depicted in Fig. 1 along with the corresponding experimental values [22].

S_E for liquid Cu, Ag and Au are calculated by employing the SW model of diffusion in Dzugutov scaling law. The computed values are in accordance with [1] which is shown in Fig. 2. η_V is also obtained through Eq. (16) and the calculated values are listed in Table 3 along with their corresponding experimental values. We have also derived the surface entropy of liquid metals through analytical expression for the temperature derivative of the SW model of D under linear trajectory principle [42]. These results are presented in Table 4 along with their experimental results [42].

The surface tension, γ is related with self-diffusion coefficients of liquids. Computed values of γ with their experimental values [42] are also presented in Table 4.

4. Discussion

It is found that the theoretical values of $g(r)$ obtained from Eqs. (5)–(7) agree well with experimental values [22].The main peak positions for liquid noble metals coincide with the experimental values although the heights of the respective first peaks in all cases are somewhat underestimated especially for liquid Ag and Cu. We find that a similar disparity is also presented with density function theory simulation under Kohn-Sham and ab-initio molecular dynamics methods [19–21] for liquid Cu. This may be due to existence of some form of cluster in Ag and Cu at their respective working temperatures under SW interaction. It is worth to mention here that we find a good agreement between computed and experimental values [22] of RDF for positions and magnitudes of subsequent peaks in all three liquids at their respective working temperatures. Recently, Mendelev et al. proposed in his publication on liquid Cu [50] that the EAM potential gives only low temperature crystal properties.

Table 4
Theoretical and experimental values of surface tension, γ (N m^{-1}), surface entropy, $S_V = -d\gamma/dT$ (mN m^{-1} K^{-1}) and isothermal compressibility, β_T (10^{-12} cm^2/dyn) of liquid metals.

Metals	Temperature (K)	γ (N m^{-1})		$S_V = -d\gamma/dT$ (mN m^{-1} K^{-1})		β_T (10^{-11} m^2 N^{-1})	
		Theort.	Expt.	Theort.	Expt.	Theort.	Expt.
Au	1423	1.20	1.14	0.27	–	1.99	1.3
Ag	1273	1.03	0.92	0.23	0.17	2.54	2.2
Cu	1423	1.03	1.31	0.25	0.28	2.00	1.5

Experimental and theoretical values of number of liquid metals (including Cu) with scattering phenomena have been reported [8] and we find that the results from SW model are in fair agreement with experimental values. However, EAM method is less accurate for liquid state properties [1,50]. The computed values of S_E for all liquids are in order of three, a similar trend was observed by other researchers for nine liquids [8]. The excess entropy measurements of most of the liquid noble metals are yet to be determined experimentally, and therefore, we are unable to compare our computed results of S_E for liquid Au and Ag with experimental values.

We find satisfactory agreement between theoretical and experimental values of surface tension, γ for liquid Cu and liquid Ag. Experimental values at working temperature for Ag and Cu were extracted from Ref. [42]. The surface entropy for liquid metals are calculated and we find a good agreement between theoretical and experimental results, which shows the one more applicability of the analytical derivation of temperature derivative of D as derived earlier [31]. We find a fair agreement between present computations with experimental results of η_V, for liquid noble metals [51,8].

The structure factor in long wavelength limit, $S(0)$, is related to isothermal compressibility of liquid metals. Table 4 shows our computed results for β_T using equation of state of SW potential. There is a fair agreement between the computed value and the experimental values [11,12,19], these shows the success of the SW perturbation theory.

5. Conclusions

The present work is concluded with the following remarks:

(1) We have computed S_E for liquid noble metals using $g(r)$ and D data of the SW model. η_V, γ and S_V were determined in terms of D. The present computed values were compared with their corresponding experimental results and we find the agreement is satisfactory.
(2) The computed $g(r)$ data were discussed with other available works as well as with experimental results. The RDF plays a major role in obtaining both equilibrium and non-equilibrium properties of liquids.
(3) New method for the determination of $S(0)$ through equation of state of SW potential is presented. $S(0)$ data were employed to compute isothermal compressibility of noble metals.
(4) Thermodynamic perturbation of SW potential over hard sphere reference system is an excellent model for the study of static and dynamic properties of liquid metals.

Acknowledgements

R. K. Mishra acknowledges the financial support from the Department of Science and Technology, Govt. of India, New Delhi under Fast Track Project (SR/FT/CS-021/2008) and R. Lalneihpuii to the University Grants Commission India (F1-17.1/2011-2012/RGNF-ST-MIZ-11977), New Delhi for awarding Rajiv Gandhi National Fellowship.

References

[1] J.J. Hoyt, M. Asta, B. Sadigh, Phys. Rev. Lett. 85 (2000) 594.
[2] G.X. Li, C.S. Liu, Z.G. ZhuJ, Non-Cryst. Solids 351 (2005) 946.
[3] X. Ma, W. Chen, Z. Wang, Y. Peng, Y. Han, P. Tong, Phys. Rev. Lett. 110 (2013) 078302.
[4] M. Dzugutov, Nature (London) 381 (1996) 137.
[5] Y. Rosenfeld, J. Phys. Condens. Matter 11 (1999) 5415.
[6] A. Samnta, S.M. Ali, S.K. Ghosh, Phys. Rev. Lett. 92 (2004) 2242.
[7] I. Yokoyama, Physica B 254 (1998) 172.
[8] I. Yokoyama, Shusaku Tsuchiya, Mater. Trans. 43 (2002) 67.
[9] W.P. Kreckelberg, M.J. Pond, G. Goel, V.K. Shen, S.P. Errington, J.M. Truskett, Phys. Rev. E 80 (2009), 061205.
[10] R.V. Gopala Rao, A.K. Murthy, Phys. Lett. A 51 (1975) 3.
[11] S. Blairs, Int. Mater. Rev. 52 (2007) 321.

[12] R.N. Singh, A. Arafin, A.K. George, Physica B 387 (2007) 344.
[13] M.M.G. Alemany, M. Calleja, C. Rey, J.L. Gallego, J. Casas, E.L. Gonzalez, Phys. Rev. B 60 (1999) 5175.
[14] J.M. Holender, Phys. Rev. B 41 (1990) 8054.
[15] M.M.G. Alemany, M. Calleja, C. Rey, J.L. Gallego, J. Casas, E.L. Gonzalez, J. Non-Cryst. Solids 250–252 (1999) 53.
[16] X.J. Han, M. Chem, Y.J. Lu, Int. J. Thermophys. 29 (2008) 1408.
[17] G.M. Bhuiyan, J.L. Bretonnet, M. Silbert, J. Non-Cryst. Solids 156–158 (1993) 145.
[18] Yu. Mitrohkin, Comput. Mater. Sci. 36 (2006) 189.
[19] P. Ganesh, M. Widom, Phys. Rev. B 74 (2006) 234205.
[20] A. Pasturel, E.S. Tasci, M.H.F. Sluiter, N. Jaksen, Phys. Rev. B 81 (2010) 140202.
[21] H.Z. Fang, X. Hui, G.L. Chen, Z.K. Liu, Phys. Lett. A 372 (2008) 5831.
[22] Y. Waseda, The Structure of Non-crystalline Materials, McGraw-Hill, New York, 1980.
[23] A. Mayer, Phys. Rev. B 81 (2010) 01202.
[24] O.J. Eder, E. Erdpresser, B. Kunsch, H. Stiller, M. Suda, J. Phys. F: Met. Phys. 10 (1980) 183.
[25] M.C. Bellissent, P. Desre, R. Bellissent, G. Tourand, J. Phys. 37 (1976) 1437.
[26] R.V. Gopala Rao, A.K. Murthy, Phys. Status Solidi B 66 (1974) 703.
[27] H. Liu, C.M. Silva, E.A. Macedo, Chem. Eng. Sci. 53 (1998) 2403.
[28] R.V. Gopala Rao, B.M. Sathpathy, Phys. Status Solidi B 110 (1982) 273.
[29] R. Venkatesh, R.K. Mishra, R.V. Gopala Rao, Phys. Status Solidi B 240 (2003) 549.
[30] R.V. Gopala Rao, R. Venkatesh, Phys. Rev. B 39 (1989) 9467.
[31] R. Venkatesh, R.K. Mishra, J. Non-Cryst. Solids 351 (2005) 705.
[32] N.E. Dubinin, V.V. Filippov, O.G. Malkhanova, N.A. Vatolin, Cent. Eur. J. Phys. 7 (3) (2009) 584.
[33] N.E. Dubinin, N.A. Vatolin, V.V. Filippov, Russian Chem. Rev. 83 (11) (2014) 987.
[34] Y.X. Yu, M.H. Han, G.H. Gao, Phys. Chem. Chem. Phys. 3 (2001) 437.
[35] R.K. Mishra, R. Lalneihpuii, R. Pathak, Chem. Phys. 457 (2015) 13.
[36] R.C. Gosh, A.Z. Ziauddin Ahmed, G.M. Bhuiyan, Eur. Phys. J. B 56 (2007) 177.
[37] G.X. Qian, M. Weinert, G.W. Fernando, J.W. Davenport, Phys. Rev. Lett. 64 (1990) 1146.
[38] M.I. Ivanov, V.V. Berezutski, J. Alloys Comp. 234 (1996) 119.
[39] P.P. Nath, R.N. Joarder, Ind. J. Pure and App Phys. 43 (2005) 180.
[40] W.H. Shih, D. Stroud, Phys. Rev. B 32 (1985) 804.
[41] H.M. Lu, Q. Jiang, J. Phys. Chem. B 109 (2005) 15463.
[42] J. Lee, W. Shimoda, T. Tanaka, Mater. Trans. 45 (2004) 2684.
[43] R.V. Gopala Rao, R.N. Joarder, Indian J. Pure Appl. Phys. 14 (1976) 905.
[44] M.S. Wertheim, Phys. Rev. Lett. 10 (1963) 321.
[45] S. Chapman, T.G. Cowling, The Mathematical Theory of Non-Uniform Gases, Cambridge University Press, London, 1970.
[46] S.G. Prakash, R. Ravi, R.P. Chhabra, Chem. Phys. 302 (2004) 149.
[47] P.P. Nath, S. Sarkar, R.N. Joardar, Pramana-J. Phys. 65 (2005) 125.
[48] M. Iwamatsu, J. Phys. Condens. Matter 2 (1990) 3053.
[49] M. Kalidoss, S. Ravi, Physica A 312 (2002) 59.
[50] M.I. Mendelev, M.J. Kramer, C.A. Becker, M. Asta, Philos. Mag. 88 (2008) 1723.
[51] E.A. Brandes, Smithells Metals Reference Book, sixth ed. Butterworths, London, 1983.

BRIEF BIO-DATA

Personal Information

Name: R. LALNEIHPUII

Date of Birth: 23rd March, 1989

Father's name: R. Lalnghinglova

Mother's name: C. Laldingliani

Permanent Address: Zobawk, Lunglei

Topic of Ph.D. Thesis: 'Theoretical and Computational Studies of Liquid Metals and Liquid Binary Alloys'

Registration No.: MZU/Ph.D/473 of 15.05.2012

Academic Qualifications

Examination	Board	Year	Division	Subjects
HSLC	MBSE	2003	1st	General
HSSLC	MBSE	2005	2nd	Maths, Phys, Chem, Bio, Eng, etc
B.Sc.	MZU	2008	1st	Chemistry-Hons (Maths, Phys, Eng-Subs)
M.Sc.	MZU	2010	1st	Chemistry

Other Exams:

1. Pre Ph.D course work in 2011.
2. Qualified State Level Eligibility Test (SLET) in 2015.

Achievements:

1) Topper in Bachelor of Science (Chemistry) in 2008.
2) Gold medalist in Master of Science (Chemistry) in 2010.
3) Recipients of RGNF
4) Received Best Oral Presentation award (2^{nd} prize) in 8^{th} National conference of the Physics Academy of North East, held on 17-19, December, 2012 at Mizoram University, Aizawl.
5) Received Best poster presentation award in 18^{th} CRSI-RSC National Symposium in Chemistry held at Punjab University, Chandigarh (5^{th}-7^{th} February, 2016).

REFERENCES

Adebayo, G.A., Akinlade, O., Hussain, L.A., (2005). Structures and auto correlation functions of liquid Al and Mg modeled via Lennard-Jones potential from molecular dynamics simulation. *Pramana J. Phys*., 64(2):269-279.

Alblas, B.P., Vander Lugt, W., (1982). Thermodynamic calculations for the liquid systems Na-K, K-Cs and Li-Pb. *Physica B* 114:59-66.

Alder, B.J., Gass, D.M., Wainwright, T.E., (1970). Studies in Molecular Dynamics. VIII. The Transport Coefficients for a Hard-Sphere Fluid. *J. Chem. Phys.* 53:3813-3826.

Alfe, D., Gillan, M.J. (1998). First-Principles Calculation of Transport Coefficients. *Phys. Rev. Lett.*, 81:5161-5164.

Ali, M., Samanta, A., Gosh, S.K., (2001). Mode coupling theory of self and cross diffusivity in a binary fluid mixture: Application to Lennard-Jones systems. *J. Chem. Phys*., 114:10419-10429.

Alonso, J.A., March, N.H., (1982). Concentration fluctuations in metallic liquid alloys. *Physica B*, 114:67-70.

Ashcroft, N.W., Langreth, D.C., (1967). Structure of Binary Liquid Mixtures. *Phys. Rev.* 156:685-691.

Asherie, N., Lomakin, A., Bendek, G.B., (1996). Phase Diagram of Colloidal Solutions. *Phys. Rev. lett*. 77:4832-4835.

Awe, O.E., Olawole, O., (2012). Correlation between bulk and surface properties in Cd-X (X=Hg, Mg) liquid alloys. *J. Non-Cryst. Solids*, 358:1491-1496.

Balucani, U., Torcini, A., Vallauri, R., (1993). Liquid alkali metals at the melting point: Structural and dynamical properties. *Phys. Rev*., B 47(6):3011-3020.

Bandyopadhyay, S., Venkatesh, R., Gopala Rao, R.V., (2002). Evaluation of partial and total structure factors, Bhatia-Thornton correlation functions, compressibility and diffusion coefficient of Pb-Pd alloy at different compositions and temperatures. *Indian J. Pure Appl. Phys*. 40:32-41.

Barajas, L., Garcia Colin, L.S., Pina. E., (1973). On the Enskog-Thorne theory for a binary mixture of dissimilar rigid spheres. *J. stat. Phys*. 7:161-183.

Baxter, R. J., (1967). Method of solution of the Percus- Yevick, Hypernetted-chain, or similar equations. *Phy. Rev.* 154(1):170-174.

Berne, B.J., Pecora, R., (2000). *Dynamics of Light Scattering: With Application to Chemistry, Biology and Physics,* 3rd ed., Dover Publication, New York.

Bhatia, A.B., Hargrove, W.H., March, N.H., (1973). Concentration fluctuations in conformal solution and partial structure factor in alloys. *J. Phys. C: solid state Phys.*, 6:621-630.

Bhatia, A.B., Thornton, D.E., (1970). Structural Aspects of the Electrical Resistivity of Binary Alloys. *Phys. Rev. B* 2:3004–3012.

Blairs, S., (2006). Correlation between surface tension, density, and sound velocity of liquid metals. *J. Colloid Interface Sc*. 302:312-314.

Blairs, S., (2007). Review of data for velocity of sound in pure liquid metals and metalloids. *Int. Mater. Rev*., 52:321-344.

Block, R., Suck, J.B., Freyland, W., Hansel, F., Glaser, W., (1977). *Proceedings of 3rd International Conference on Liquid Metals,* The Institute of Physics, Bristol, London, 126-132.

Born, M., Green, H.S., (1949). *A general kinetic theory of Liquids*, University Press, Cambridge.

Boulahbak, M., Jakes, N., Wax, J.F., Bretonnet, J.L., (1998). Transferable pair potentials for the description of liquid alkali metals. *Chem. Phys*. 108: 2111-2116.

Brandes, E. A., (1983). *Smithells Metals Reference Book*; 6th Ed., Butterworths & Co Ltd: London, 15-2.

Brillo, J., Chathoth, S.M., Koza, M.M., Meyer, A., (2008). Liquid $Al_{80}Cu_{20:}$ Atomic diffusion and viscosity. *Appl. Phys. Lett*. 93:121905 (1-3).

Brillo, J., Bytchkov, A., Egry, I., Hennet, L., Mathiak, G., Pozdnyakova, I., Price, D.L., Thiaudiere, D., Zanghi, D., (2006). Local structure in liquid binary Al-Cu and Al-Ni alloys. *J. Non-Cryst. Solids*. 352:4008-4012.

Brillo, J., Lauletta, G., Vaianella, L., Arato, E., Giuranno, D., Novakovic, R., Ricci, E., (2004). Surface Tension of Liquid Ag-Cu Binary Alloys. *ISIJ International*, 54(9):2115-2119.

Brillo, J., Pommrich, A.I., Mayer, A., (2011). Relation between Self-Diffusion and Viscosity in Dense Liquids: New Experimental Results from Electro Levitation. *Phy. Rev. Lett*., 107:165902(1-4).

Cahoon, J.R., (2004). The first coordination number for liquid metals. *Can. J. Phys.*, 82: 291- 301.

Canales, M., González, D.J., González, L.E., Padró, J.A., (1998). Static structure and dynamics of the liquid Li-Na and Li-Mg alloys. *Phys. Rev. E* 58: 4747-4757.

Cao, Q.L., Wang, P.P., Shao, J.X., Wang, F.H., (2016). Transport properties and entropy-scaling laws for diffusion coefficients in liquid $Fe_{0.9}Ni_{0.1}$ up to 350 GPa. *RSC Adv.*, 6: 84420-84425.

Chapman, S., Cowling, T.G., (1970). *The Mathematical Theory of Non-Uniform Gases*, Cambridge University Press, London.

Cheng, H., Lü, Y.J., Chen, M., J. (2009). Inter-diffusion in liquid Al-Cu and Ni-Cu alloys, *Chem. Phys*.131: 044502 (1-6).

Cheng, W., Zhang, L., Du, Y., Huang, B., (2014). Viscosity and diffusivity in melts: from unary to multicomponent systems. *Philos. Mag*. 94: 1552-1577.

Clark, D.B., (1989). The ideal gas law at the center of the sun. *J. Chem. Educ*. 66: 826.

Cui, J., Elliot, J.R., (2001). Phase envelopes for variable width square well chain fluids. *J. Chem. Phys*. 114: 7283-7290.

Dahlborg, U., Besser, M., Calvo-Dahlborg, M., Janssen, S., Juranyi, F., Kramer, M.J., Morris, J.R., Sordelet, D.J., (2007). Diffusion of Cu ions in AlCu alloys of different composition by quasielastic neutron scattering. *J. Non-cryst. Sol*., 353: 3295-3299.

Dahlborg, U., Besser, M., Kramer, M.J., Morris, J.R., Calvo-Dahlborg, M., (2013). Atomic dynamics in molten Al-Cu alloys of different compositions and at different temperatures by cold neutron scattering. *Physica B*, 412: 50-60.

Dalgic, S., Colakogullari, M., (2006). Self-Diffusion Coefficients in Liquid Ag Using the Embedded Atom Model Based Effective Pair Potentials. *Turk J Phys*. 30: 303-310.

Davis, H.T., Polyvos (1967). Contribution to the Friction Coefficient from Time Correlations between Hard and Soft Molecular Interactions. *J. Chem phys* (46): 4043-4047.

Davis, H.T., Rice, S.A., Sengers, J.V. (1961). The kineitc theory of dense fluid IX. The fluid of rigid sheres with a square- well attraction. *J. Chem. Phys.* 35: 2210-2233.

Davis, H.T., Luks, K.D., (1965). Transport Properties of a Dense Fluid of Molecular Interacting with a Square-Well Potential, *J. Chem. Phys*. 69: 869-880.

Dubinin, N.E., Filippov, V.V., Malkhanova O.G., Vatolin, N.A., (2009). Structure factors of binary liquid metal alloys within the square-well model. *Cent. Eur. J. Phys*. 7(3):584-590.

Dubinin, N.E., Vatolin, N.A., Filippov, V.V., (2014). Thermodynamic perturbation theory in studies of metal melts. *Russian Chem. Rev.* 83(11):987-1002.

Dymond, J.H., (1985). Hard-sphere theories of transport properties. *Chem. Soc. rev.*, 14: 317-356.

Dzugutov, M., (1996). Addendum: A universal scaling law for atomic diffusion in condensed matter. *Nature, London,* 381:137-139.

Echendua, O.K., Mbamalaa, E.C., Anunsionwua, B.C., (2010). *Phys. and Chem. of Liquids*, 1:1-12.

Enderby, J. E., North, D. M., (1967). The partial structure factors of liquid alloys. *Advances in Physics.* 16(62):171-175.

Enderby, J.E., North, D.M., Percus-Yevick, (1968). Structure factors for liquid alloys. *Phys. Chem. Liquids.* 1:1-11.

Eskin , D., Du, Q., Ruvalcaba, D., Katgerman, L. (2005). Experimental study of structure formation in binary Al–Cu alloys at different cooling rates. *Matt. Sc. Eng. A* 405:1-10.

Faber, T. E., (1972). *Introduction to the theory of liquid metals*, Cambridge University press, Cambridge.

Fei, W., Bart, H.J., (1998). Prediction of diffusivities in liquids. *Chem. Eng. Technol*, 2: 659-665.

Flory, J., (1942). Thermodynamics of high polymer solutions. *J. Chem. Phys*. 10:51-61.

Fowler, R.H., (1937). A Tentative Statistical Theory of Macleod's Equation for Surface Tension, and the Parachor. *Proc. Roy. Soc A*, 159:229-246.

Ganesh, P., Widom, M., (2006). Signature of nearly icosahedral structures in liquid and supercooled liquid copper. *Phys. Rev. B*, 74:134205 (1-4).

Gingrich, N.S., (1943). The Diffraction of X-Rays by Liquid Elements. *Rev. Mod. Phys*. 15: 90-110

Glasstone, S., Laidler, K.J., Eyring, H., (1941). *The Theory of Rate Processes*, Mc Graw – Hill, New York.

Gingrich, N.S., Henderson, R.E., (1952). The Diffraction of X-Rays by Liquid Alloys of Sodium and Potassium. J. Chem. Phys. 20:1117-1120.

Glazov, V.M., Aivazov, A.A., (1980). *Entropy of metals and semiconductor*, Moscow, Russia.

Glazov, V. M., Chizheskaya, S. N., Glagoleva, N. N., (1969). *Liquid semiconductor*, Plenum, New York.

Gonz'alez, D.J., Gondz'alez, L.E., (2008). Microscopic dynamics in liquid binary alloys: orbital-free ab-initio molecular dynamics studies. *Condens. Matter. Phys*. 11(53):155-168.

Gopala Rao, R.V., Murthy, A.K., (1974). Mean spherical model and structure factor of liquid mercury and aluminium. *Phys. Stat. Sol. (b)*, 66:703-707.

Gopala Rao, R.V., Murthy, A.K., (1975). Structure of liquid noble metals, *Phys. Letts.* A 51:3-4.

Gopala Rao, R.V., Murthy, A.K., (1975). Self Diffusion in Liquid Metals. *Z. Natur Forsch*, 30a:619-622.

Gopala Rao, R. V., Das, R., (1987). Theoretical computation of coherent scattering intensities, partial structure factors, and diffusion coefficients of magnesium-bismuth melt. *Phys. Rev. B* 36:6325-6330.

Gopala Rao, R.V., Satpathy, A., (1990). Theoretical evaluation of neutron scattering intensities, partial structure factors, and diffusion coefficients of the alloy of the peculiar metal Bi in Cu-Bi alloy. *Phys. Rev. B* 41:995-1002.

Gopala Rao, R.V., Sathpathy, B.M., (1982). Partial Structure of Liquid Sodium—Cesium Alloys. *Phys. Stat. Sol.(b).* 110:273-279.

Gopala Rao, R.V., Venkatesh, R., (1989). Computation of total and partial structure factors, coordination number, and compressibility with self- and mutual-diffusion coefficient in Hg-In alloy. *Phys. Rev. B* 39:9467-9475.

Gopala Rao., R.V., Das Gupta, B., (1985). Partial structure factors of diffusion coefficients of liquid K-Cs alloys. *Phy. Rev. B.* 32(10):6429-6436.

Gosh, R.C., Ziauddin Ahmed, A.Z., Bhuiyan, G.M., (2007). Investigation of surface entropy for liquid less simple metals. *Eur. Phys. J. B* 56:177-181.

Hafner, J., Kahl, G., (1984). The structure of the elements in the liquid state. *J. Phys F: Metal Phys.* 14:2259-2278.

Hansen, J.P., McDonald, I.R., (1986). *Theory of simple liquids*, Academic Press, London, New York.

Harrision, W.A., (1966). *Pseudopotential in the theory of metal*, W.A. Benjamin, Inc., New York.

Herrera, J.N., Cummings, P.T., Estrada, H.R. (1999). Static structure factor for simple liquid metals. *Mol. Phys*. 96:835-847.

Helfand, E., (1961). Theory of the Molecular Friction Constant. *Phys. Fluids*., 4: 681-690.

Hoyt, J.J., Asta, M., Sadigh, B., (2000). Test of the Universal Scaling Law for the Diffusion Coefficient in Liquid Metals. *Phys. Rev. Lett.*, 85:594-597.

Huang, L., Wang, C.Z., Ho, K.M., (2011). Structure and dynamics of liquid $Ni_{36}Zr_{64}$ by ab-initio molecular dynamics. *Phys. Rev. B* 83:184103(1-8).

IAMP Data base of SCM-LIQ Tohoku University, (website address: http.//www.iamp.tohoku.ac.jp/database/scm/LIQ)

Itami, T., Mizuno, A., Aoki, H., Arai, Y., Goto, K., Amano, S., Tateiwa, N., Kaneko, M.,. Fukazawa, T., Nakamura, R., Nishioji, H., Ogiso, A., Nakamura, T., Kohikawa, N., Matsumoto, S., Munejiri, S., Uchida, M., Shinichi, S., (2000). The Study of Diffusion in Complex Metallic Liquids With High Melting Points: The study of Self-Diffusion and Mutual-Diffusion of Liquid Cu-Ag Alloys. *J. Jpn. Soc. Microgravity Appl*., 17(2): 64-69.

Ivanov, M.I., Berezutski, V.V., (1996). Thermodynamics of Au-Gd melts and percolation theory application for compound-forming liquid alloys. *J. Alloys. Comp.* 234: 119-124.

Iwamatsu, M., (1990). The long-wavelength-limit structure factor of liquid alkali metals with the classical plasma reference system. *J. Phys. Condens. Matter* 2: 3053-3059.

Jakse, N., Pasturel, A., (2015). Relationship between structure and dynamics in liquid $Al_{1-x}Ni_x$ alloys. J. Chem. Phys. 143: 84504 (1-7)

Jakse, N., Pasturel, A., (2016). Excess entropy scaling law for diffusivity in liquid metals. *Scientific Reports*. 6:20689 (1-11)

Jha, I.S., Koirala, I., Singh, B.P., Adhikari, D., (2014). Concentration dependence of thermodynamic, transport and surface properties in Ag-Cu liquid alloys. *Appl. Phys. A*, 116:1517-1523.

Kalidoss, M., Ravi, S., (2002). New method of determining the structure factor of real liquids and their mixtures using ultrasonic velocity. *Physica A* 312:59-69.

Keating, D.T., (1963). Interpretation of the Neutron or X-Ray Scattering from a Liquid-Like Binary. *J. Appl. Phys*., 34: 923-925.

Kirkwood, J.G., (1946). The Statistical Mechanical Theory of Transport Processes I. General Theory. *Chem. Phys*., 14: 180-201.

Kita , Y., Van Zytveld, J.B., Morita, Z., Iida, T., (1994). Covalency in liquid Si and liquid transition metals Si alloys: X-ray diffraction studies. *J. Phys. Condens. Matter* 6: 811-830.

Koirala, I., Singh B.P., Jha, I.S., (2014). Transport and Surface Properties of Molten Cd- Zn Alloys. *J. Inst. Sc. Tech.*, 19(1):14-18.

Korkmaz, S.D., Korkmaz, S., (2009). Investigation of atomic transport and surface properties of liquid transdition metals using scaling law. *J. Mol. Liq* 150: 81-85

Korkmaz, S.D., Yazar, U.N.N., Korkmaz, S., (2006). A comparative study of the atomic transport properties of liquid alkaline metals using scaling laws. *Fluid Phase Equilibria*. 249: 159-164.

Korkmaz, S.D., Korkmaz, S., (2007). Atomic transport properties of liquid alkaline earth metals: a conmparision of scaling laws proposed for diffusion and viscosity model Simulation. *Mater. Sci. Eng.* 15; 285-294.

Kreckelberg, W.P., Pond, M.J., Goel, G., Shen, V.K., Errington, S.P., Truskett, J.M., (2009). Generalized Rosenfeld scalings for tracer diffusivities in not-so-simple fluids: Mixtures and soft particles. *Phys. Rev. E* 80: 061205 (1-13).

Lado, J. (1971) Numerical Fourier transforms in one, two, and three dimensions for liquid state calculations. *Comput. Phys*. 8, 417-433.

Lebowitz, J.L., Rubin, E., (1963). Dynamical Study of Brownian Motion. *Phys. Rev.* 131: 2381-2396.

Lai, S.K., Akinlade, O., Tosi, M.P., (1990). Thermodynamics and structure of liquid alkali metals from the charged-hard-sphere reference fluid. *Phys. Rev. A* 41: 5482-5790.

Lal, M., Singh, D.P., (1993). Acoustical investigation of As-Sb-Se based glasses and chemical bond approach. *Indian J. Phys. A* 67: 445-451.

Lang, A., Kahl, G., Likos, C.N., Lowen, H., Watzlawek, M., (1999). Structure and thermodynamics of square well and square shoulder fluids. *J. Phys. Condens. Matter*. 11: 10143-10161.

Lebowitz, J. L., (1964). Exact solution of generalized Percus-Yevick equation for mixture of hard spheres, *Phys. Rev. A* 133: 895-899

Lebowitz, J.L., Percus, J.K., (1966). Mean Spherical Model for Lattice Gases with extended Hard Cores and Continuum Fluids. *Phys. Rev.* 144: 251-258.

Lee, J., Shimoda, M., Tanaka, T., (2004). Surface Tension and its Temperature Coefficient of Liquid Sn-X (X=Ag, Cu) Alloys. *Mat. Trans.* 45: 2864-2870.

Li, G.X., Lang, Y.F., Zhu, Z.G., Liu, C.S., (2003). Microstructural Analysis of the Radial Distribution Function for Liquid and Amorphous Al. *J. Physics: Cond. Matter*, 15: 2259-2267.

Li, G.X., Liu, C.S., Zhu, Z.G., (2005). Excess entropy scaling for transport coefficients: diffusion and viscosity in liquid metals. *J. Non-Cryst. Solids*, 351: 946-950.

Li, G.X., Liu, C.S., Zhu, Z.G., (2005). Scaling law for diffusion coefficients in simple melts. *Phys Rev. B*, 71: 094209 (1-7).

Li, G.X., Liu, C.S., Zhu, Z.G., (2004). Universal scaling law for atomic diffusion and viscosity in liquid metals. *Chin. Phys. Lett*. 21, 2489-2492.

Li, M., Gong, X.G., (2004). *Ab initio* molecular dynamics simulation on temperature-dependent properties of Al–Siliquid alloy. *J. Phys. Cond. Matter*, 16: 2507-2514.

Liu, H., Silva, C.M., Macedo, E.A., (1998). Unified approach to the self-diffusion coefficients of dense fluids over wide ranges of temperature and pressure – hard-sphere, square-well, Lennard-Jones and real substances. *Chem. Eng. Sc*., 53: 2403-2422.

Lu, H.M., Jiang, Q., (2005). Surface Tension and Its Temperature Coefficient for Liquid Metals. *J. Phys. Chem. B*. 109: 15463-15468.

Lukens, W.E., Wagner, C.N.J., (1975). The structure of Liquid Silver-Copper Alloys. *Z. Naturforsch*, 30 a: 242-249.

Manning, J.R., (1961). Diffusion in a Chemical Concentration Gradient. *Phys. Rev*., 124:470-482.

Ma, X., Chen, W., Wang, Z., Peng, Y., Han, Y., Tong, P., (2013). Test of the universal scaling law of diffusion in colloidal monolayers. *Phys. Rev. Lett*. 110: 078302 (1-5).

McLaughlin, I.L., Davis, H.T., (1966). Kinetic Theory of Dense-Fluid Mixtures. I. Square-Well Model. *J. Chem. Phys.* 45: 2020-2031.

March, N.H., (1999). Local coordination, electronic correlations and relation between thermodynamic and transport properties of sp liquid metals. *J. Non-Cryst. Sol*., 250-252: 1-8.

Mc. Quarrie, D. A., (1976). *Statistical Mechanics*, Horper & Row, New York.

Mendelev, M. I., Kramer, M. J., Becker, C. A., Asta, M., (2008). Analysis of semi-empirical interatomic potentials appropriate for simulation of crystalline and liquid Al and Cu. *Phil. Mag.*, 88(12): 1723–1750.

Mishra, P.P., Milanarun, M., Jha, N., Mishra, A.K., (2002). Thermodynamic properties of liquid glass-forming Ca–Mg alloys. *J. Alloys. Compounds.* 340:108-113.

Mishra, R.K., Venkatesh, R., (2008). Theoretical evaluation of structural and various associated properties of Al-Si melts. *Chem. Phys.* 354: 112-117.

Murdy, S., Shtablavy, I., Shcherba, I., (2008). Liquid eutectic alloys as a cluster solutions. *Archives. Matt. Sc. Eng*., 34:14-18.

Nath, P.P., Joarder, R.N., (2005). Characteristic Bhatia-Thornton static structure and diffusion coefficients of liquid LiNa and KPb alloys. *Ind. J. Pure & App Phys*. 43: 180-183.

Nath, P.P., Sarkar, S., Joardar, R.N., (2005). An effective pair potential for liquid semiconductor, Se: Structure and related dynamical properties. *Pramana J. Phys.* 65(1); 125-135.

Nogi, K., Ogino, K., McLean, A., Miller, W. A., (1986). The temperature coefficient of the surface tension of Pure liquids metals. *Metallurgical Transactions B*, 17:163-170.

Novakovic, R., (2010). Thermodynamics, Surface properties and microscopic functions of liquid Al-Nb and Nb-Ti alloys. *J. Non-Cryst. Solids,* 356: 1593-1598.

Novakovic, R., Ricci, E., Giuranno, D., Passerone, A., (2005). Surface and transport properties of Ag-Cu liquid alloys. *Surface Science,* 576: 175-187.

Odusote, Y.A., (2008). Investigation of ordering phenomenon in Me-Pt (Me= Fe, Ni) liquid alloys. *Sci. Technol. Adv. Matter.* 9: 015001(1-7).

Panfilovich, K.B., Sagadeev, V.V., (2000). Thermal radiation of liquid metals. *J. Eng. Phys. Thermophys*. 73(6): 1170 -1175.

Pasturel, A, Jakse, N., (2015). On the role of entropy in determining transport properties in metallic melts. *J Phys.: Condens. Matter,* 27: 325104 (1-6).

Peng et al., (2015). Origin of the metal-insulator transition in ultrathin films of La2/3Sr1/3MnO3. *Phys Rev. B,* 92: 119906

Percus, J.K., (1962). Approximation Methods in Classical Statistical Mechanics. *Phys. Rev. Lett*. 8: 462-465.

Percus, J.K., Yevick, G.J., (1957). Analysis of Classical Statistical Mechanics by Means of Collective Coordinates. *Phys. Rev*., 110; 1-13.

Phillies, G. D. J., (2000). *Elementary Lectures in Statistical Mechanics*, Spinger-Verlag, New York, Inc.

Polyvos, J.A., Davis, H.T., (1967). Contribution to the Friction Coefficient from Time Correlations between Hard and Soft Molecular Interactions. *J. Phys. Chem.* 46: 4043 - 4047.

Prakash, S,G., Ravia, R., Chhabra, R.P., (2004). Corresponding states theory and transport coefficients of liquid metals. *Chem. Phys*. 302; 149-159.

Prasad, L.C., Singh, R.N., Singh, V.N., Singh, G.P., (1998). Correlation between Bulk and Surface Properties of Ag-Sn Liquid Alloys. *J. Phys. Chem. B*, 102 (6): 921–926.

Prasad, L.C., Singh, R.N., (1991). Surface segregation and concentration fluctuations at the liquid-vapor interface of molten Cu-Ni alloys. *Phys. Rev. B* 44:13768.

Rah, K., Eu, B.C., (2002). Self-diffusion coefficient of liquid nitrogen. *Mol. Phys.*, 100(20): 3281-3283.

Randall, J.T., (1934). *The diffraction of X – rays and electrons by amorphous solids and gases*, Wiley, New York.

Ravi, S., Kalidoss, M., Srinivasanmoorthy, R., Amoros, R., (2001). A new empirical structure factor for real liquids using internal pressure. *J. Fluid Phase Equilibria.* 178; 33-44.

Resibois, P, Davis, H.T., (1964). Transport equation of a Brownian particle in an external field. *Physica* 30, 1077-1091.

Rice, S.A., Gray, P., (1963). *Statistical Mechanics of Simple Liquids*, Wiley Inter Science, New York.

Ross, J., (1956). Statistical mechanical theory of transport processes. IX. Contribution to the Theory of Brownian Motion. *J. Chem. Phys*. 24: 375-380.

Rosenfeld, Y., (1999). Quasi-universal melting-temperature scaling of transport coefficients in Yukawa systems. *J. Phys.: Condens. Matter,* 11: 5415-5427.

Samanta, A., Ali, S.M., Ghosh, S.K., (2004). New universal scaling laws of diffusion and Kolmogorov-Sinai entropy in simple liquids. *Phys. Rev. Lett*., 92: 2242 (1-4).

Schmitz, J., Brillo, J., Egry, I., Schmid-Fetzer, R. (2009). Surface tension of liquid Al–Cu binary alloys. *In. J. Mat. Res*., 100 (11); 1529 -1535.

Schmitz, J., Brillo J., Egry, I., (2014). Surface tension of liquid Al-Cu and wetting at the Cu/Sapphire solid-liquid interface. *Eur. Phys. J. Special Topics,* 223: 469-479.

Shih, W.H., Stroud, D., (1985). Theory of the surface tension of liquid metal alloys. *Phys. Rev. B* 32 : 804-811.

Shimoji, M., Itami, T., (1986). *Diffusion and Defect Data, Atomic Transport in Liquid Metals*, Trans Tech Publication, Switzerland.

Singh, N.K.P., Singh, R.N., Choudhary, R.B., (1991). Thermodynamic investigation of atomic order in Al-Mg liquid alloys .*J. Phys. Condens. Matter,* 3; 3635-3644.

Singh, R.N., Ali, I., (2013). Elastic Moduli and Phonon Dispersion Curves for Amorphous Metals and Alloys. *Int. J. Appl. Phys. and Math*. 3: 275-279.

Singh, R.N., Arafin, A., George, A.K., (2007). Temperature-dependent thermo-elastic properties of s-, p-and d-block liquid metals. *Physica B*, 387: 344-351.

Singh, R.N., Mishra, I.K., Singh, V.N., (1990). Local order in Cd-based liquid alloys. *Phys. Condens. Matter*, 2: 8457-8462.

Singh, R.N., (1993). Higher Order Conditional Probabilities and Short Range Order in Molten Alloys. *Phys. Chem. Liq*., 25: 251-267.

Singh, R.N., Sommer, F., (1992). Temperature dependence of the thermodynamic functions of strongly interacting liquid alloys. *J. Phys. Condens. Matter*. 4(24): 5345

Singh, R. N., Sommer, F., (1997). Segregation and Immiscibility in liquid binary alloys. *Rep. Prog. Phys.*. 60: 57-150.

Singh, R. N., Sommer, F., (2006). Thermodynamic investigation of viscosity and diffusion in binary liquid alloys. *Phys. Chem. liq: In. J*., 36(1):17-28.

Siwiec, G., Oleksiak, B., Smalcerz, A., (2013). J. Wieczorek, Surface Tension of Cu-Ag Alloys. *Archives of Metallurgy and Materials*, 58(1): 193-195.

Skhrishevsij, A.F., (1980). *The structure Analysis of liquids and Amorphous materials*, Nauka, Moskva, Russia.

Speedy, R.J., (1987). Diffusion in the hard sphere fluid. *Mol. Phys*. 62:509 – 515

Speedy, R.J., Prielmeir, F.X., Vardag, T., Lang, E.W., Ludermann, (1989). Diffusion in simple fluids. *Mol. Phys*., 66:577-590

Stadler, R., Alfe, D., Kresse, G., de Wijs, A., Gillan, M.J., J. Non–Cryst. Solids. 82 (1999) 250-252.

Sonvane Y.A., Thakor, PB, Jani AR (2012). Atomic transport and surface properties of some simple liquid metal using one component plasma system. J. Theor. Appl. Phys, 6(43):1-6.

Tao, D.P., (2005). Prediction of the Coordination Numbers of Liquid Metals. *Metall. Mater. Trans*. 36A: 3495-3497.

Tatarinova, L. I., (1988*). Structure of amorphous solid and liquid substances,* pp. 15-37, 41-57, Moscow, Russia.

Tham M.K., Gubbins, K.E., (1971). Kinetic theory of multicomponent dense fluid mixtures of rigid spheres. *J. Chem. Phys.* 55: 268-279.

Thiele, E., (1963). Equation of state of hard spheres. *J. Chem. Phys.* 39(2): 474 - 479.

Tribula, M., Jakse, N., Gasior, W., Pasturel, A., (2015). Thermodynamics and concentration fluctuations of liquid Al-Cu and Al-Zn alloys. *Arch. Metall. Mater*. 60: 649-655.

Van den Berg, H.P., Hoheisel, C., (1990). Dynamic cross correlation in isotopic two-component liquids: Molecular-dynamics calculation results compared with predictions of kinetic theory. *Phys. Rev. A*, 42: 3368-3373.

vardeman C.F., Gezelter, J.D.M, (2001). Comparing models for diffusion in Supercooled Liquids: the eutectic composition of the Ag-Cu alloy. *J. Phys. Chem. A* 105:2568-2574.

Venkatesh, R., Mishra, R.K., (2005). Evaluation of activation energies and other properties from structural studies of liquid metals and their extension to liquid Ag-In alloys. *J. Non-Cryst. Sol*. 351: 705-710.

Venkatesh, R., Mishra, R.K., Gopala Rao, R.V., (2003). Structural, thermodynamic and other associated properties of partially ordered Ag-In alloy. *Phys. Stat. Solidi (b),* 240: 549-560.

Wang, N., Jiang, T., Yang, Y., Tian, J., Hu, S., Peng, S., Yan, L., (2015). Embedded atom model for the liquid U-10Zr alloy based on density functional theory calculations. *RSC Adv*., 5: 61495-61501.

Wang, S.Y., Kramer, M.J., Xu, M., Wu, S., Hao, S.G., Sordelet, D.J., Ho, K.M.,Wang, C.Z., (2009). Experimental and ab initio molecular dynamics simulation studies of liquid $Al_{60}Cu_{40}$ alloy. *Phys. Rev. B* 79: 144205(1-9).

Warren, B.E., Gingrich, N.S., (1934). Fourier Integral Analysis of X-Ray Powder Patterns. *Phys. Rev.,* 46: 368-399.

Waseda, Y., (1980). *The Structure of Non-crystalline Materials, liquids and amorphous solids*. McGraw-Hill, New York.

Wax, J. F., Akbali, R., Bretonnet, J.L., (2002). Temperature dependence of the diffusion coefficient in liquid alkali metals. *Phys. Rev. B* 65(1): 14301.

Wertheim, M. S., 1963. Exact solution of the Percus- Yevick integral equation for hard spheres. *Physical Review Letters.* 10(8): 321-323.

Xin, Y.Y., Han, M.H., Gao, G.H., (2001). Self-diffusion in a fluid of square-well spheres. *Phys. Chem. Phys*., 3: 437-443.

Xiong, L.H., Yoo, H., Lou, H.B., Wang, X.D., Cao, Q.P., Zhang, D.X., Jiang, J.Z., Xie, H.L., Xiao, T.Q., Jeon, S., Lee, G.W., (2015). Evolution of atomic structure in $Al_{75}Cu_{25}$ liquid from experimental and ab initio molecular dynamics simulation studies. *J. Phys: Cond.. Matt.* 27: 035102 (1-7).

Yokoyama, I., (1998). A relationship between excess entropy and diffusion coefficient for liquid metals near the melting point. *Physica B* 254:172-177.

Yokoyama, I., (2000). A relationship between structural, thermodynamic, transport and surface properties of liquid metals: a hard-sphere description.*Physica B* 291:145-151.

Yokoyama, I., Tsuchiya, S., (2002). Excess entropy, diffusion coefficient, viscosity coefficient and surface tension of liquid simple metals from diffraction data. *Mater Trans.* 43: 67-72

Yu, Y.X., Gao, G.H., (1999). Self-diffusion coefficient equation for polyatomic fluid *Fluid Pahse Equilibria.* 166: 111-124.

Yu, Y.X., Han, M.H., Gao, G.H., (2001). Self-diffusion in a fluid of square-well spheres. *Phys. Chem. Chem. Phys*. 3: 437-443.

Zaccarelli, E., Foffi, G., Dawson, K.A., Sciortino, F., Tartaglia, P., (2001). Mechanical properties of a model of attractive colloidal solutions. *P., Phys. Rev. E,* 63: 031501 (1-11).

Zalid, F., Bhuiyan, G.M., Sultana, S., Khaleque, M.A., Rashid, R.I.M.A., Rahman, S.M.M., (1999). Investigations of the Static and Dynamic Properties of Liquid Less Simple Metals. *Phys. Stat. Sol.(b).* 215: 987-998.

Zhakova, L.A. and Afanayeva, L.S., (2008). A method of more correct detection of the shortest atomic distance in liquid metals. J. Phys. Conference series, 98:012012.

Zhang, B., Griesche, A., Meyer, A., (2009). Relation between self diffusion and interdiffusion in Al-Cu melts. *Diffusion-fundamentals.org* 11(100): 1-8.

Zhang, B., Griesche, A., Meyer, A., (2010). Diffusionin Al-Cu Melts Studied by Time-Resolved X-Ray Radiography. *Phys. Rev. Lett.* 104: 035902 (1- 4).

Zhou, Y., Karplus, M., Ball, K.D., Berry, R.S., (2002). The distance fluctuation criterion for melting: Comparison of square-well and morse potential models for clusters and homopolymers. *J. Chem. Phys*. 116:2323-2329.

Zhou, Y., Karplus, M., Wichert, J.M., Hall, C.K., (1997). Equilibrium thermodynamics of homopolymers and clusters: Molecular dynamics and Monte Carlo simulation studies of systems with square-well interactions. *J. Chem. Phys*. 107:10691.

Zwanzig, R.W., (1954). High temperature equation of state by a perturbation method. *J. Chem. Phys*. 22: 1420-1426.

ABSTRACT

The study on structural, dynamical and surface properties of liquid metals and alloys helps in various metallurgical processes and also their study in solid state. The study of liquid state is considered to be very complicated due to irregular structure of liquids. Theoretical development on the structural and associated properties (dynamic, transport, surface, thermodynamics) of liquids become a big challenge in present time for complete understanding of liquid state. Metals have been extensively studied in the liquid phase by using classical and quantum statistical mechanics to understand their microscopic as well as macroscopic properties under equilibrium and non-equilibrium conditions.

In present study, the structure of liquids is described by means of the correlation function called the structure factor, which is shown to play an important role to obtain both equilibrium and non-equilibrium properties. The theoretical methods, computational results and their discussion on various structural aspects and their derived associated properties of liquid metals and binary liquid mixtures especially considering Al-Cu and Ag-Cu alloys have been presented. The computed structural functions were successfully employed in the same system for computing diffusion coefficients, surface tension, surface entropy, shear viscosity. Further, recently developed universal scaling law, which correlates diffusion coefficient with excess entropy in real fluids, was tested for the considered systems with square well potential. The scaling law study can predict correctly the diffusivity of pure fluids as well as binary fluid mixtures over a wide range of densities.

The first chapter deals with a detailed survey of literature which includes the integral equations of Born – Green – Yvon (BGY), hyper-netted chain (HNC), and the

Percus – Yevick (PY) which relate the potential function with the radial distribution function. In addition we give equations connecting radial distribution function (RDF) and thermodynamic quantities like compressibility, surface properties etc. The various correlation functions and the Ornstein-Zernike (OZ) equation are presented in diagram form for more clear understanding to viewers.

We give the square well potential and the result of the hard sphere solution of PY integral equation obtained by Wertheim and Thiele. The mean spherical model approximation (MSMA) was used to obtain the direct correlation function (DCF) outside the core.

The theory connecting scattering intensities and the structure factor is given. Finally the transport properties related to surface properties and the connected equations have been briefly given.

In Chapter-2 the Square well model was applied to a sample of liquid metals to compute the microscopic structural functions like structure factor, radial distribution function, coordination number. Transport properties eg. diffusion coefficients and shear viscosity of liquid metals were also presented. The computed results were found in good agreement with experimental values for most of the liquids.

In Chapter-3 the transport properties of liquids together with structural and thermodynamic information provide an important base for theories of the liquid state especially when applied with success by computing the derived properties and comparing them with the available literature values.

Thus diffusion coefficient data were employed to determine the Debye temperature, surface tension and surface entropy in all the considered liquid metals. Further, newly

developed scaling law for diffusion given by Dzugutov was tested for the SW interaction as in order to confidently label the universal scaling law, the hypothesis must be tested with different form of the inter-atomic potential. This study demonstrates that the Dgututov scaling law is valid for SW liquid metals.

Further, structure factor in the long wavelength limit of liquid metals was established through equation of state of the square well potential. The computed data of long wavelength limit of structure factor were employed to determine the isothermal compressibility of liquid metals.

In Chapter-4 we have shown how the detailed partial structure of alloys can be obtained from Lebowitz solution of hard sphere mixtures with a square well perturbing tail. These computed concentration dependent partial structure factors are incorporated in the calculations of totals structure factors of Al – Cu and Ag – Cu alloys at different atomic percent of Cu. We used mean spherical model to compute the total and partial direct correlation functions in the attractive and repulsive regions of the interacting potential in both alloys (Al-Cu and Ag-Cu) at different compositions. Thus the different partial DCFs $C_{ij}(r)$ are Fourier transformed to obtain $C_{ij}(k)$, from which the partial structure factors are computed.

It is important to point out that in the present calculations no experimental data of the alloys is used to generate the partial and total structure factors. The potential parameters were those obtained for pure metals fitted with the peak positions of the structure factors of pure constituents. With these potential parameters (the partial and total) structure factors were evaluated, and then Fourier transformed to get the partial and total radial distribution

functions. We also obtained total and partial coordination numbers from partial and total pair correlation functions respectively.

At this juncture it is important to note that with one total structure factor it is not possible to calculate the three partial structure factors. Of course it is possible to do different experiments with different isotopic substitution. Hence the present detailed model calculations are of immense help and important.

In Chapter-5 the Bhatia - Thornton fluctuations namely the number - number, concentration - concentration, and number - concentration correlation functions have been shown to be related to the partial structure factors linearly and hence these thermodynamically important quantities are also computed from the partial structure factors at various compositions of alloys in the entire momentum space with special emphasis on the values at long wave limit from which we evaluate the chemical short range order parameter to comprehend the segregating and compound formation tendencies in binary melts.

Further using Kirkwood-Buff's equation, isothermal compressibility has been calculated as a function of composition in Al - Cu and Ag - Cu alloys.

In Chapter–6 the self and mutual diffusion coefficients along with Onsager's coefficient, D_{id} were calculated by incorporating thermodynamic factor due to concentration-concentration correlation in the long wavelength, $S_{CC}(0)$ in Darken's equation. The theoretically calculated partial and total structure factors were employed to derive the self and mutual diffusion coefficients in Al - Cu and Ag - Cu alloys at different compositions of Cu. For this we use the Helfand's linear trajectory principle generalized by Davis and Polyvos for a binary mixture.

New equations have been formulated for the temperature dependence of diffusion coefficient for binary mixtures. These equations are extended to Al-Cu and Ag-Cu alloys at different concentrations of Cu to determine the activation energy for diffusion under Arrhenius law and the results are in good agreement with available literature values.

It is worth to mention here that in all the calculations of structural, transport and thermodynamic properties the potential parameters of the pure constituents have been used and no experimental data of the alloys have been employed.

Thus, in this Thesis

(1) TSFs and g(r) of liquid metals (Na, K. Cs, Mg, Al, In, Pb, Ag, Cu and Au) were determined. The computed structural parameters were employed to derive transport, thermo physical and surface properties in the considered liquid metals.

(2) Partial and total structure factors, partial and total radial distribution functions and coordination numbers in Al - Cu and Ag - Cu alloys at different concentrations of Cu.

(3) Bhatia – Thornton correlation functions in the entire momentum space with special emphasis on the values at long wave limit i.e. $S_{CC}(0)$, chemical short range order parameter and compressibility of the same alloys at different concentrations.

(4) The self and mutual diffusion coefficients have been calculated for the constituents of the same alloys through the use of Helfand linear trajectory principle at various concentrations. Extension of equations for the computation of activation energy in binary mixtures has been given.

(5) The universal scaling law was tested with the SW interaction in one component liquid metals to binary liquid alloys.

It is worth to mention that the entire work on above studies have already been published/ or communicated for its publications in the reputed scientific journals. The following are their references

1. Raj Kumar Mishra, **R. Lalneihpuii**, Raghvendu Pathak. Investigation of structure, thermodynamic and surface properties of liquid metals using square well potential. Chemical Physics, 457 (2015), 13-18.

2. Raj Kumar Mishra, **R. Lalneihpuii.** Test of the universal scaling law for square well liquid metals. Journal of Non-Crystalline solids, 444 (2016), 11-15.

3. **R. Lalneihpuii**, Raj Kumar Mishra. Transport and surface properties of liquid metals using their diffusion data. Science and Technology Journal, 4:2 (2016), 123-126. ISSN: 2321-3388.

4. Raj Kumar Mishra, **R. Lalneihpuii**, R Pathak. Concentration-Concentration orrelation in Long wavelength Limit and Short Range Order in Binary Alloys. Basic and Applied Physics, 175-182. ISBN 978-81-8487-517-1, Narosa Publication, New Delhi.

5. R Pathak, **R. Lalneihpuii**, Raj Kumar Mishra. Statistical mechanical Studies of liquid metals. Green Chemistry for Greener Environment. 135-141. ISBN 978-81-928823, Educreation Publication, New Delhi,

6. Concentration dependent structural, transport surface and scaling properties in liquid Al-Cu alloys (Communicated).

7. Bhatia-Thornton characteristics structure factors, dynamic and ordering in liquid Al-Cu alloys within the square well model (Communicated).